COMPLIANT ROBOTIC STRUCTURES - PART III

Final Report to DARPA

June 1, 1986 - August 31, 1987

James F. Wilson

Department of Civil and Environmental Engineering

Duke University

Durham, North Carolina 27706

November, 1987

Sponsored by the Defense Advanced Research Projects Agency (DOD), ARPA Order No. 5092. The views, opinions, and findings contained in this report are those of the authors and should not be construed as an official Department of Defense position, policy, or decision, unless so designated by other official documentation.

SECURITY CLASSIFICATION OF THIS PAGE

REPORT DOCUMENTATION PAGE

Form Approved
OMB No. 0704-0188
Exp. Date: Jun 30, 1986

1a. REPORT SECURITY CLASSIFICATION unclassified	1b. RESTRICTIVE MARKINGS
2a. SECURITY CLASSIFICATION AUTHORITY	3. DISTRIBUTION/AVAILABILITY OF REPORT APPROVED FOR PUBLIC RELEASE DISTRIBUTION UNLIMITED
2b. DECLASSIFICATION/DOWNGRADING SCHEDULE	
4. PERFORMING ORGANIZATION REPORT NUMBER(S) DUKE-CE-001-87-3	
6a. NAME OF PERFORMING ORGANIZATION Duke University 6b. OFFICE SYMBOL (If applicable) CE	7a. NAME OF MONITORING ORGANIZATION ONRRR
6c. ADDRESS (City, State, and ZIP Code) Durham, NC 27706	7b. ADDRESS (City, State, and ZIP Code) Georgia Institute of Technology 2060 O'Keefe Building Atlanta, GA 30332
8a. NAME OF FUNDING/SPONSORING ORGANIZATION DARPA (DOD) 8b. OFFICE SYMBOL (If applicable)	9. PROCUREMENT INSTRUMENT IDENTIFICATION NUMBER MDA903-84-C-0243
8c. ADDRESS (City, State, and ZIP Code) DARPA/ISTO 1400 Wilson Boulevard Arlington, VA 22209	10. SOURCE OF FUNDING NUMBERS PROGRAM ELEMENT NO / PROJECT NO / TASK NO / WORK UNIT ACCESSION NO
11. TITLE (Include Security Classification) Compliant Robotic Structures - Part III	
12. PERSONAL AUTHOR(S) Wilson, James F.	
13a. TYPE OF REPORT Final Report 13b. TIME COVERED FROM 6/1/86 TO 8/31/87 14. DATE OF REPORT (Year, Month, Day) 1987, November 15. PAGE COUNT	
16. SUPPLEMENTARY NOTATION	

17. COSATI CODES			18. SUBJECT TERMS (Continue on reverse if necessary and identify by block number)
FIELD	GROUP	SUB-GROUP	control, cylindrical shells, elastica, manipulators, nonlinear deformations, robotics

19. ABSTRACT (Continue on reverse if necessary and identify by block number)

This is the third and final report of a three-year study of compliant robotic structures. These structures are continuously flexible limbs designed to extend, bend, or twist when pressurized. Conceptual designs are tempered by a knowledge of muscle structure in selected animals.

The results of this third year study are reported in three chapters. Chapter I presents solutions to the elastica of an arbitrarily end-loaded, cantilevered limb. Chapter II focuses on the design details and experimental evaluations of new types of bending and torsion limb elements. Chapter III deals with the control and experimental demonstrations of a high flexure manipulator arm.

20. DISTRIBUTION/AVAILABILITY OF ABSTRACT ☒ UNCLASSIFIED/UNLIMITED ☐ SAME AS RPT ☐ DTIC USERS	21. ABSTRACT SECURITY CLASSIFICATION unclassified
22a. NAME OF RESPONSIBLE INDIVIDUAL Robert L. Rosenfeld	22b. TELEPHONE (Include Area Code) 202-694-3624 22c. OFFICE SYMBOL ISTO

DD FORM 1473, 84 MAR 83 APR edition may be used until exhausted
All other editions are obsolete

SECURITY CLASSIFICATION OF THIS PAGE

SUMMARY

This is the third and final report of a three-year study on compliant robotic structures. Such structures are designed of continuously flexible elastomeric tubes that either extend as bellows, or bend transversely, or twist about the longitudinal axis when subjected to internal pressure. The motion of such a tube under controlled internal pressure depends on its directional stiffness, achieved through the orientation of both the wall corrugations and reinforcing fibers. Tube elements in series, or end-to-end, make up a robotic limb. A single limb may be employed as a manipulator arm. Several limbs acting in parallel may be used as a compliant gripping device that conforms to the object being manipulated; and multiple limbs in parallel may be used as legs for walking machines.

In the present report, we have concentrated on the analysis, the design, and the experimental evaluation of the above mentioned elements. In these studies, we have tempered our conceptual designs with a knowledge of muscle structure in selected animals. We describe a computer-aided control scheme applied to a demonstration project: a manipulator arm made up of bending elements in series. This 50 cm arm successfully manages smooth, open-loop, pick-and-place manipulations with cycle times as small as 4.2 seconds and with placement reproducibility within 5% of the target point.

ACKNOWLEDGMENTS

Coauthors of this report are Joseph M. Snyder, Jihad Ghattas, Zhenhai Chen and Rhett T. George, Jr. We thank Glenn Butcher for his help in implementing the demonstration manipulator arm; and Jack Rebman of the Lord Corporation for his aid in the design and construction of the rubber limb elements. We also acknowledge Robert L. Rosenfeld, our DARPA project manager, for his continuing support.

James F. Wilson

Professor and
Principal Investigator

TABLE OF CONTENTS

Chapter I

STATIC BEHAVIOR OF HIGH FLEXURE MANIPULATOR ARMS

Joseph M. Snyder and James F. Wilson

INTRODUCTION

A high flexure manipulator arm is shown in Figure 1. The arm, which may carry an end payload, is comprised of several small tubular elements and is moved to various positions by adjusting the internal pressure of these elements. A single element of this arm is shown in Figure 2. The element is fabricated from a polymeric material, has a thin corrugated bellows section for part of its circumference, and a flat reinforced strip along one side. Rigid caps are provided at each end. As shown in Figure 2, the neutral axis of bending of the element is located in the flat strip, eccentric from the center of pressure on the end caps. When the element is pressurized it behaves as the beam shown in Figure 3, where the pressure load, F_d, rotates to follow the tangent to the elastic line and is offset by distance d_d. The purpose of the present study is to present a mathematical model to predict the large static deformations of a single element when it is pressurized slowly and lifts an end payload, W_d.

The element is modeled as an end loaded elastic cantilever beam for which self-weight is negligible compared to the applied loads. Since the range of deformation of the beam is too large for the application of linear beam theory, the beam is analyzed using the exact curvature relations. The shape of the elastic curve of a beam derived from the exact curvatures is called the elastica.

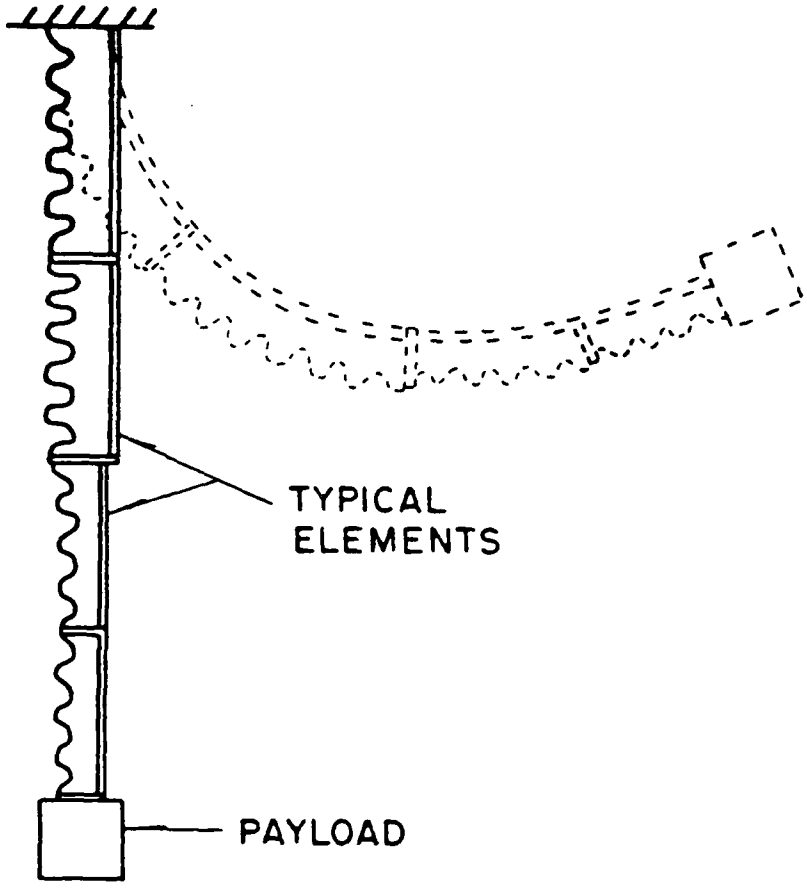

Fig. 1 The high flexure manipulator arm

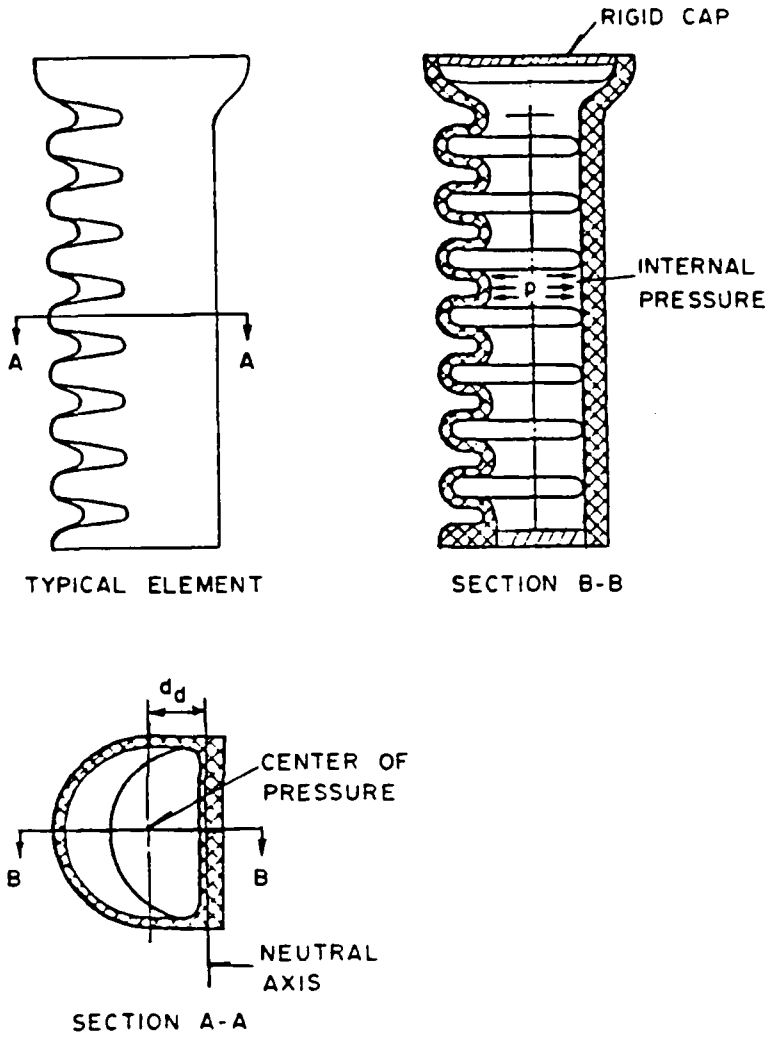

Fig. 2 Detail of a typical element of the manipulator arm

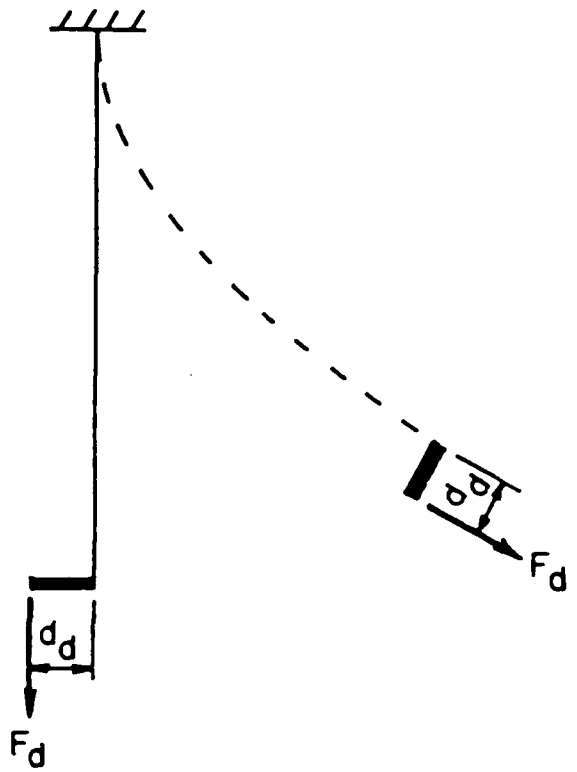

Fig. 3 Beam model of an element with no external load where F_d is due to internal pressure

The elastica has been studied for over 200 years. Euler (1744) performed the first systematic study of the elastica. An account of this early work is given by Timoshenko (1953). Love (1944) presented solutions for the "inflexional" elastica, loaded with equal and opposite forces at each end as shown in Figure 4a; and the "non-inflexional" elastica, with no inflection points, as shown in Figure 4b. Timoshenko (1961) presented an elastica solution for a cantilever beam loaded with a single longitudinal end load and Hummel and Morton (1927) gave a solution for a single transverse end force. Lau (1982) presented a solution for the general end load problem shown in Figure 5. All of these solutions were non-explicit analytical expressions using elliptic integrals. Additional references on the elastica may be found in the literature survey by Schmidt and DaDeppo (1971)

The present paper deals with numerical solutions for the elastica of a cantilever beam subjected to general end loads, where the beam models a pressurized tubular element with an arbitrarily oriented dead weight payload. The results, presented in nondimensional form, can be utilized in two ways: to develop a model for the static behavior of the entire arm and to model the arm stiffness needed for a dynamic analysis of arm motion.

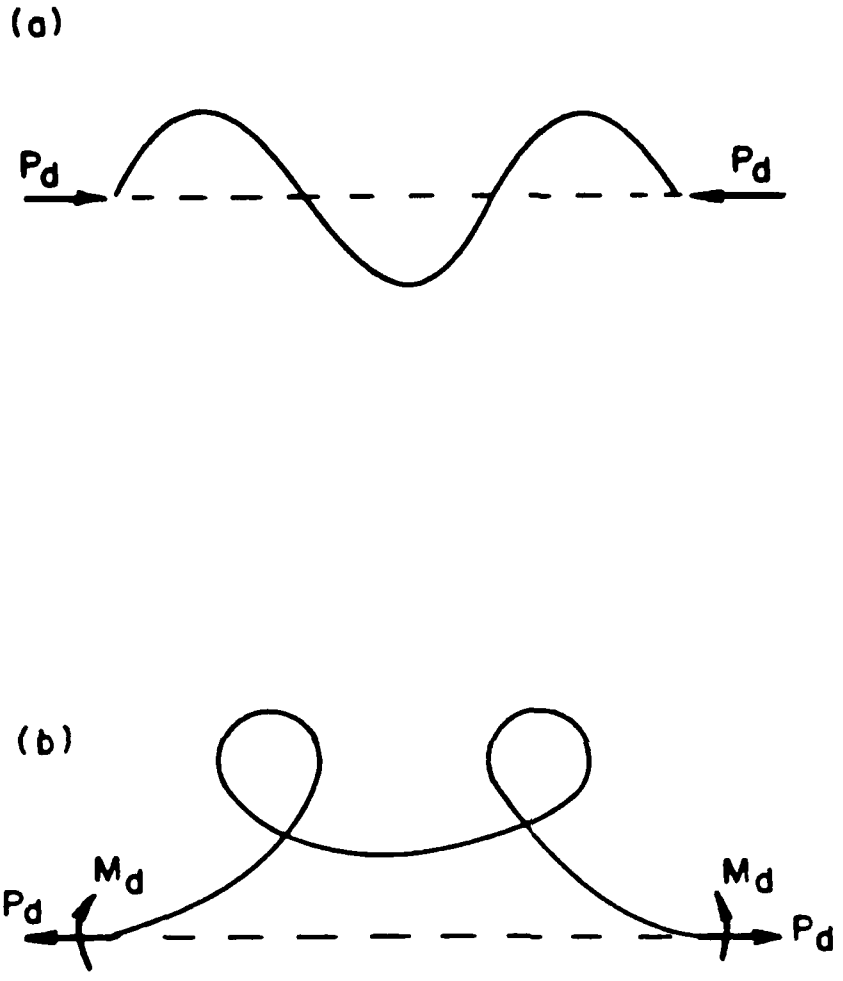

Fig. 4 The inflexional elastica (a) and the noninflexional elastica (b)

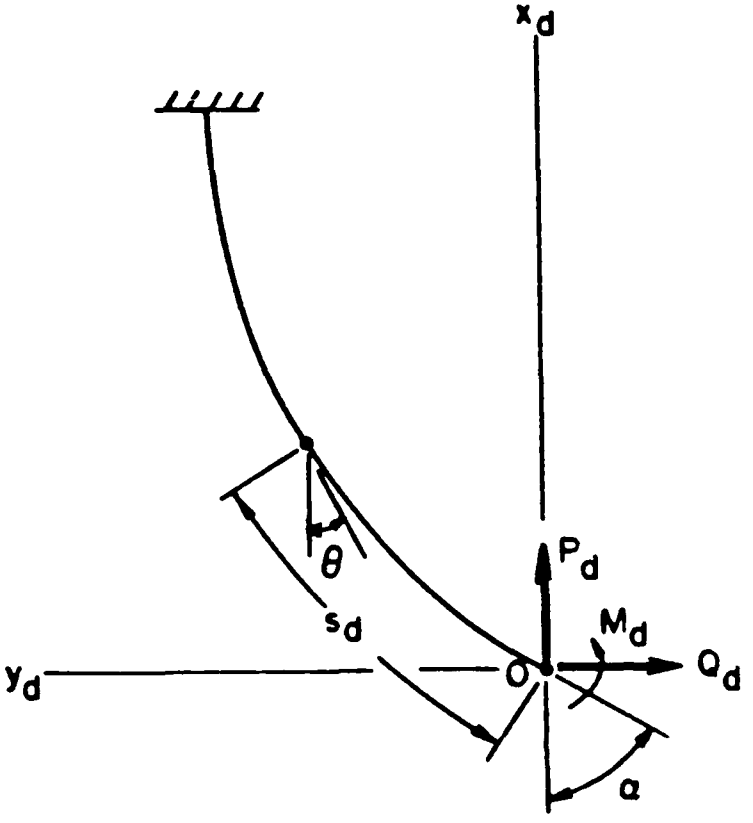

Fig. 5 The elastica subjected to general end loads

MATHEMATICAL MODEL

Consider the cantilever beam with end loads P_d, Q_d, and M_d as shown in Figure 5. The origin of the x_d,y_d axes is at the tip of the beam and the loads P_d and Q_d remain parallel to these axes. The basic assumptions of the element model are:

i) the beam is weightless and all loads are concentrated at its tip

ii) the beam material is linear elastic

iii) the beam is inextensible

iv) the effects of Poisson's ratio and transverse shearing deformations on the bending deflections are negligible

v) unloaded, the beam is straight with length L

vi) loaded, the curvature of the beam, $d\theta/ds_d$, is nonpositive.

Based on these assumptions, the differential equation of the elastica is

$$EI\frac{d\theta}{ds_d} = -P_d y_d - Q_d x_d - M_d \tag{1}$$

where E is the modulus of elasticity and I is the second moment of area of the beam cross section. With the following nondimensional parameters

$$s = \frac{s_d}{L} \tag{2a}$$

$$x = \frac{x_d}{L} \tag{2b}$$

$$y = \frac{y_d}{L} \tag{2c}$$

$$P = \frac{P_d L^2}{EI} \tag{2d}$$

$$Q = \frac{Q_d L^2}{EI} \tag{2e}$$

$$M = \frac{M_d L}{EI} \tag{2f}$$

equation (1) is transformed to the following nondimensional form

$$\frac{d\theta}{ds} = -Py - Qx - M \tag{3}$$

When equation (3) is differentiated with respect to s and the following relations are used

$$dx = \cos\theta \, ds \tag{4a}$$

$$dy = \sin\theta \, ds \tag{4b}$$

equation (3) becomes

$$\frac{d^2\theta}{ds^2} = -P\sin\theta - Q\cos\theta \tag{5}$$

This equation is integrated as

$$\int_M^{\frac{d\theta}{ds}} \frac{d\theta}{ds} \, d\left(\frac{d\theta}{ds}\right) = \int_\alpha^\theta (-P\sin\theta - Q\cos\theta) \, d\theta \tag{6}$$

where α is the slope of the elastic curve at the tip of the beam. The result is

$$\frac{1}{2}\left(\frac{d\theta}{ds}\right)^2 - \frac{1}{2}M^2 = P(\cos\theta - \cos\alpha) + Q(\sin\alpha - \sin\theta) \tag{7}$$

When equation (7) is solved for $d\theta/ds$, which is nonpositive in this problem, the following equation is obtained

$$ds = \frac{-d\theta}{\sqrt{2P(\cos\theta - \cos\alpha) + 2Q(\sin\alpha - \sin\theta) + M^2}} \tag{8}$$

Equation (8) is stated more concisely as

$$ds = \frac{-d\theta}{\sqrt{a + b\cos(\theta+\theta_0)}} \tag{9}$$

where

$$a = M^2 - b\cos(\alpha + \theta_0) \tag{10a}$$

$$b = 2\sqrt{P^2 + Q^2} \tag{10b}$$

$$\theta_0 = \arctan\left(\frac{Q}{P}\right) \text{ , where } -\pi<\theta_0\leq\pi \tag{10c}$$

Equation (9) is integrated over the length of the beam to obtain

$$1-s = \int_{\theta_0}^{\theta+\theta_0} \frac{d\phi}{\sqrt{a + b\cos\phi}} \tag{11}$$

where $\phi=\theta+\theta_0$. Equation (11) is a non-explicit,closed form solution for the rotation of the beam, θ, at the arc length coordinate s. The nondimensional coordinates at s are

$$x = \int_{\theta_0}^{\theta+\theta_0} \frac{\cos(\phi-\theta_0)\ d\phi}{\sqrt{a + b\cos\phi}} \tag{12a}$$

$$y = \int_{\theta_0}^{\theta+\theta_0} \frac{\sin(\phi-\theta_0)\ d\phi}{\sqrt{a + b\cos\phi}} \tag{12b}$$

Equations (11) and (12) may be expressed in terms of elliptic integrals, but this provides no advantage in obtaining numerical results for this problem. The solutions remain non-explicit and must be solved numerically. Given the nondimensional loads P, Q, and M and the arc length coordinate s, compatible solutions $(\theta,x,y;\alpha)$ for the shape of the elastica may be calculated from equations (10) - (12). The loading is expressed next.

LOADING CONDITIONS

The static behavior of a single element is modeled by the beam with the loads and orientations shown in Figure 6. W_d and N_d are the force and moment due to the weight of the payload at the tip of the element. Gravity is assumed to act at the constant angle β as shown. F_d is the pressure load at the tip, acting at eccentricity d_d from the neutral axis, see Figure 2. The direction and magnitude of W_d remains unchanged as the element rotates, while F_d rotates to match the slope at the tip of the element. N_d varies with both α and the configuration of the payload.

Define the following nondimensional loading parameters:

$$F = \frac{F_d L^2}{EI} \tag{13a}$$

$$W = \frac{W_d L^2}{EI} \tag{13b}$$

$$N = \frac{N_d L}{EI} \tag{13c}$$

$$d = \frac{d_d}{L} \tag{13d}$$

The nondimensional loads of equations (10) are

$$P = -F\cos\alpha - W\cos\beta \tag{14a}$$

$$Q = F\sin\alpha + W\sin\beta \tag{14b}$$

$$M = N + F\,d \tag{14c}$$

which are used with equations (11) and (12) to calculate the elastica of the element model.

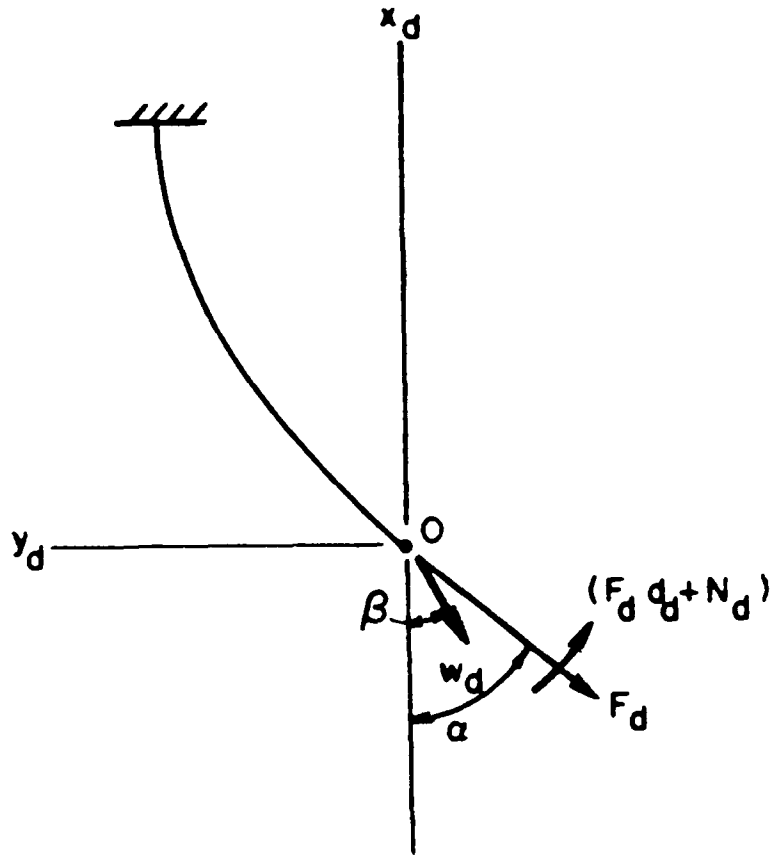

Fig. 6 Loading of an element of the manipulator arm

ALTERNATE EQUILIBRIUM STATES

An elastica problem may possess more than one possible solution. Figure 7 illustrates two of the possible equilibrium states for an elastica loaded with an end force F_1. If F_1 is applied directly to the unloaded beam, the configuration of Figure 7a will result. However, the configuration of Figure 7b will result if the load F_2 is applied to the beam before F_1 is applied and removed after F_1 is applied. This example illustrates that the loading history must be defined for an elastica solution to be unique. The elastica solutions that follow are unique because for a fixed initial payload the internal pressure loading is monotone increasing, which is consistent with the curvature assumptions used in the derivation of equations (11) and (12).

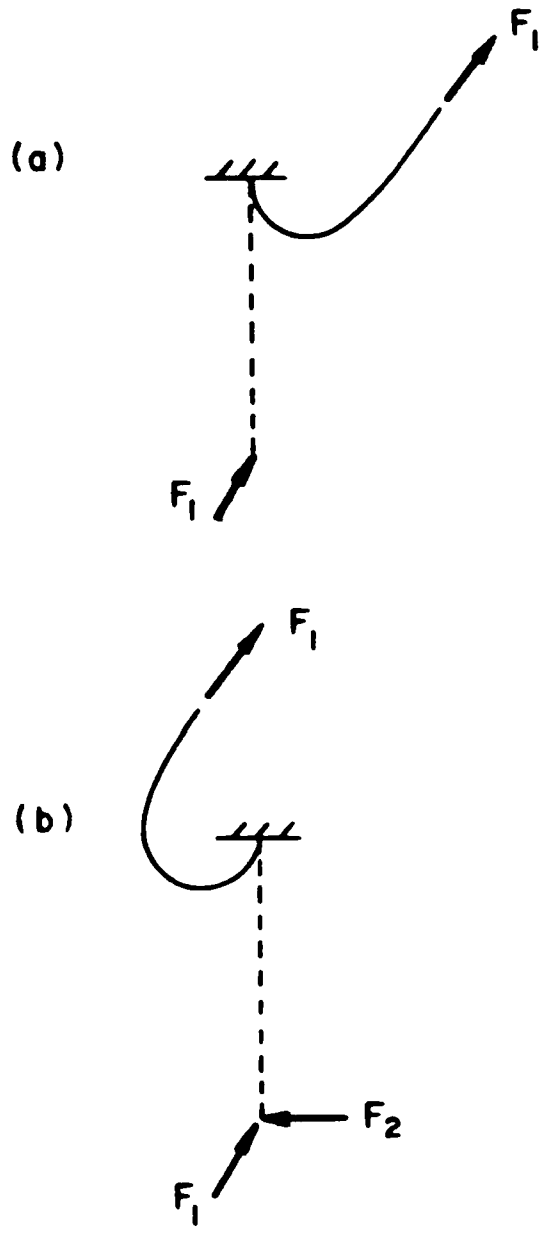

Fig. 7 Two possible equilibrium states for an elastica with the same end load

NUMERICAL RESULTS

The problem shown in Figure 8 represents a vertical element lifting a point mass of weight W_d. The point mass is located at the tip of the element, on the neutral axis so that N_d=0. This problem was solved numerically in nondimensional form using equations (10)-(12) and (14). To solve the problem, given d, F, and W, equation (11) is first solved for α (s=0) using bisection and secant iteration. After α is calculated, the equations are used in an explicit manner to determine the planar coordinates at a sufficient number of points on the neutral axis to describe its deformed shape. Numerical quadrature is used to evaluate all integrals in the equations. The computer code used for these calculations is in Appendix A. Figures 9-16 show the calculated results for a range of nondimensional parameters representative of practical experimental elements. Each of these figures shows, for given values of d and W, the elastica of the element when subjected to different values of the nondimensional pressure load, F. For clarity, these figures employ the fixed X-Y coordinate system of Figure 8, normalized by the element length L.

Figures 9 and 10 show the elastica with no dead weight load (W=0). As expected, for a given level of pressure loading, F, the curvature and the tip rotation increase as the eccentricity, d, of the pressure load increases. Figures

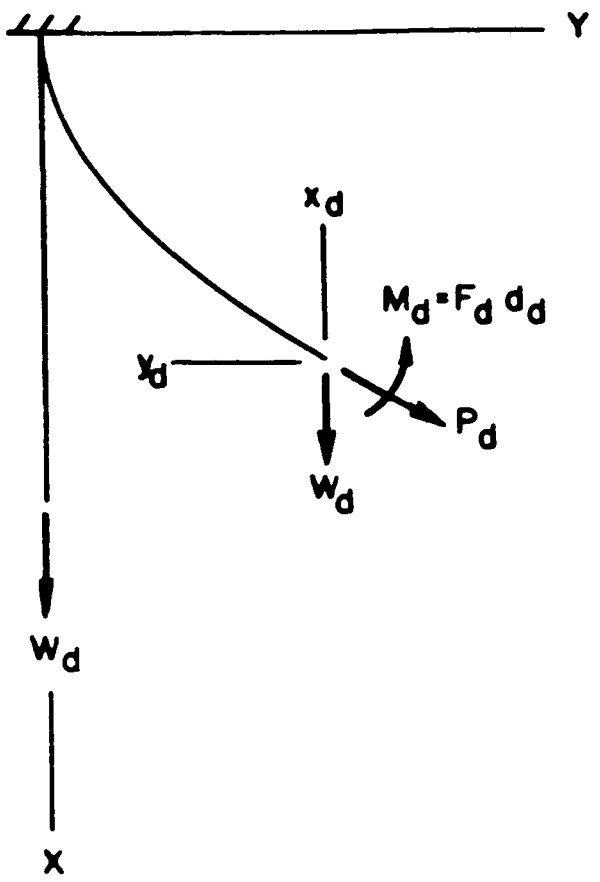

Fig. 8 Coordinate system and loading conditions for the numerical examples of Figures 9 - 19

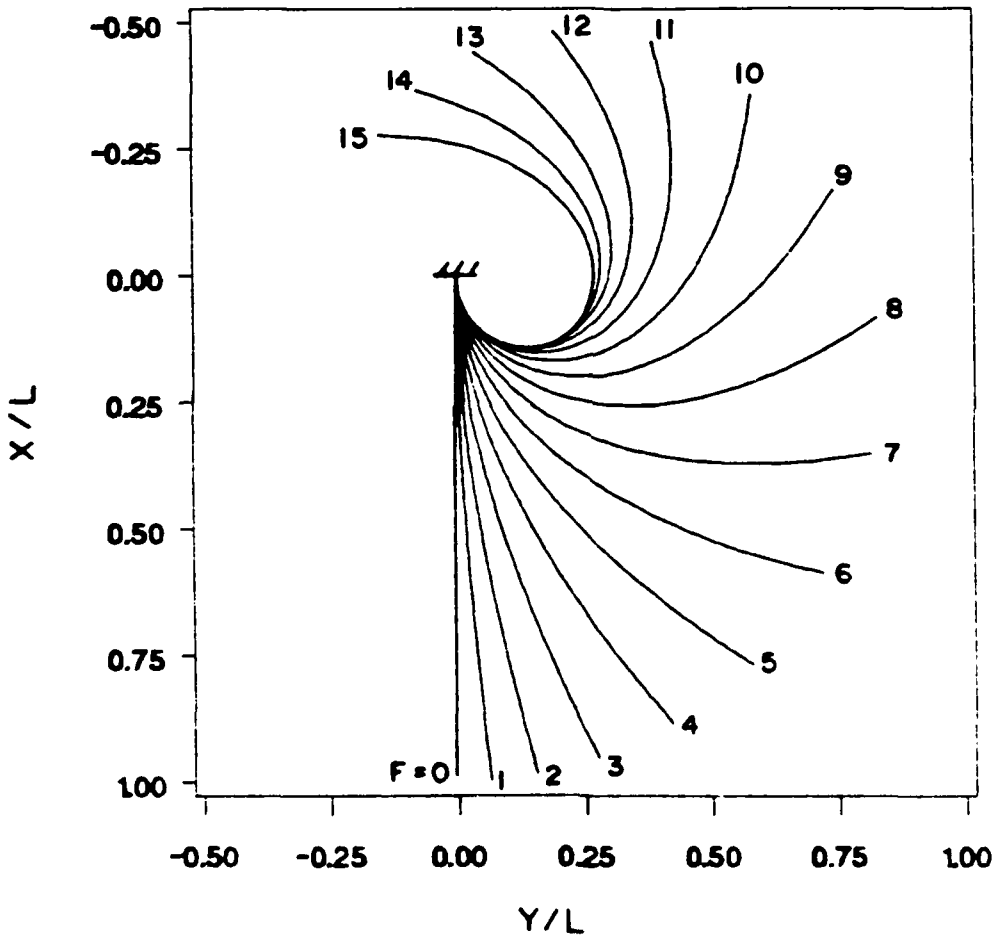

Fig. 9 Element elastica for a practical range of pressure loads, where W=0 and d=0.1

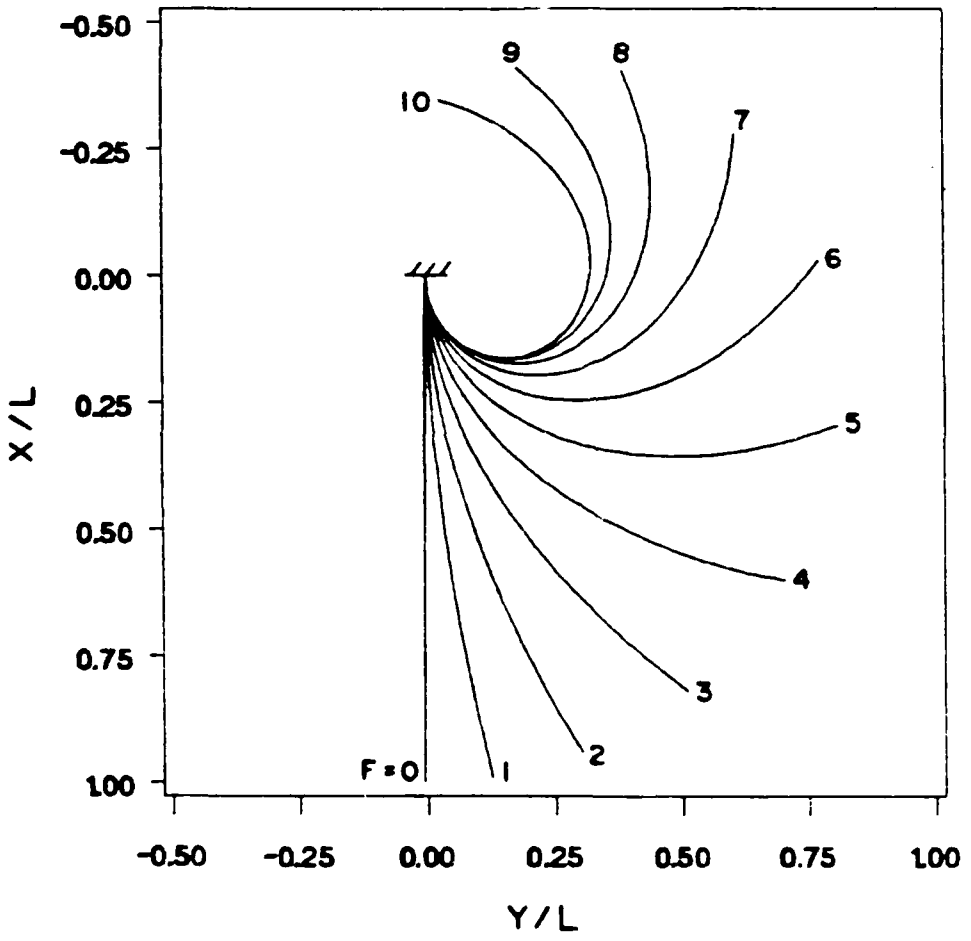

Fig.10 Element elastica for a practical range of pressure loads, where W=0 and d=0.2

11-16 show that shortly after the tip of the element rotates past ninety degrees, a relatively small increment of pressure load causes a "flip-over", or large change in shape of the elastica. This behavior, not observed when W=0 (Figures 9 and 10), becomes more pronounced as W increases. Flip-over is of special interest because it can cause significant problems in the control of the manipulator arm.

Figures 11 and 12, for which W=2.5, present a more detailed view of the flip-over phenomenom. Figure 11a, for which d=0.1, shows the shape of the elastica as F varies from 0 to 15. A large change in shape occurs as F increases from 11.8 to 11.9. Figure 11b shows the shape of the elastica as F increases from 11.8 to 11.9 in increments of one hundredth. The element still changes shape in an abrupt manner as F is increased using these finer load increments, the change occurring between F=11.84 and F=11.85. This abrupt flip-over also occurs in the elasticas presented in Figures 13 through 16. Figure 12a, for which d=0.2, shows the shape of the elastica as F varies from 0 to 10. A large change in shape occurs as F increases from 8 to 9. Figure 12b shows the shape of the element model as F increases from 8 to 9 in increments of one tenth. The element changes shape in a regular manner as F is increased using these finer load increments.The behavior illustrated by Figure 12b represents

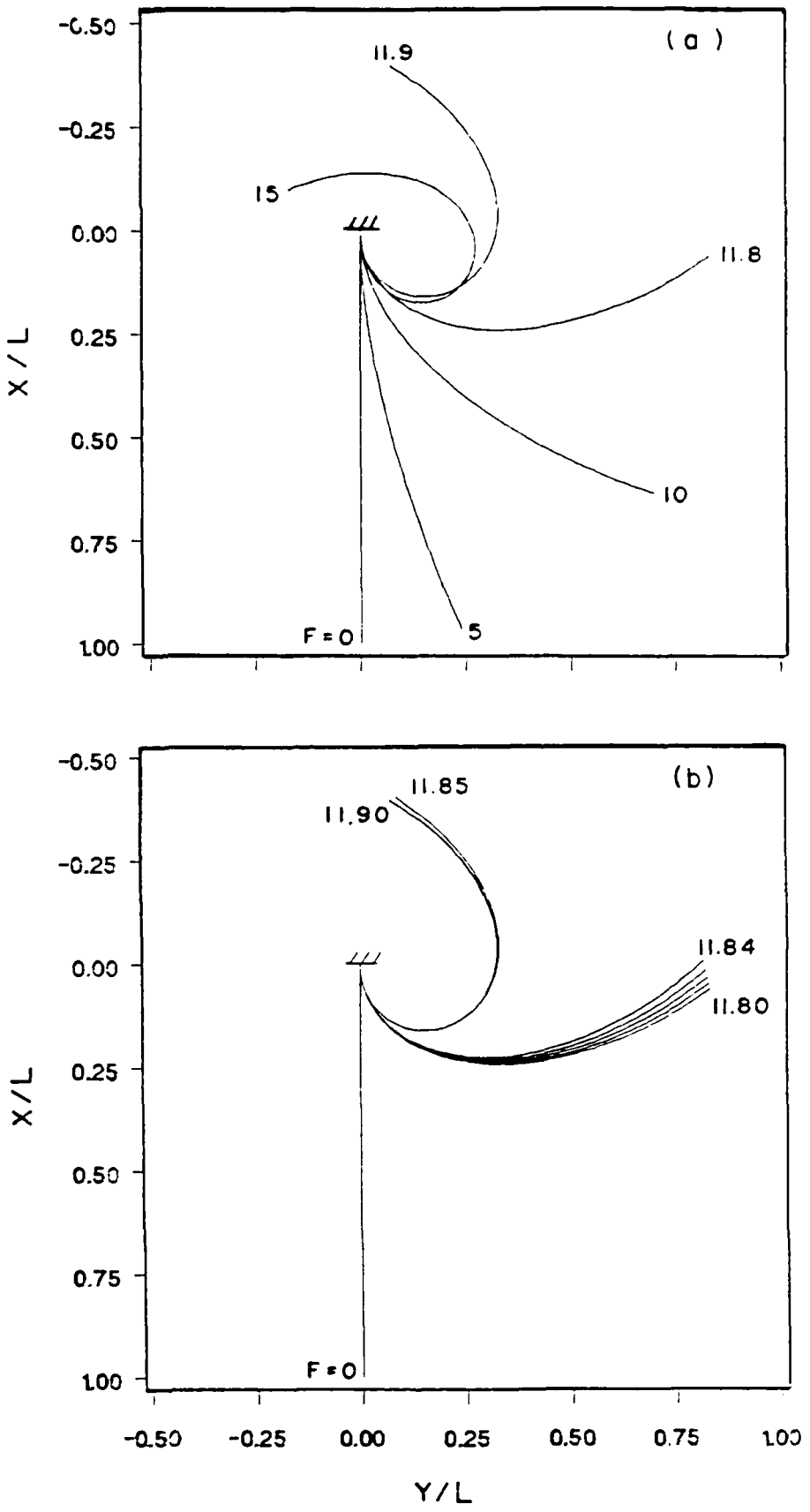

Fig.11 Element elastica for W=2.5 and d=0.1 where (a) shows overall behavior and (b) shows detailed behavior near flip-over

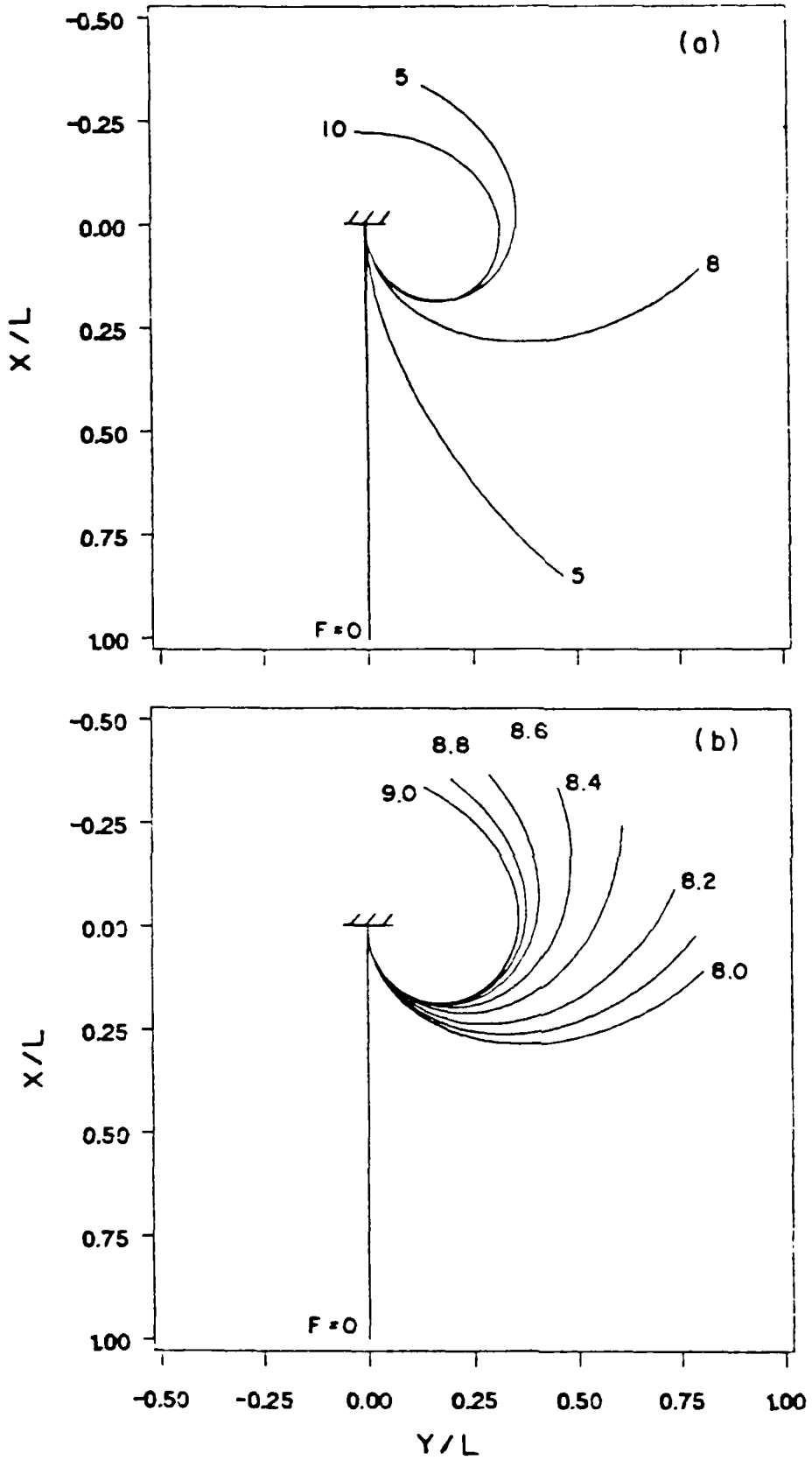

Fig.12 Element elastica for W=2.5 and d=0.2 where (a) shows overall behavior and (b) shows detailed behavior near flip-over

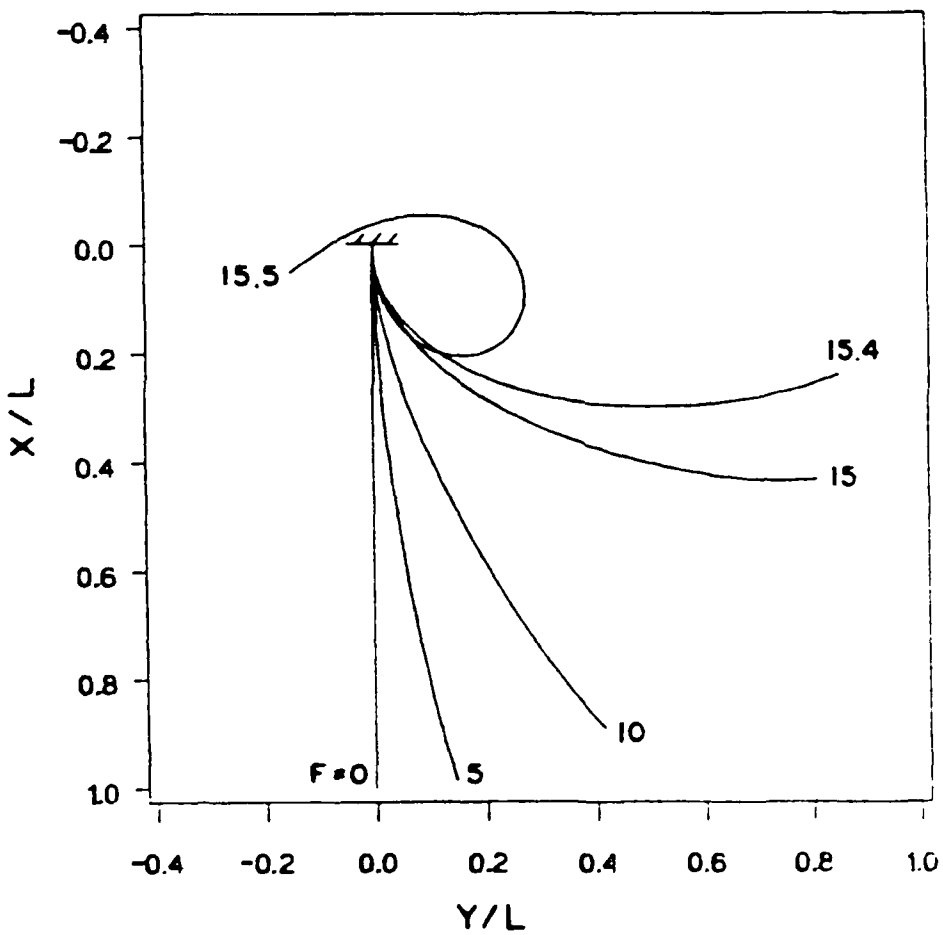

Fig.13 Element elastica for a practical range of pressure loads, where W=5.0 and d=0.1

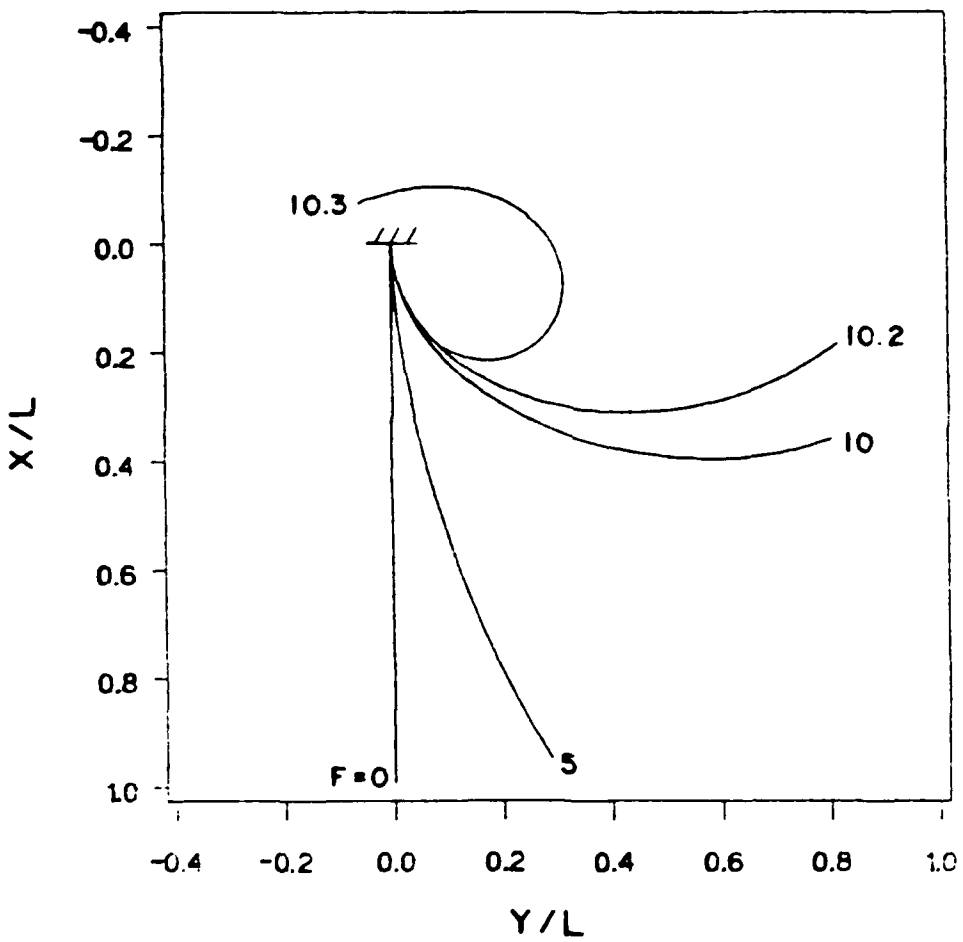

Fig.14 Element elastica for a practical range of pressure loads, where W=5.0 and d=0.2

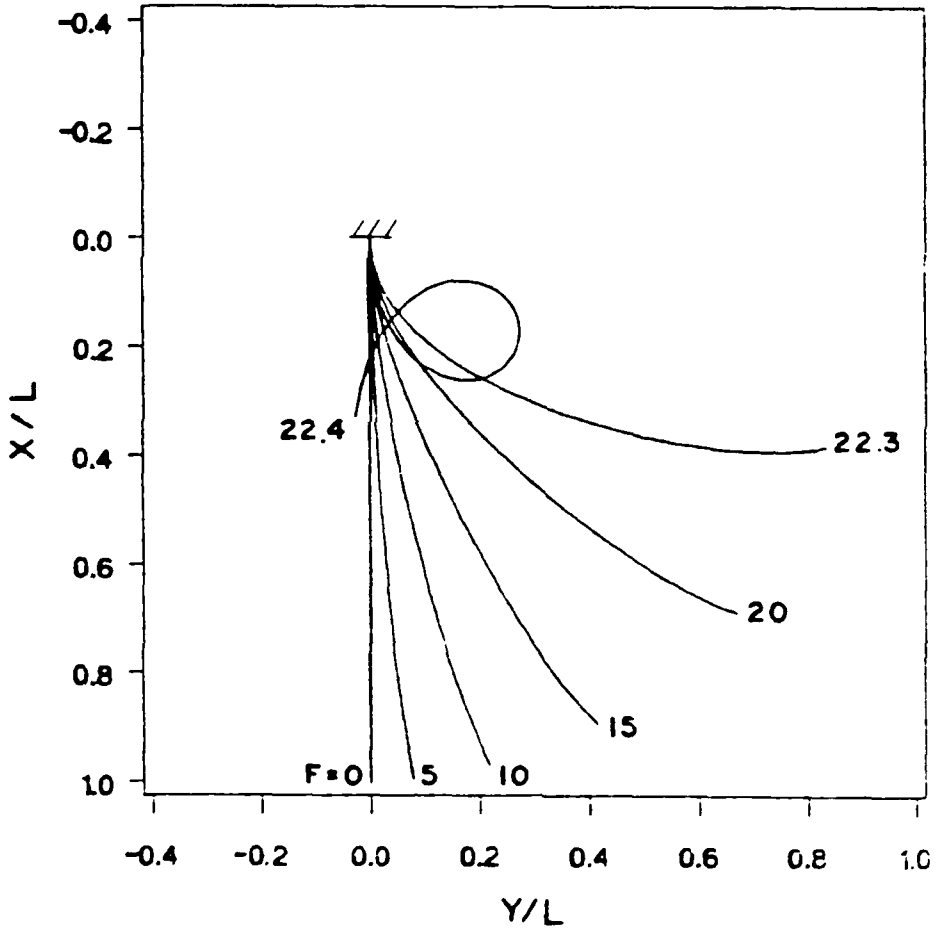

Fig.15 Element elastica for a practical range of pressure loads, where W=10.0 and d=0.1

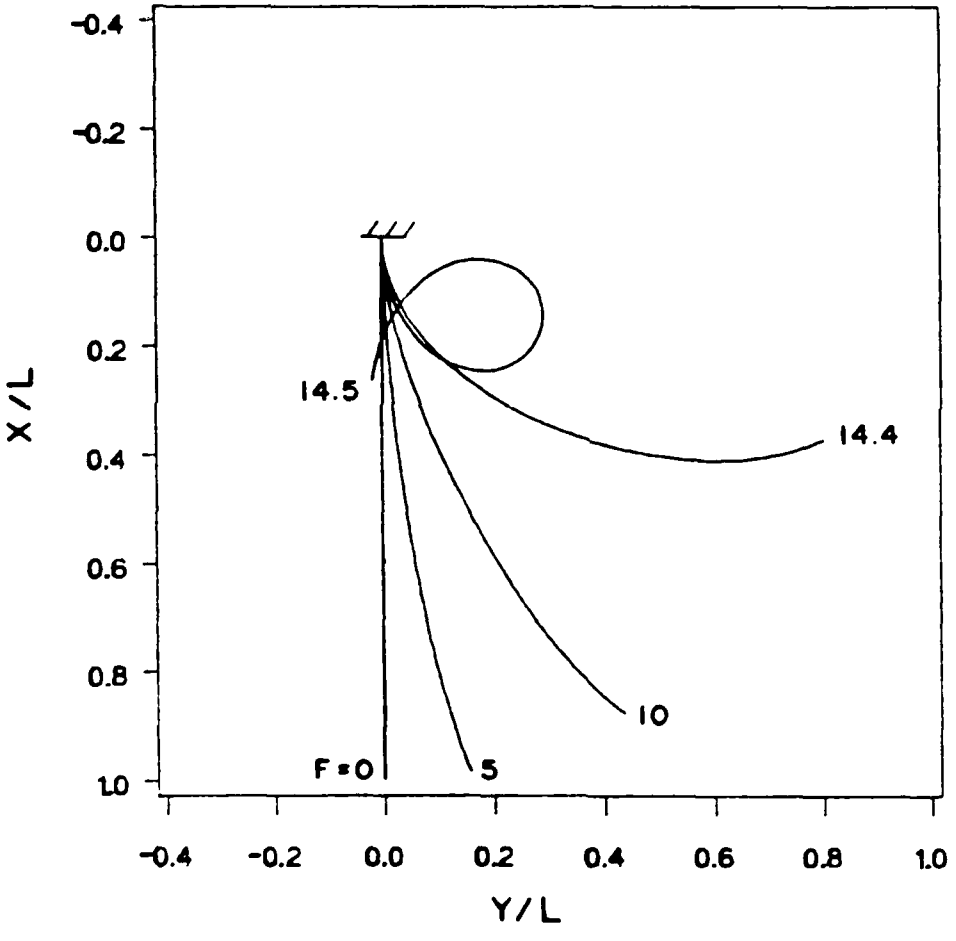

Fig.16 Element elastica for a practical range of pressure loads, where W=10.0 and d=0.2

a transition between the regular behavior exhibited in Figures 9 and 10, where W=0, and the abrupt flip-over which occurs in the remaining figures.

Table 1 presents the pressure load at the onset of flip-over, F_{cr}, the tip rotation at the onset of flip-over, α_{cr}, and the change in tip rotation due to flip-over, $\Delta\alpha$, for a range of values of W and d. F_{cr} is reported to the nearest hundredth and $\Delta\alpha$ is computed by subtracting α_{cr} from the tip rotation calculated for F_{cr}+.01. When W=2.5 and d=0.2, F_{cr} is reported to an integer value and α_{cr} and $\Delta\alpha$ are not reported because the change in shape is not abrupt and hence these quantities cannot be precisely identified. The data of Table 1 is presented graphically in Figures 17, 18, and 19. These data show that flip-over becomes more pronounced with increasing payload, W, and with decreasing eccentricity, d.

TABLE 1 Critical System Parameters for Flip-Over
(Angles in radians)

	d = 0.1			d = 0.2		
PAYLOAD W	PRESSURE LOAD F_{cr}	TIP ROTATION α_{cr}	CHANGE IN TIP ROTATION $\Delta\alpha$	PRESSURE LOAD F_{cr}	TIP ROTATION α_{cr}	CHANGE IN TIP ROTATION $\Delta\alpha$
2.5	11.848	2.37	1.75	8	NA	NA
5.0	15.412	2.00	3.40	10.203	2.26	2.81
7.5	18.985	1.88	3.98	12.357	2.14	3.59
10.0	22.399	1.88	4.28	14.422	2.05	4.09
12.5	25.635	1.88	4.52	16.410	2.04	4.41

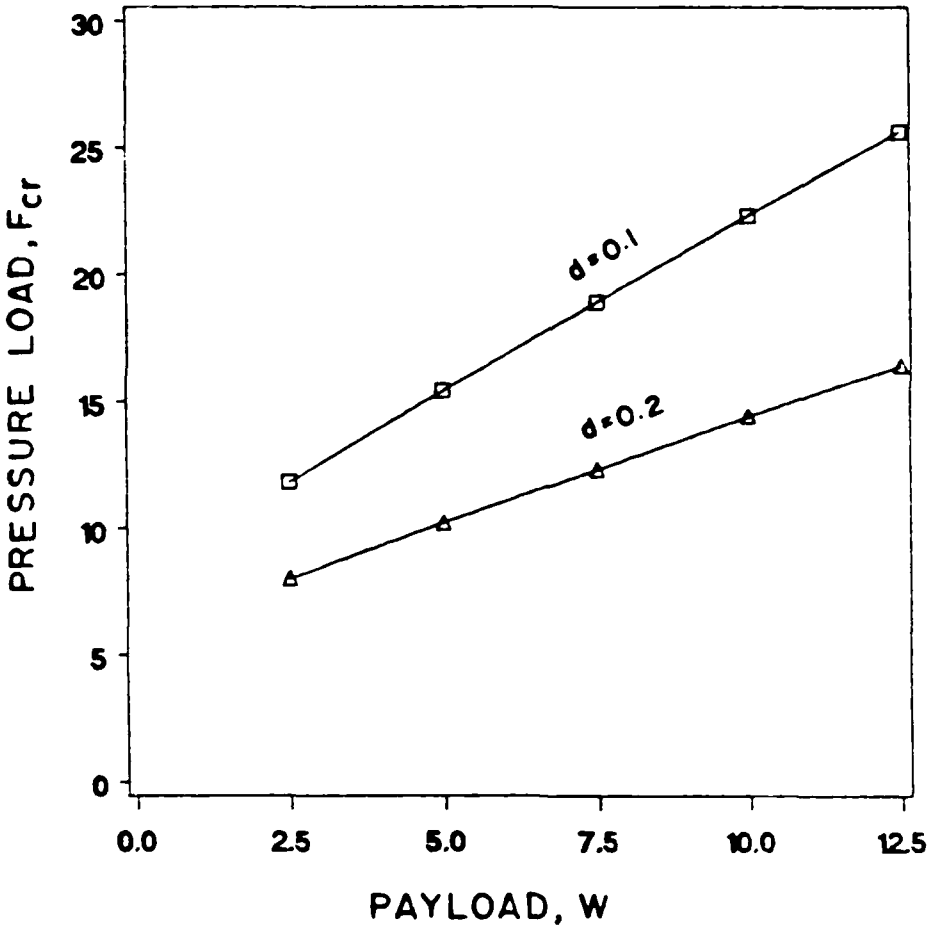

Fig.17 Pressure load at the onset of flip-over

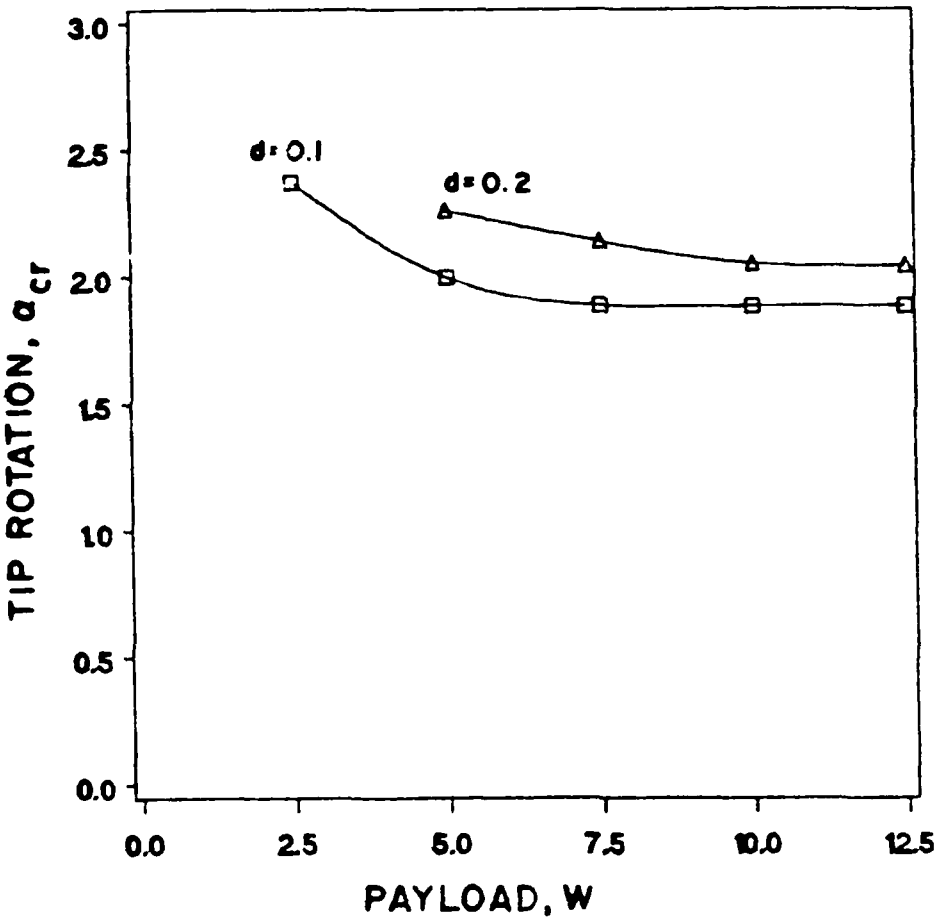

Fig.18 Tip rotation at the onset of flip-over

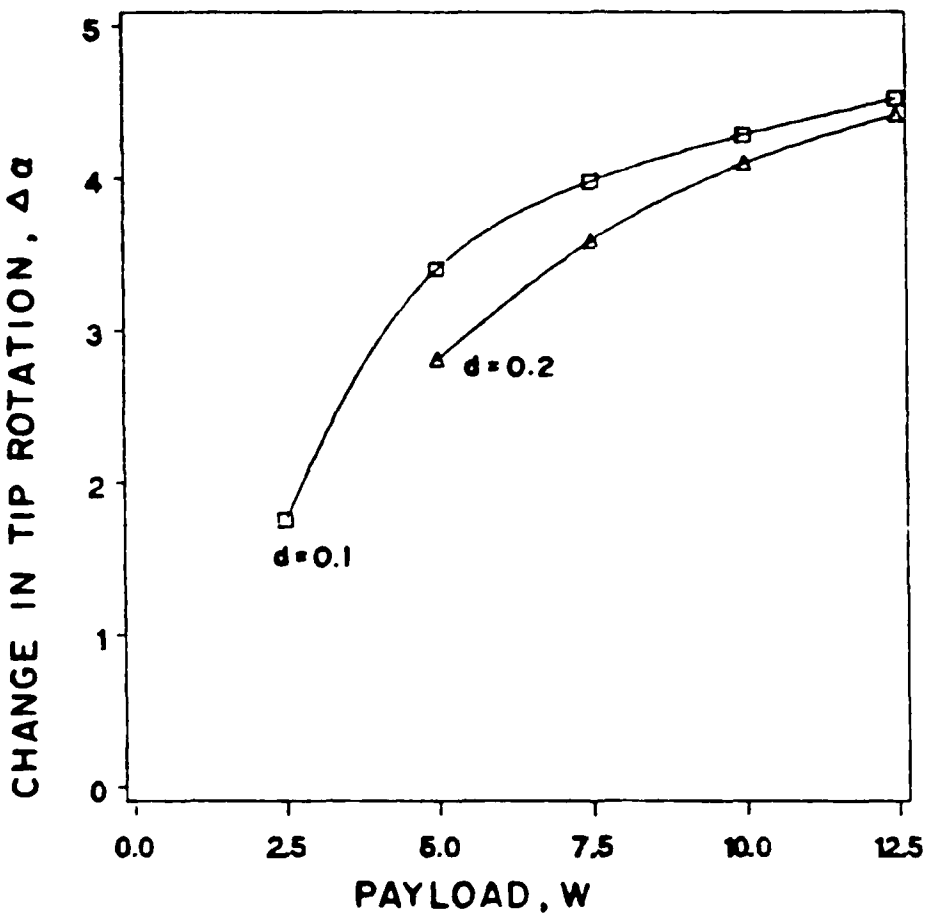

Fig.19 Change in tip rotation due to flip-over

CONCLUDING REMARKS

Flip-over is the result of interaction between the payload W and the pressure load F. The payload always acts in the same direction while the pressure load is a follower load that rotates with the tip of the elastica. Before flip-over, an initial payload tends to return the elastica to its undeformed shape. When the element is near vertical (α near 0) both F and W impose a tensile load on the element, increasing its stiffness and causing deformations to be relatively small. When the tip rotation exceeds ninety degrees, the vertical component of F opposes W. This reduces the restraining effect of W on element deformation so that small changes in the pressure load lead to flip-over.

References

Euler, L., 1744, Methodus Inveniendi Lineas Curvas Maximi Minimive Proprietate Gaudentes (Additamentum I, De Curvis Elasticis), Lausanne and Geneva

Hummel, F.H. and Morton, W.B., 1927, "On the Large Bending of Thin Flexible Strips and the Measurement of their Elasticity," Philosophical Magazine, Vol.4, Ser.7

Lau, J.H., 1982, "Large Deflections of Beams with Combined Loads," Journal of the Engineering Mechanics Division, ASCE, Vol.108, No.EM1

Love, A.E.H., 1927, A Treatise on the Mathematical Theory of Elasticity, 4th Ed., Dover Publications, New York

Schmidt, R. and DaDeppo, D.A., 1971, "A Survey of Literature on Large Deflections of Nonshallow Arches. Bibliography of Finite Deflections of Straight and Curved Beams, Rings, and Shallow Arches," The Journal of the Industrial Mathematics Society, Vol.21, Part 2

Timoshenko, S.P., 1953, History of Strength of Materials, Dover Publications, New York

Timoshenko, S.P. and Gere, J.M., 1961, Theory of Elastic Stability, 2nd Ed., McGraw-Hill, New York

Chapter II

DESIGN AND EXPERIMENTAL EVALUATION OF NEW LIMB ELEMENTS

Jihad N. Ghattas and James F. Wilson

INTRODUCTION

Elastic limb elements are used as structural components of flexible robotic manipulator arms. Two kinds of elements, bending and torque elements, can be linked end to end to form an entire manipulator arm. See Figure 1. Such elements incorporate flexible bellows, and can be pressurized independently to effect the motion of the manipulator arm. Pressurization of bending elements causes them to bend, enabling the arm to lift its payload (Wilson, 1984a). Pressurization of torque elements causes them to rotate, providing twisting action for the arm (Wilson and Orgill, 1986).

Most robotic arms in use today consist of hinged or pivoted joints connected by rigid links. Flexible manipulators utilizing pressurized elastic elements have several advantages over such rigid-link arms, including:

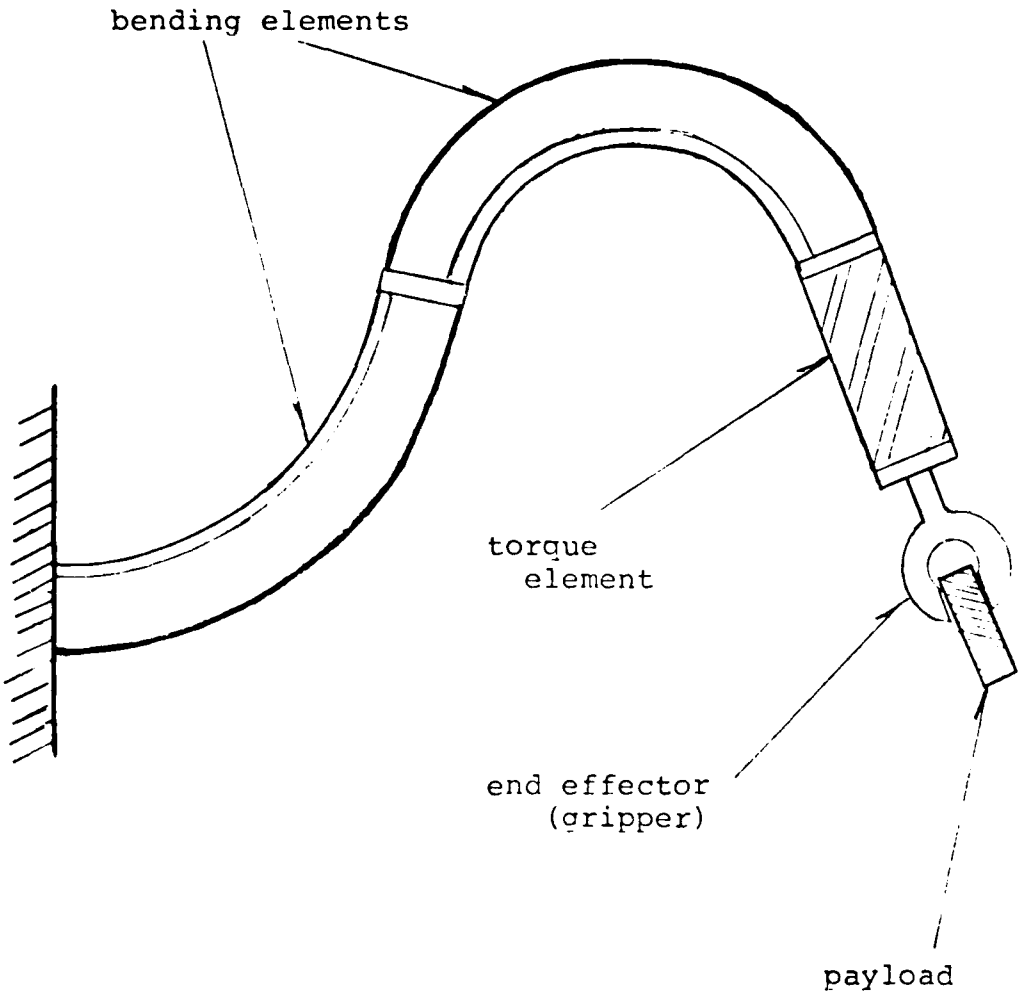

Figure 1: Robotic manipulator arm comprised of bending and torque elements. Bending elements lift payload; torque elements provide twisting, or "wrist" action. Pressure to each element is independently controlled.

1) Increased durability in harsh environments due to the impact resistance and ruggedness of elastomeric materials.
2) Reduction in arm self weight due to the remote location of the power source (air pressure supply).
3) Increased speed due to the reduction in self weight.
4) Increased lifting capacity relative to self weight.

Disadvantages include an increased complexity in precisely controlling the arm's position with pressurized air.

There are several previous studies that are relevent to the present work. For instance, the instability of bellows subjected to internal pressure was studied by Haringx (1952). Wilson (1984b) evaluated mathematical models for computing the overall stiffness for bellows of various shapes. Wilson and Orgill (1986) analyzed uniformly stressed orthotropic cylindrical shells using linear theory. Such a model may be used to describe the overall deformation characteristics of the torque element.

In this chapter, the mechanical behavior of bending and torque elements are experimentally evaluated. Then the measured relationships among deflection, internal pressure, and external loading are compared to linear theory.

DESCRIPTION OF ELEMENT CONFIGURATIONS

Three types of elements were evaluated. These were:

1) Bending elements with uniform size of bellows gaps. Both elements with one and two bellows (the single- and double-sided elements) were evaluated.
2) Bending elements with bellows gaps of optimum size. Two sizes were evaluated: small and large.
3) Torque element.

In addition, a bending element with six bellows (the "satellite" configuration) was considered, although quantitative tests were not performed on it because of irreparable pressure leaks.

All elements were made of type A150 black rubber. The modulus of elasticity of this rubber was previously measured in the range of 740 to 2330 psi., corresponding to the uncycled and cycled tensile specimens, respectively (Wilson, 1986). End fittings were aluminum in the case of the bending elements, and brass in the case of the torque element. End fittings were designed to allow the controlled intake and exhaust of air while preventing leakage of air from the element.

Bending Elements with Uniform Size Bellows Gaps.

The "single-sided" bending element consists of a solid slab attached to a corrugated bellows. See Figure 2. The bellows consists of cylindrical shells with radii r_1 and r_2 connected by annular plates. A detail of the bending element is shown in Figure 3. The single-sided element shown in Figure 2 has equal interior and exterior gaps (a = b in Figure 3). The thickness of the bellows wall is t.

The bellows portion of the bending element can be modelled as a cylidrical tube with effective wall thickness t_e, radius R equal to the bellows mean radius, or $(r_1+r_2)/2$, and an effective modulus of elasticity E′ based on the material modulus E and the bellows geometry (Wilson, 1984b). See Figure 4a. The entire bending element is modeled as a composite, cantilever beam of length L with transverse end load F_o and moment M_0 and M_p. See Figure 4b. The effect of longitudinal end loading is neglected. From elementary beam theory, the transverse tip deflection is

$$\delta = \frac{F_o L^3}{3EI_b} + (M_0 - M_p)\frac{L^2}{2EI_b} \qquad (1)$$

where E is the material modulus and I_b is the overall second area moment of the composite beam section consisting of: (1) the slab with modulus E and (2) the tube model of the bellows with modulus equal to its effective modulus E′.

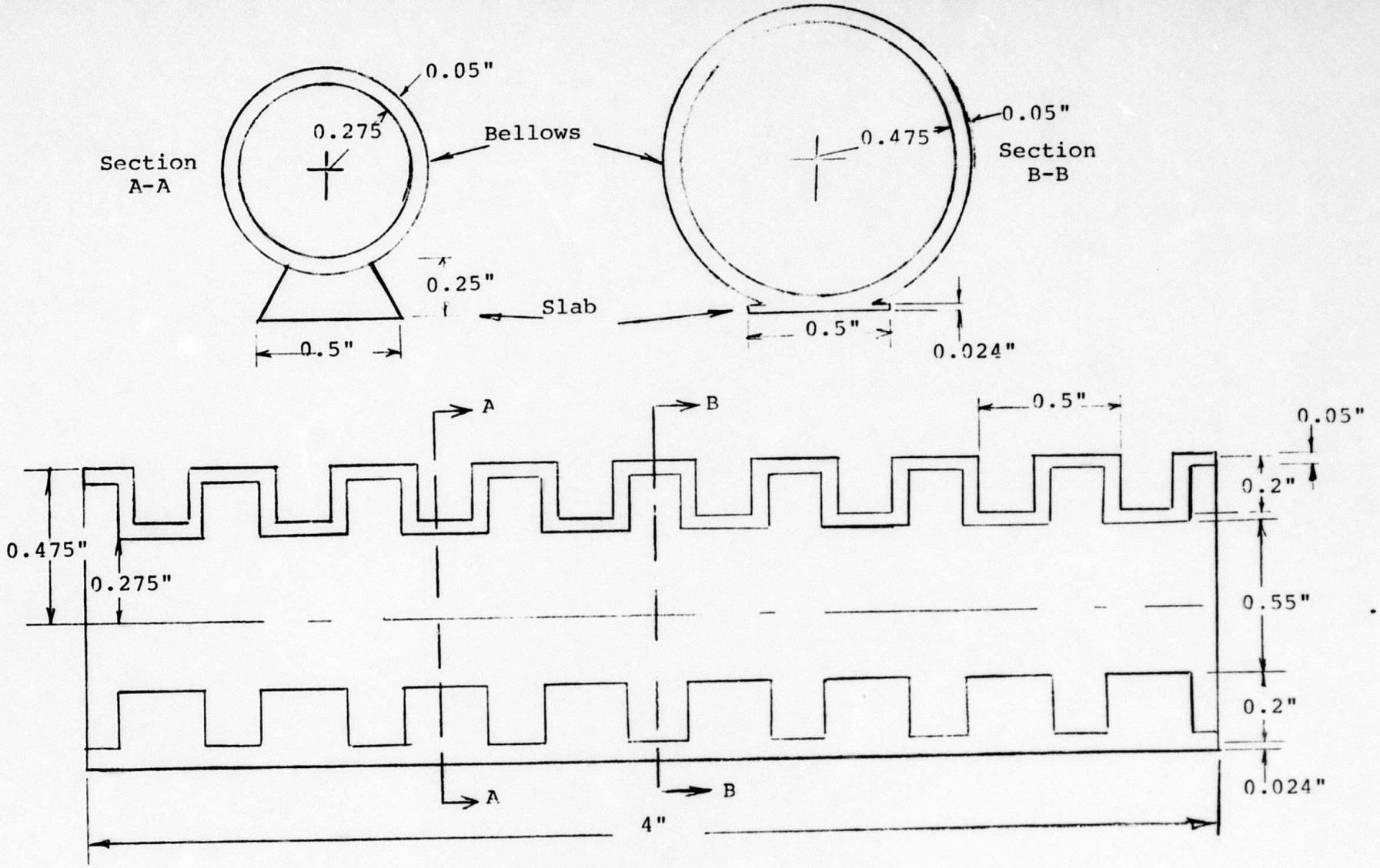

Figure 2: Bending element, single-sided with uniform size bellows gaps.

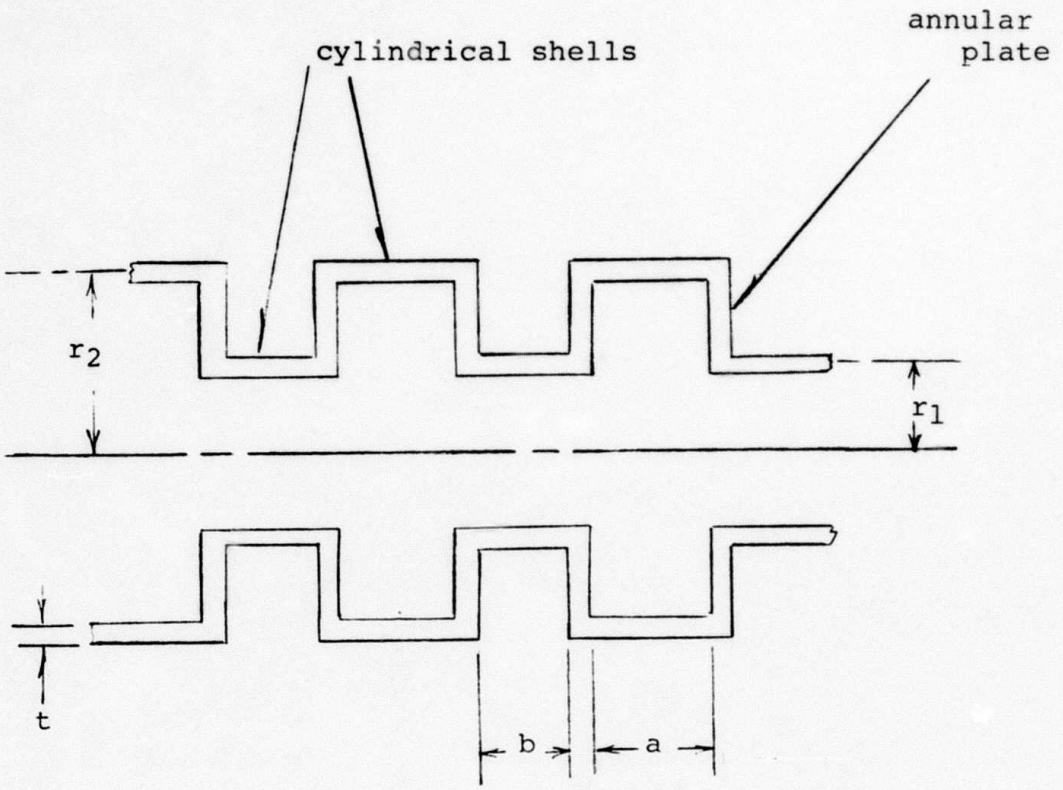

Figure 3: Detail of bending element bellows.

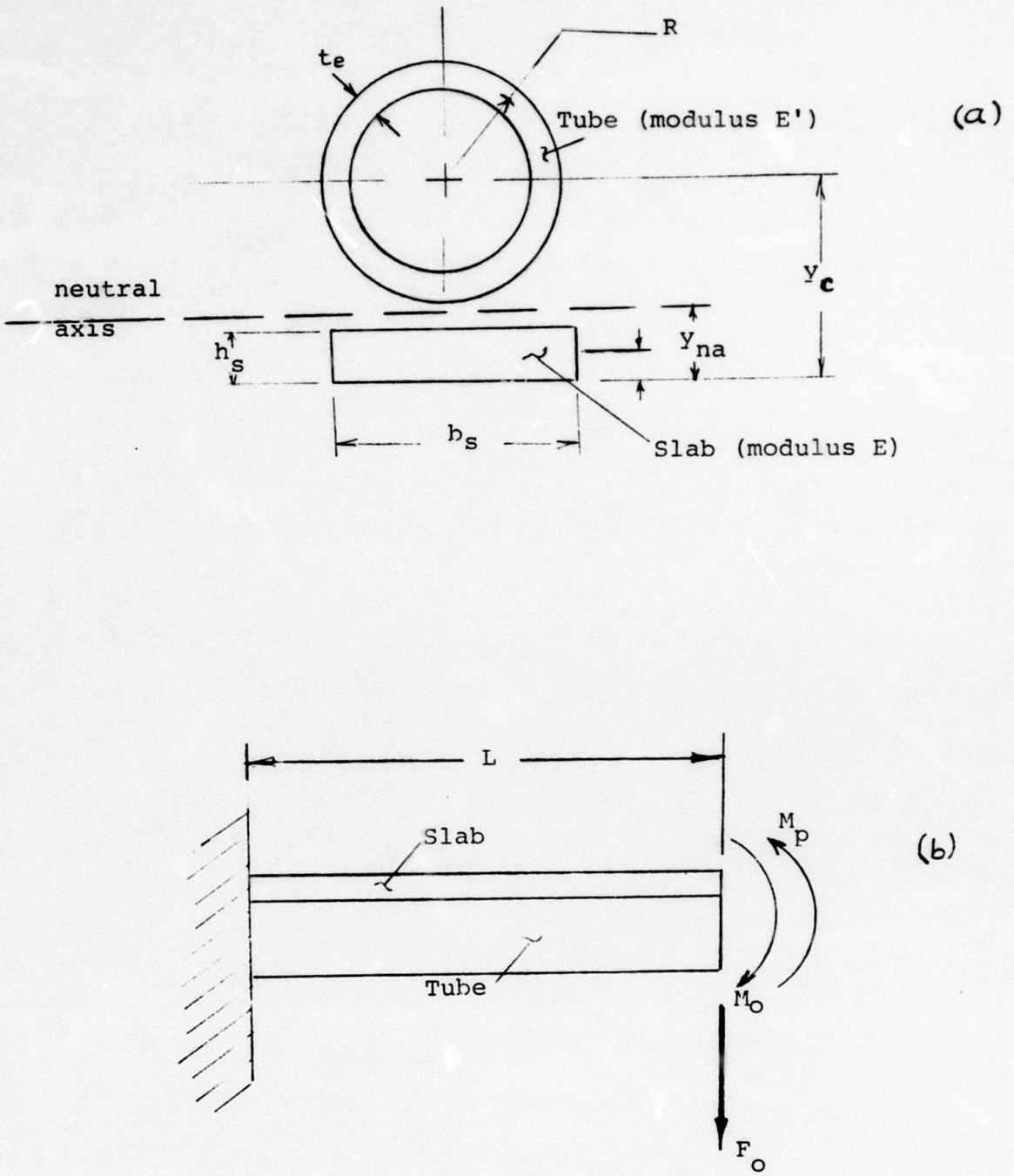

Figure 4: Composite beam model of bending element comprised of slab and tube model of bellows (4a). 4b: cantilevered beam with loading.

I_b is calculated by first locating the neutral axis, or

$$y_{na} = \frac{A_c y_c + A_s y_s}{A_c + A_s} \tag{2}$$

where the cross-sectional areas of the cylinder and slab are

$$A_c = 2\pi R t_e \tag{3}$$

and

$$A_s = b_s h_s \tag{4}$$

The effective thickness t_e of the cylindrical tube is

$$t_e = \frac{E'}{E} t \tag{5}$$

The second moment of area about the section neutral axis is then

$$I_b = \pi R^3 t_e + A_c(y_c - y_{na})^2 + \frac{b_s h_s^3}{12} + A_s(y_s - y_{na})^2 \tag{6}$$

The moment M_p due to pressurization is given by the the net force of the air pressure at the tube end acting at a distance $(y_c - y_{na})$ from the neutral axis. The net force acts at the tube center and is the product of the pressure and the effective area at the tube end, or $p\pi R^2$. Thus, M_p becomes

$$M_p = p\pi R^2(y_c - y_{na}) \tag{7}$$

Program LINDEFL.FOR, listed in Appendix B, calculates element deflections using Equations (1)-(7) where E′ is based on the Haringx bellows model.

The "double-sided" bending element consists of two single-sided elements with their slabs bonded to each other. See Figure 5. The two bellows are on opposite sides of the attached slabs and can be pressurized independently of

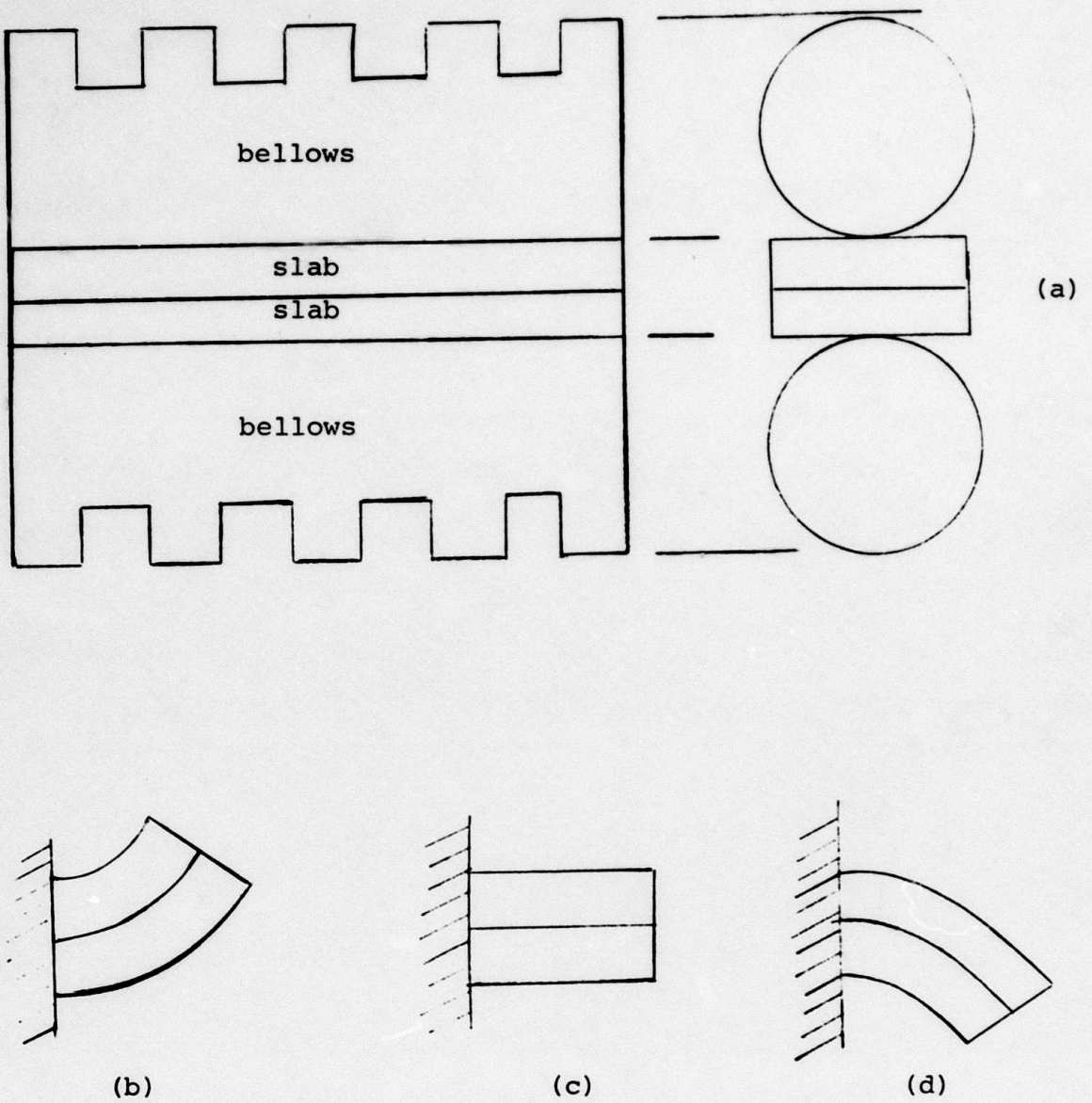

Figure 5: Double-sided bending element (a). Element bends up when pressure in lower bellows > pressure in upper bellows (b); pressure in lower and upper bellows equal (c); pressure in upper bellows > pressure in lower bellows (d).

each other. The advantages of the double-sided configuration are:

1) The element can bend under pressure to both sides of the element's neutral axis (instead of just to one side, as in the case of the single-sided element).
2) Motion can be better controlled, since motion due to the action of one bellows can be opposed or even reversed by the action of the opposing bellows.

Bending Elements with Optimum Size Bellows Gaps.

The bending elements with the optimum size of bellows gaps have configurations similar to the single-sided elements above, except that the interior and exterior gaps (a and b in Figure 3) are not equal. Dimensions a and b, as well as radii r_1 and r_2 and wall thickness t, were selected so as to maximize the performance of the element (Ghattas, 1988). The performance is characterized by the maximum degree to which the element can bend toward the bellows side without a closing of its gaps. The element must also meet deflection and payload capacity requirements.

The dimensions of the small and large elements are shown in Figures 6 and 7. These elements exhibit a maximum bending angle as described above of 69 and 108 degrees, respectively. This is a significant improvement over the

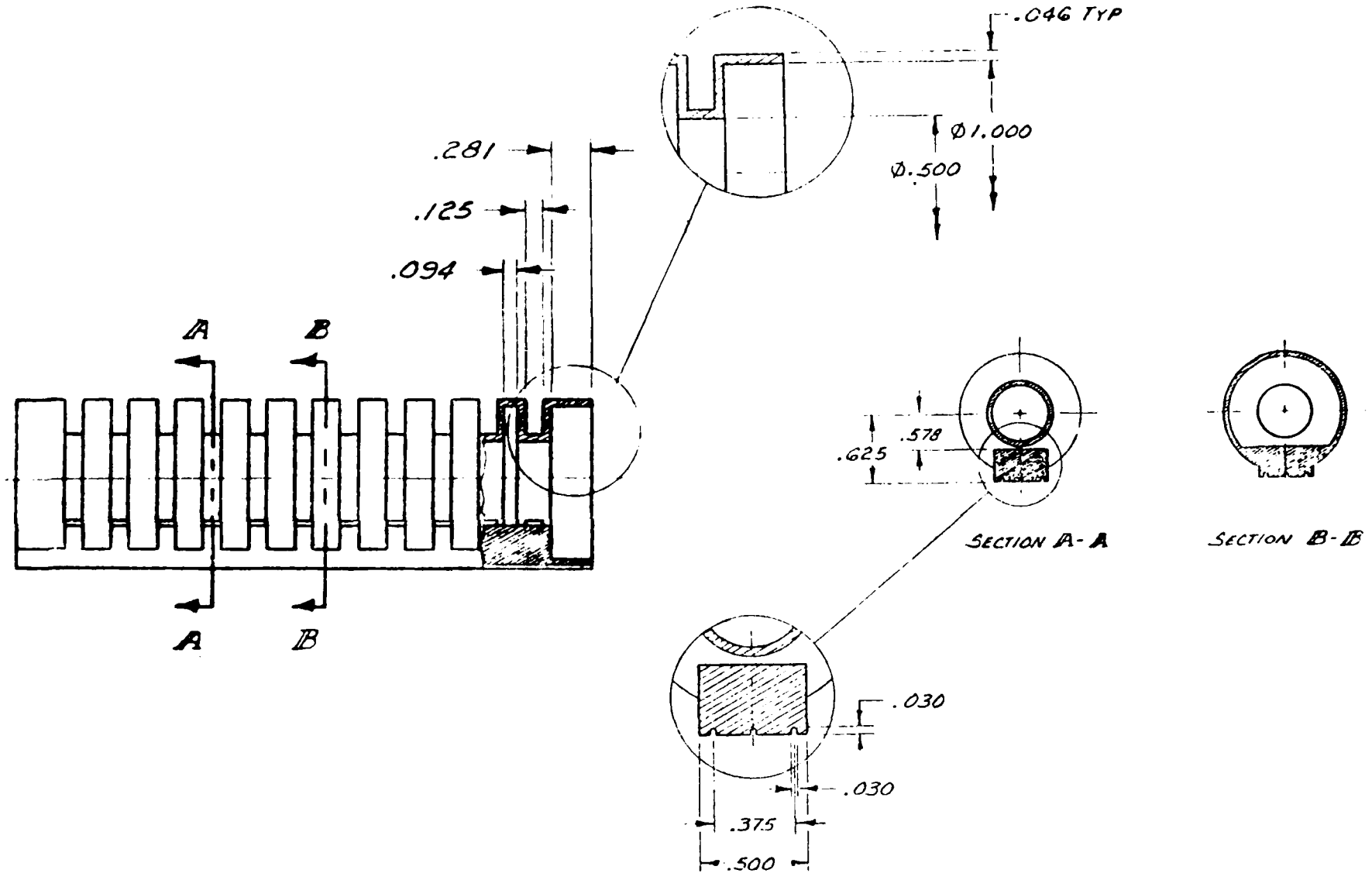

Figure 6: Bending element, small, with optimum size bellows gaps.

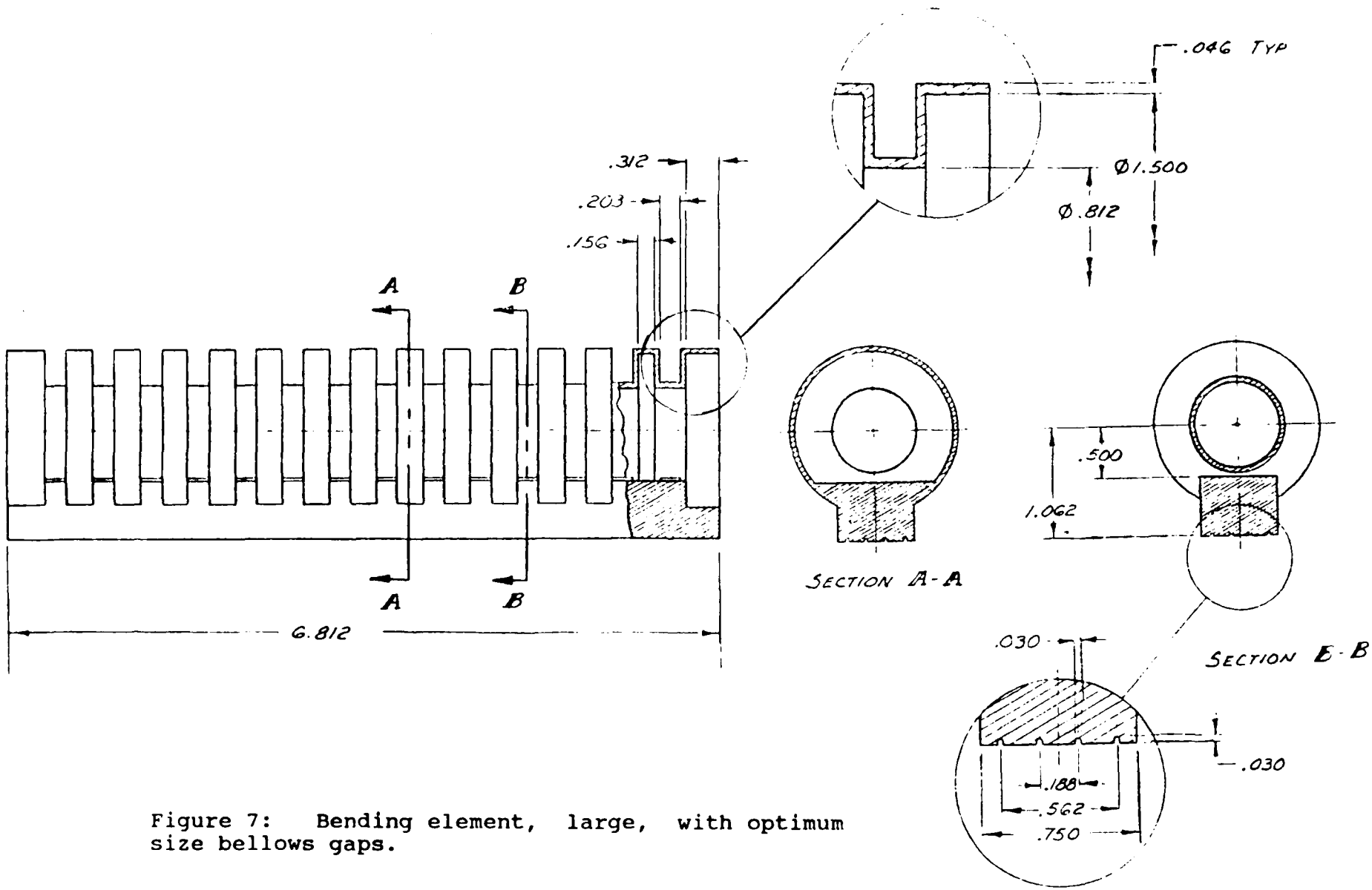

Figure 7: Bending element, large, with optimum size bellows gaps.

maximum angle for their counterpart elements in which a = b and the maximum bending angle was 45 degrees.

Torque Element.

The torque element is a cylindrical tube with bellows corrugations at a helix angle of 70 degrees. The dimensions of the torque element are shown in Figure 8.

The end rotation of the torque element is given by Wilson and Orgill (1986) as

$$\phi = \frac{L}{R}(1+\epsilon_{zz})\gamma_{\theta z} \tag{8}$$

where L is the length of the element, R is the mean radius of the element, ϵ_{zz} is the longitudinal strain, and $\gamma_{\theta z}$ is the shear strain. In the latter reference, the longitudinal and shear strains are computed for various element and loading parameters.

Satellite Bellows Configuraton.

The bending element with the satellite bellows configuration consists of six bellows arranged circumferencially (as "satellites") about a flexible central core. Such a configuration is shown in Figure 9. As shown below, six satellites is the number which yields the highest moment due to pressurization for a given arm ouside diameter.

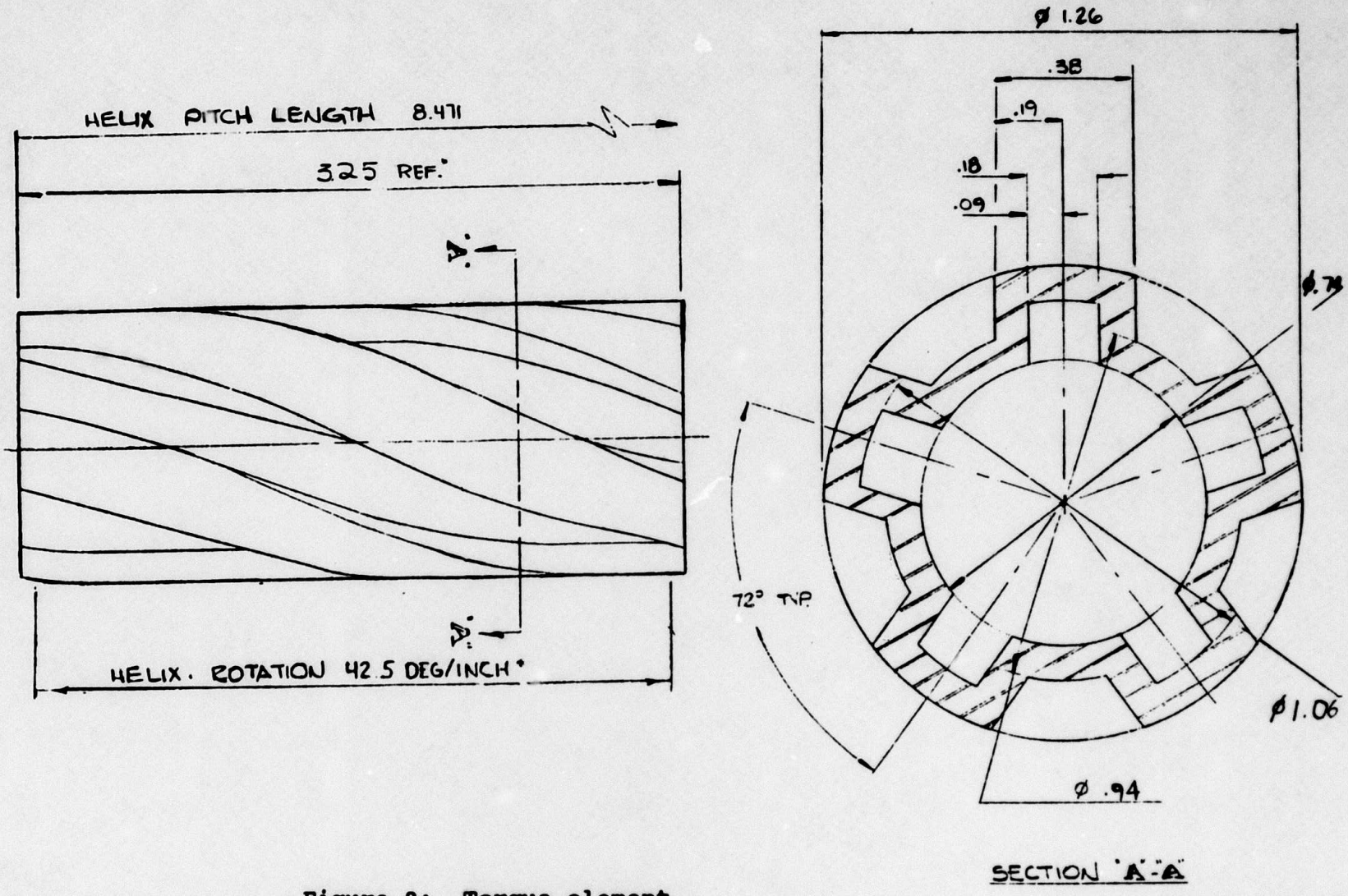

Figure 8: Torque element.

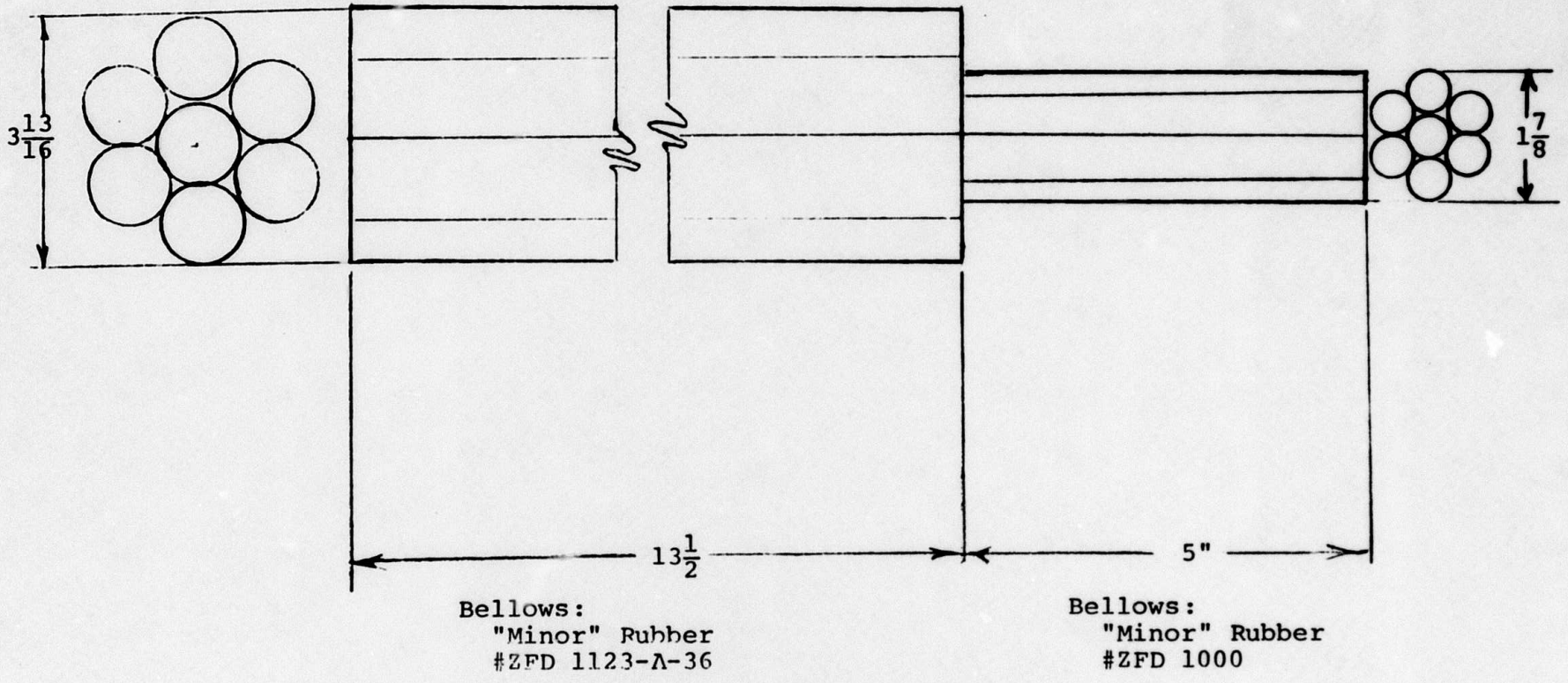

Figure 9: Bending element with satellite bellows configuration (two such elements connected end to end).

The advantages of the satellite configuration are the same as those of the double-sided element over the single-sided element. In addition, motion is not limited to the plane. Out-of-plane motion is possible because the circumferencial arrangement of the bellows enables the element to bend around not just one neutral axis, but any neutral axis in the cross section. For example, in Figure 10, if bellows 1, 2, and 3 are pressurized equally, the element will bend about neutral axis a. However, if bellows 2, 3, and 4 are pressurized equally, the element will bend about neutral axis b. Bending about any intermediate axis can be achieved by unequally pressurizing the bellows, or by pressurizing some other combination of bellows.

The optimum number of satellite bellows was determined to be six. The optimum number m is the number that yields the highest bending moment for a given outside diameter OD of the entire cluster and a given internal pressure p. The moment M due to the pressurization of all bellows to one side of the neutral axis is given by the product of the net force due to the air pressure p (pressure times the effective area at the end of the bellows) and the distances of those bellows from the neutral axis. Referring to Figures 11 and 12 for the distances of the bellows centroids from the neutral axis, the expression for moment M becomes

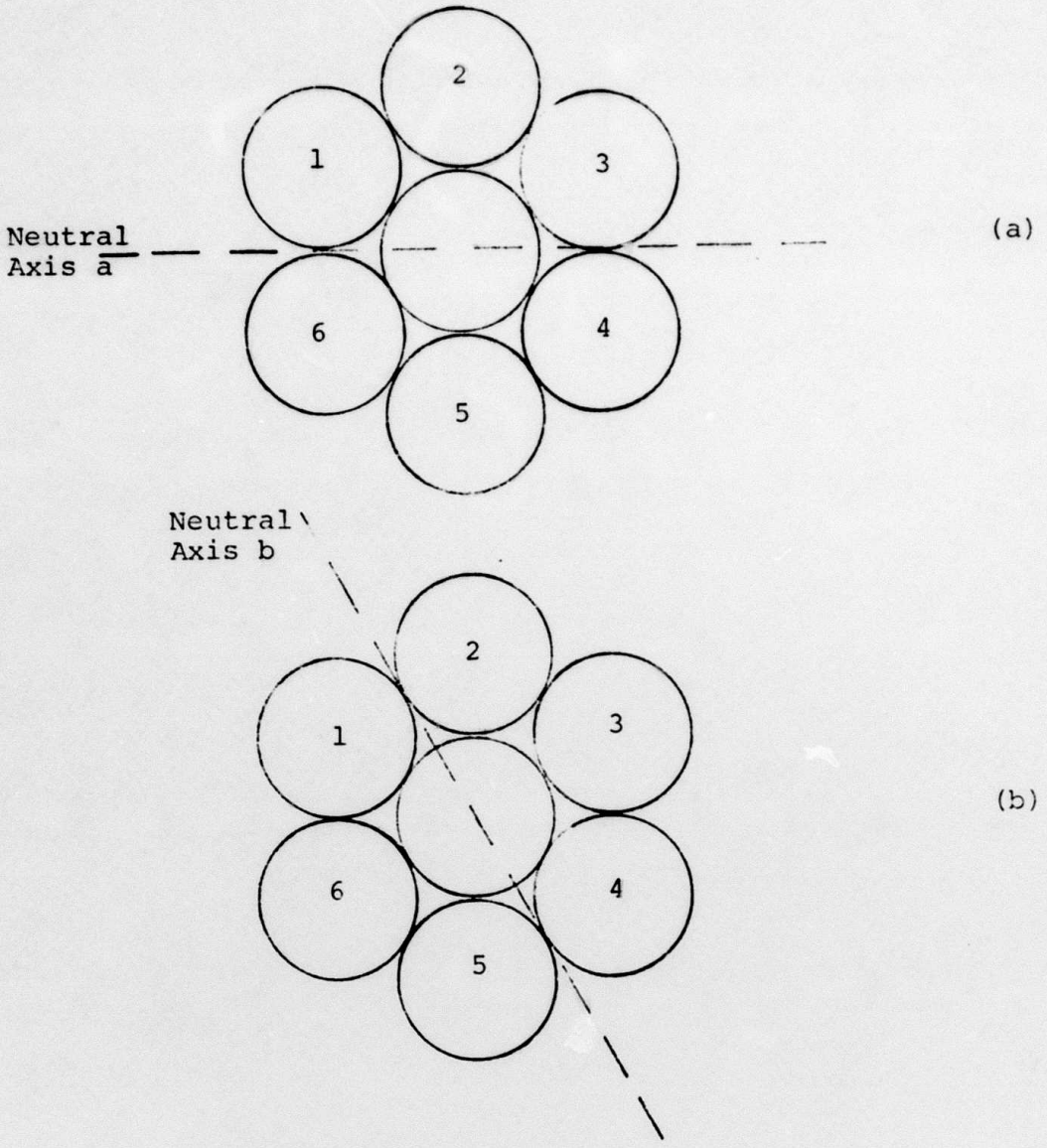

Figure 10: Variable neutral axis of satellite configuration. (a): 1, 2, 3 pressurized yields bending about neutral axis a. (b): 2, 3, 4 pressurized yields bending about neutral axis b.

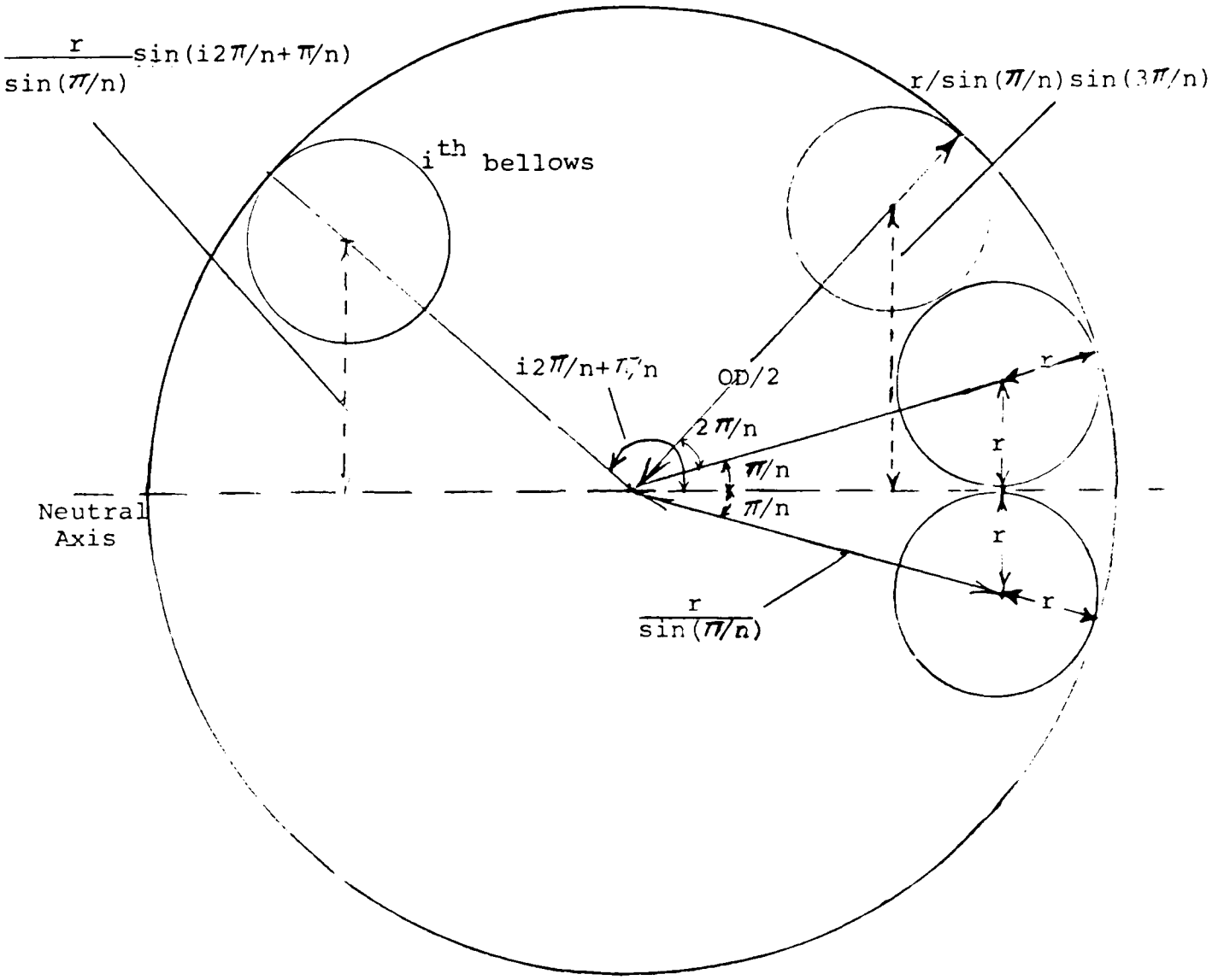

$$OD/2 = \frac{r}{\sin(\pi/n)} + r \; ; \quad r = \frac{OD}{2[1 + 1/\sin(\pi/n)]}$$

Figure 11: Element with m number of satellite bellows, m even

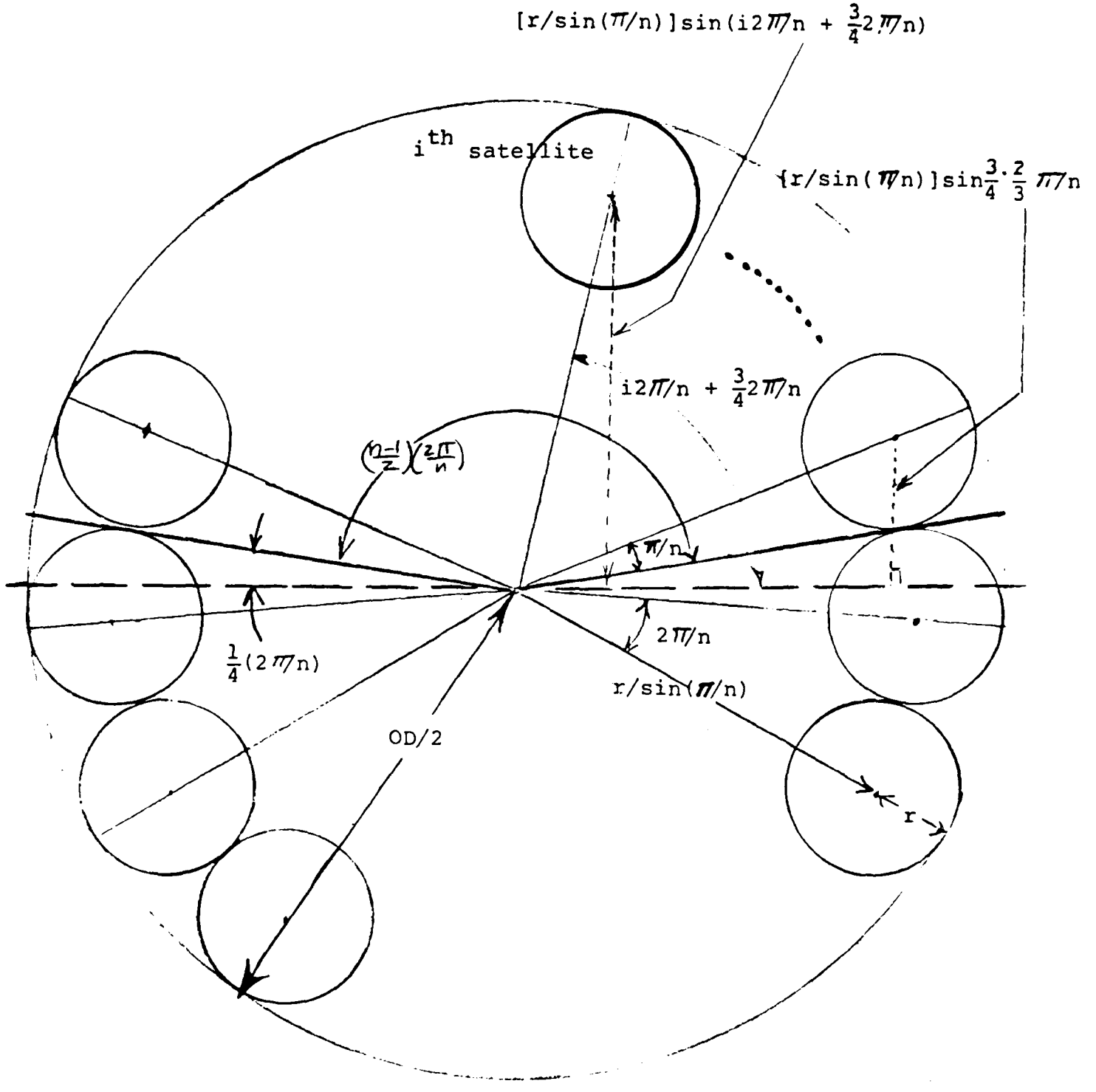

Figure 12: Element with m satellite bellows; m is odd. Neutral axis is through section which yields highest moment.

$$M = p\pi r^2 \sum_{i=0}^{INT(m/2-1)} \sin\left(\frac{2\pi i}{m}+\alpha\right) \tag{9}$$

Note that the cluster OD determines the bellows outside radius, i.e. (from Figure 11)

$$r = \frac{OD}{2\left(1+\frac{1}{\sin(\pi/m)}\right)} \tag{10}$$

Substituting this expression into that for moment due to internal pressure gives the result

$$M = \frac{4p\pi}{9\sin(\pi/m)}\left[\frac{OD}{2\left(1+\frac{1}{\sin(\pi/m)}\right)}\right]^3 \sum_{i=0}^{INT(m/2-1)} \sin\left(\frac{2\pi i}{m}+\alpha\right) \tag{11}$$

where

$$\alpha = \left\{ \begin{array}{c} \frac{1}{2}(2\pi/m) \quad \text{(for m even)} \\ \text{or} \\ \frac{3}{4}(2\pi/m) \quad \text{(for m odd)} \end{array} \right\} \tag{12}$$

and INT is the integer function that trucates after the decimal point.

To find the highest moment for a given pressure p and cluster outside diameter OD, M was computed for various satellite numbers m. The results tabulated in Figure 13 show that for six satellite bellows, the moment will be highest. For m>6, the moment decreases as the satellites become infinitely small but their distances to the neutral axis approach OD/2.

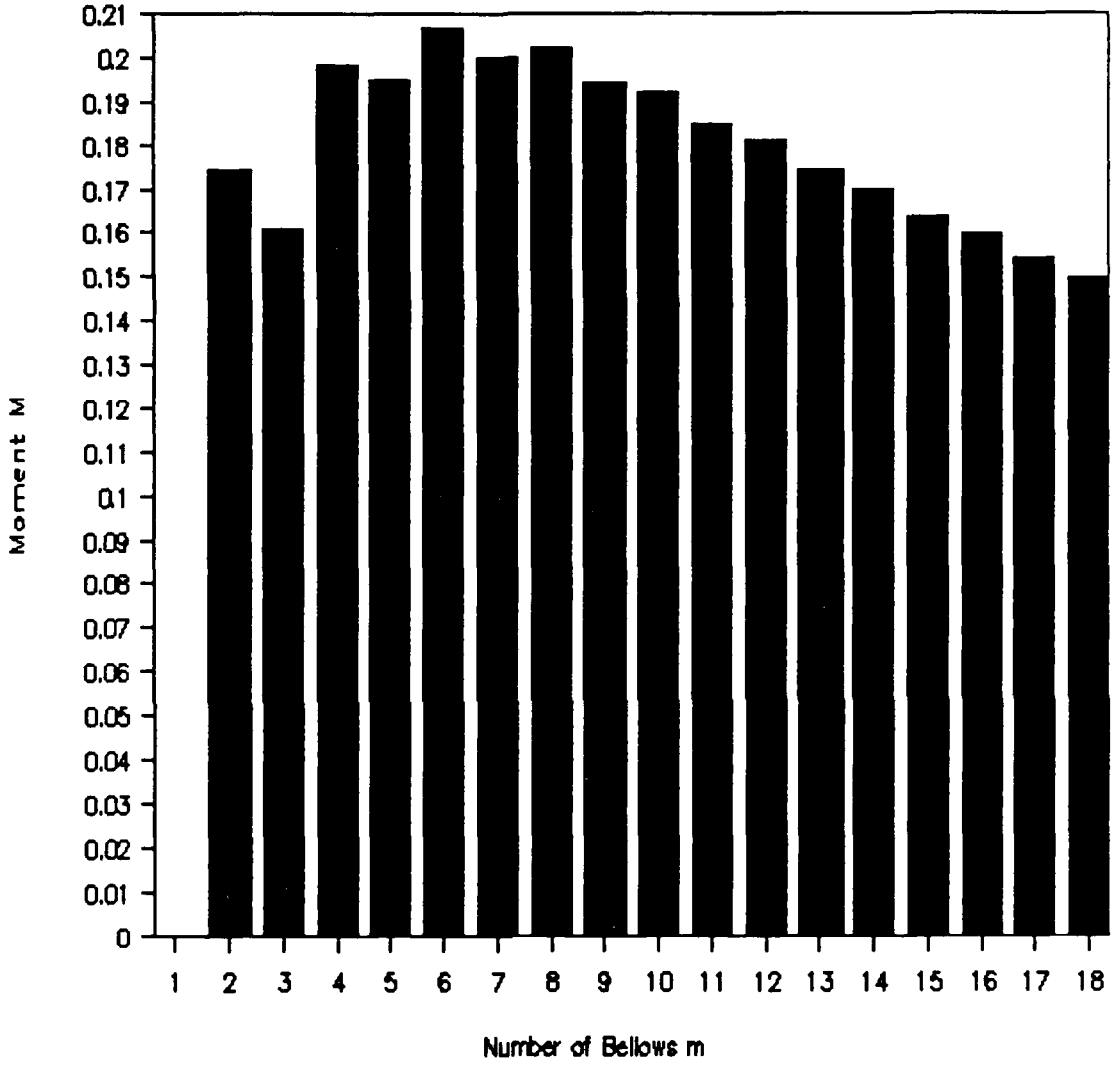

Figure 13: moment in element with unit pressure and outside diameter 2 as a function of number of satellite bellows.

The limb shown in Figure 9 consists of two bending elements, each with six comercially available satellite bellows of dipped latex rubber that surround a central core made of a smooth rubber tube. Successive pressurization of the satellite elements did produce bending about different neutral axes. However, because of the inconsistency of the bellows wall thicknesses, irreparable air leaks occurred even at pressures as low as 10 psi and experiments of a quantatative nature could not be performed.

DESCRIPTION OF THE EXPERIMENTS

The purpose of the experiments was to test the behavior of the elements and to compare their behavior to the results predicted by linear theory. The five types of elements tested were:

1) Uniform bellows gap bending element.
2) Double-sided, uniform gap bending element.
3) Small, optimum bellows gap bending element.
4) Large, optimum bellows gap bending element.
5) Torque element.

Experiments performed on the bending elements were:

1) Measurements of tip deflection under internal pressurization. Internal pressure in the bellows was incrementally increased and the resulting tip deflection measured. No load was applied.
2) Measurements of load capacity. Load at tip was incrementally increased and the pressure required to maintain the tip at zero deflection was measured.
3) These same measurements were made on the double-sided element where the initial pressure p_i in each side was chosen as 4 and then 8 psi.

Experiments performed on the torque element were:

1) Measurments of end rotation under internal pressurization. Internal pressure was incrementally increased and the resulting end rotation measured. No torque was applied.
2) Measurements of torque capacity. Torque applied at tip was incrementally increased and the pressure required to maintain zero end rotation was measured.
3) Measurements of end rotation under torque applied at end. Applied torque was incrementally increased and the resulting end rotation measured. Internal pressure was maintained at 0 psi.

The experimental apparatus used in the bending tests is shown in Figure 14. The tip deflection of each cantilevered bending elements was measured with a depth micrometer with an accuracy of ±0.0005 in. Loads were applied by suspending weights from the tip each element.

The experimental apparatus used in the torsion tests is shown in Figure 15. Pure torque was applied to this element through the system of weights and pulleys. End rotation was determined by measuring the deflection of a rod attached to the end of the torque element.

All elements were pressurized with laboratory air which passed through a regulator that controlled pressure up to 30 psi with an accuracy of ±0.2 psi.

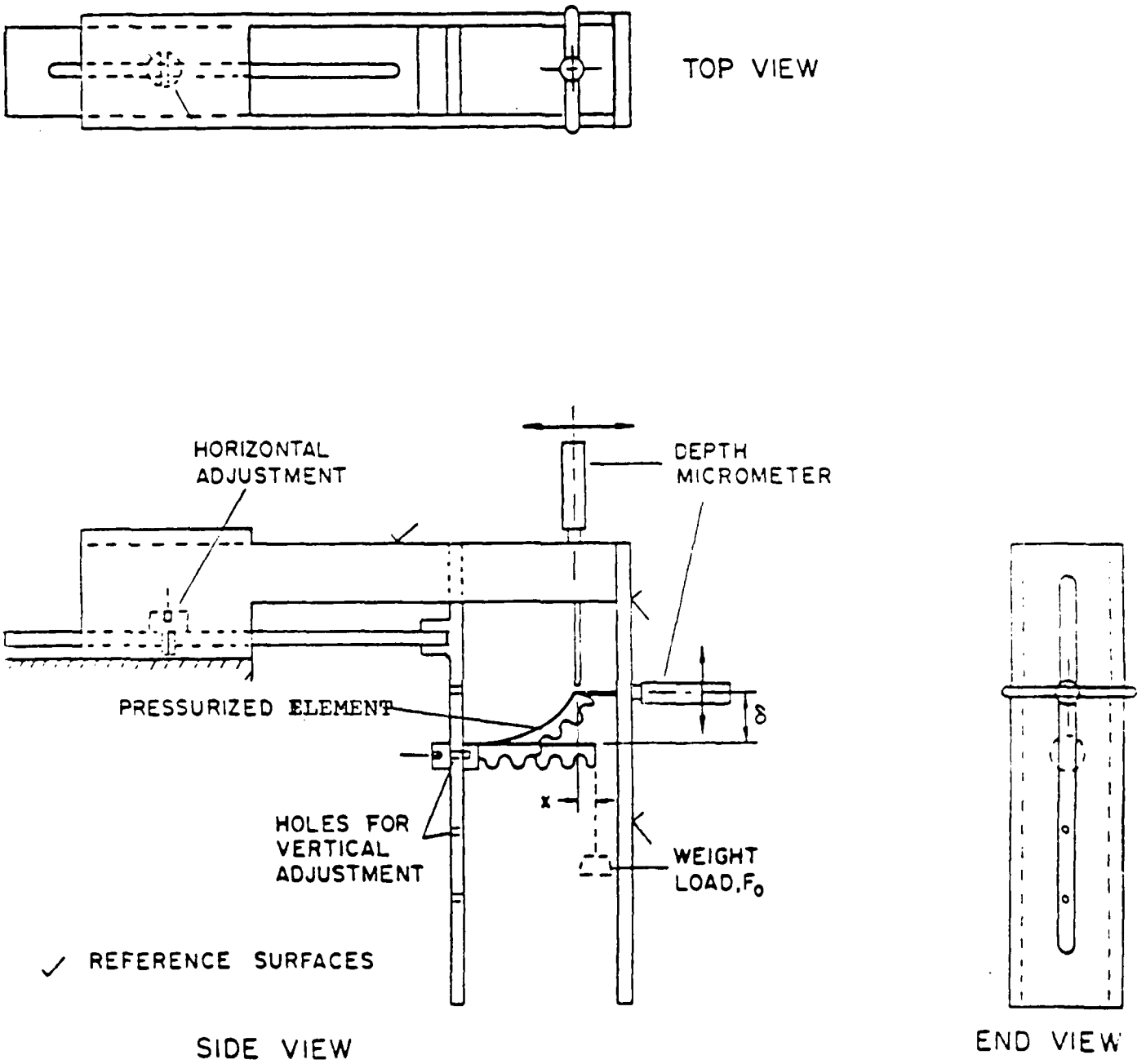

Figure 14: Testing apparatus for bending and torque element static response tests.

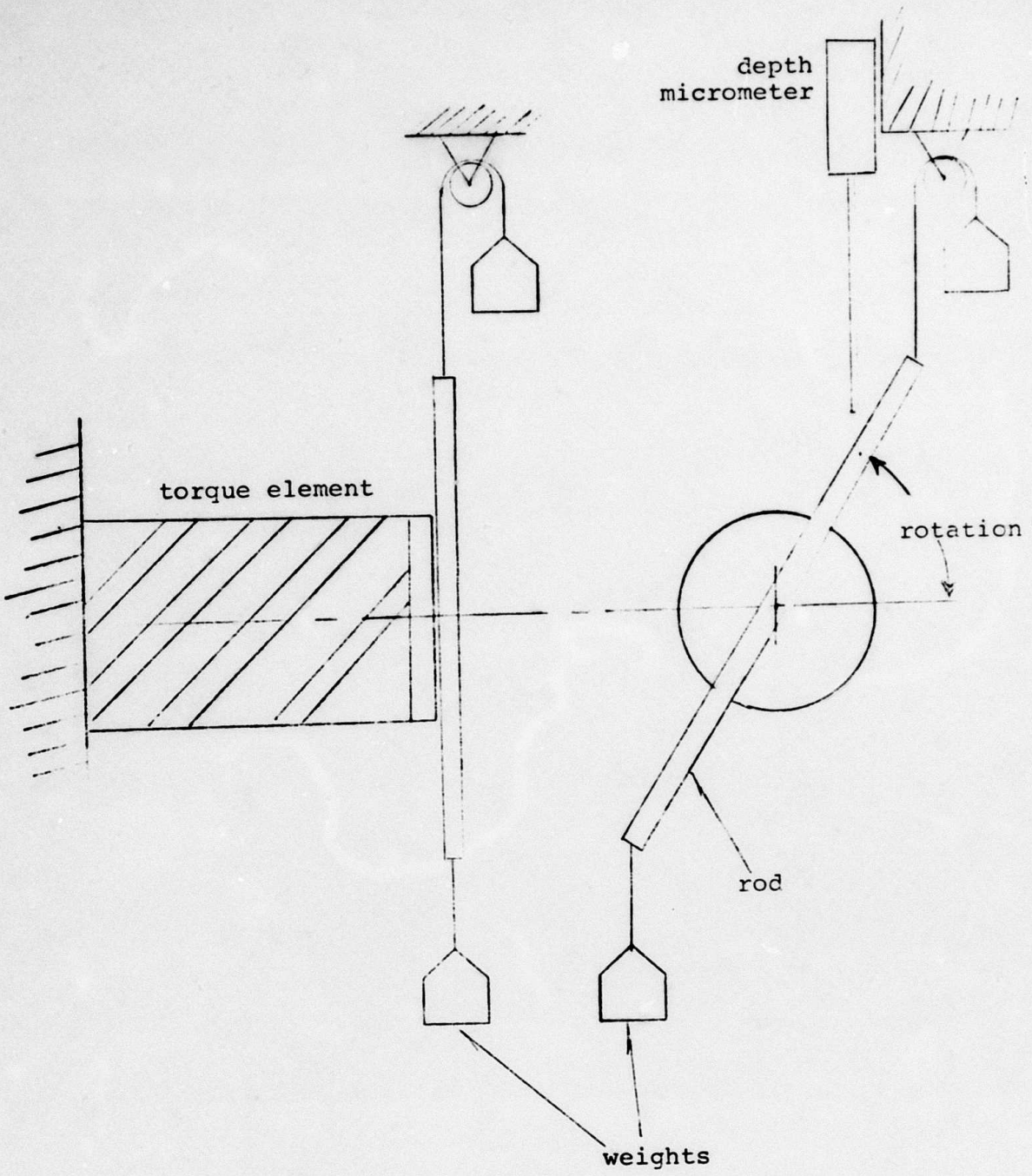

Figure 15: Method of applying pure torque to element and measuring end rotation.

EXPERIMENTAL RESULTS AND COMPARISONS TO THEORY

The test results for the static response of bending and torque elements are graphed in Figures 16-26. Also shown on the graphs are the best-fit lines for the data in the linear range of response of the elements. Their slopes are tabulated in Tables 1 and 2. As can be seen in the graphs, most tests exhibited essentially linear response over a certain range, after which the response became nonlinear.

The results are also compared to predicted behavior. To predict element behavior, bellows stiffnessess were computed using the Haringx model (Wilson, 1984b). The bellows stiffnesses were used to calculate the relationships among pressure, deflection, and end load for the bending elements and among pressure, rotation, and end moment for the torque element. These are also tabulated in Tables 1 and 2, where they are compared to the experimental values.

Program LINDEFL.FOR was used to compute the theoretical values for the bending elements and is listed in Appendix B. Torque element behavior was calculated using results from Wilson and Orgill (1986). Values were computed for both the lower and upper bounds of the range of the material modulus E. For A150B black rubber, experiments show: E = 740 psi if uncycled and E = 2330 psi after cycling.

Bending Element

Deflection/Pressure:

Figures 16-19 show the vertical tip deflection for bending elements subjected to internal pressure. The bending elements initially responded linearly, but the response became nonlinear at higher pressure and deflection. This is to be expected since linear theory is valid only for small deformations.

The slopes of the linear response ranges are listed in Table 1, where they are compared to computed values. From equation (1), we can see that when there is no end load F_0 and no end moment M_0, the vertical tip deflection δ becomes

$$\delta = M_p \frac{L^2}{2EI_b} \tag{13}$$

where M_p is the moment due to the internal pressure p acting over the effective area at the bellows end at a distance from the bellows center to the neutral axis of the beam. The computed values of δ/p based on equations (2)-(7) and (13) are listed in Table 1.

Figure 17 shows the response of the double-sided element for 0, 4, and 8 psi. internal pressure in the opposing bellows. No significant increase in element stiffness was observed with increasing opposing pressure.

Pressure/Load:

Figures 20-23 show the load capacity of the bending

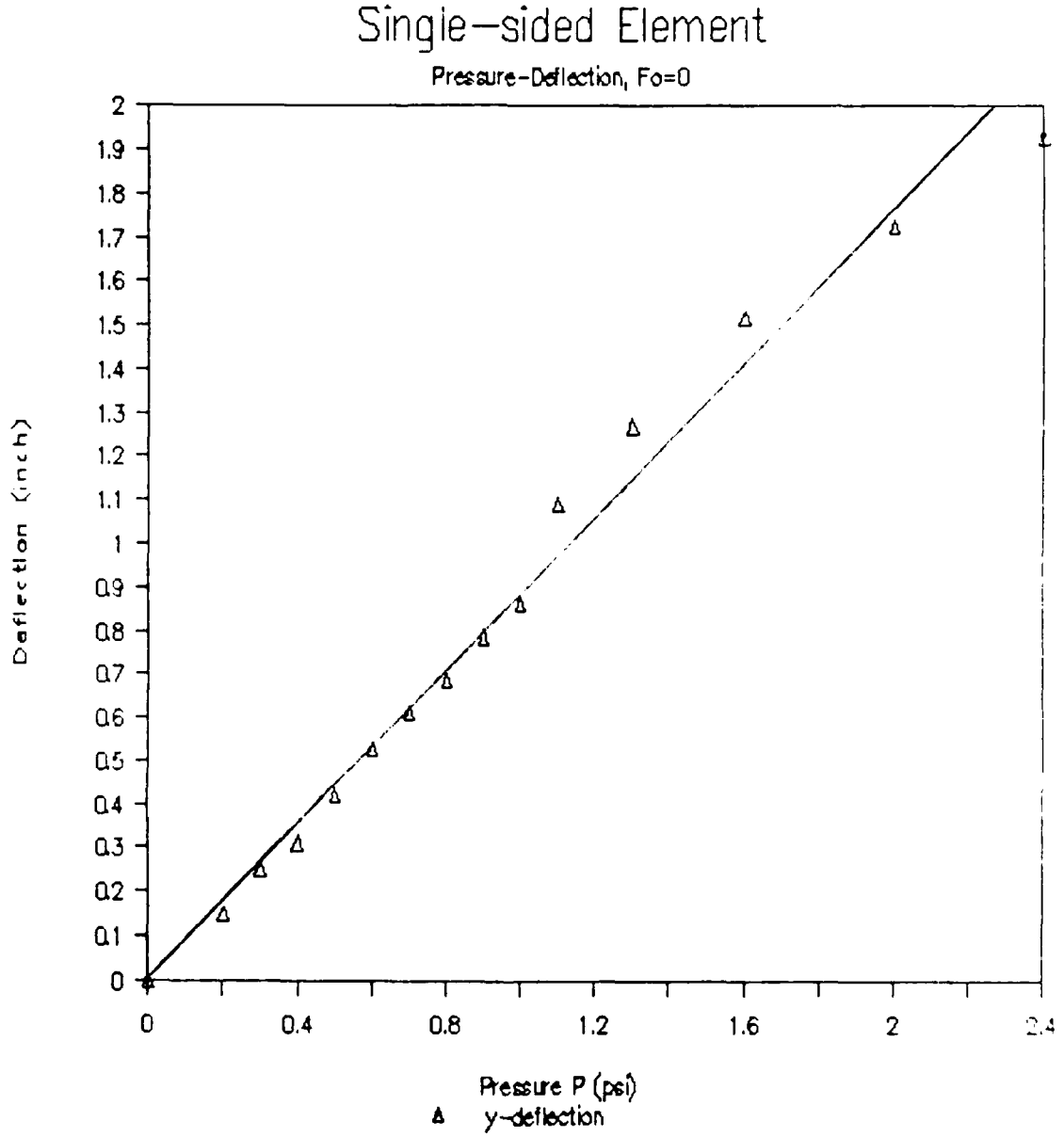

Figure 16: Experimental vertical tip deflection as a function of pressure for single-sided, uniform-gap bending element, with no load at tip.

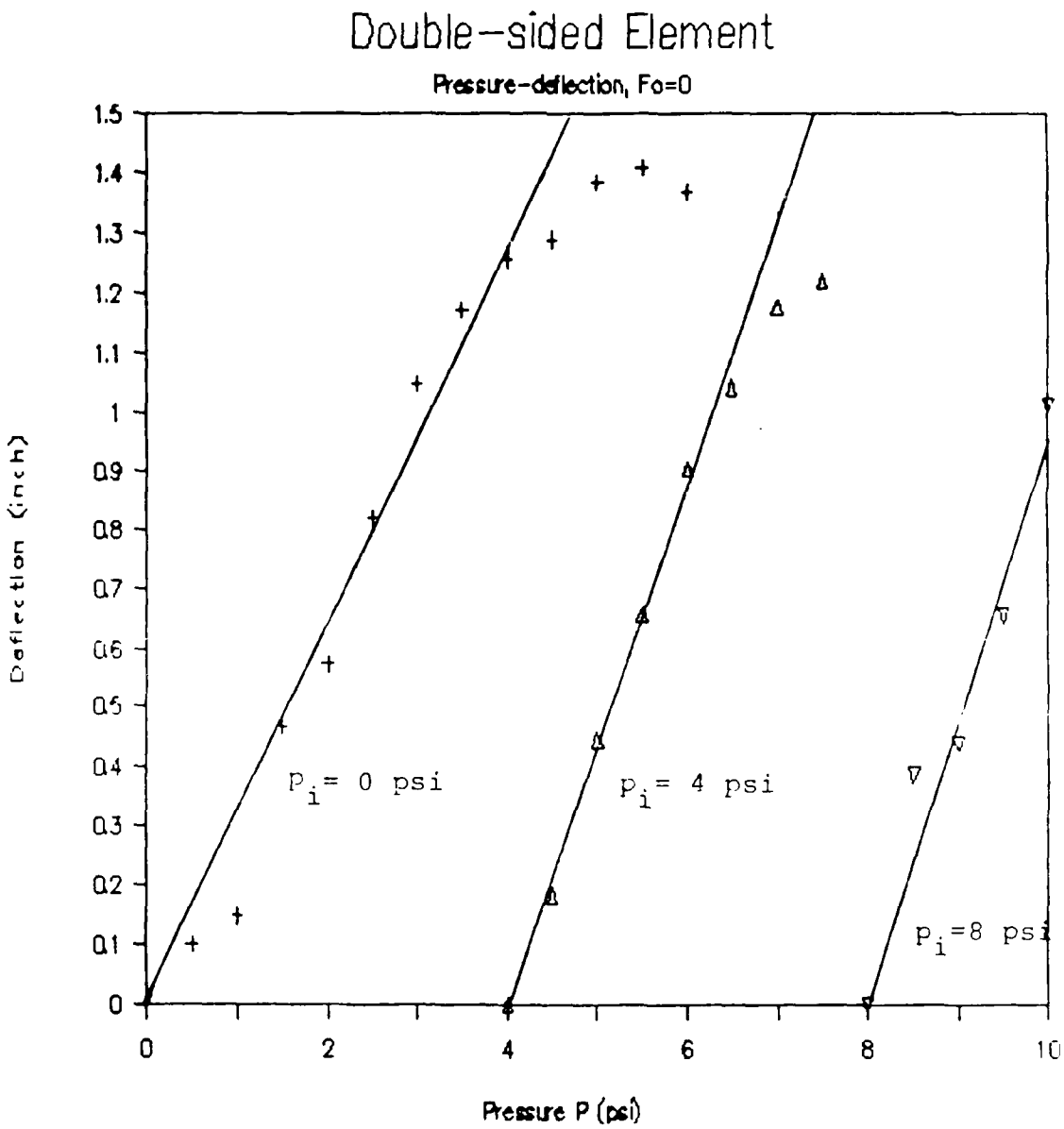

Figure 17: Experimental vertical tip deflection as a function of pressure for double-sided, uniform-gap bending element, with no load at tip, and with pressure in opposing bellows at 0, 4, and 8 psi.

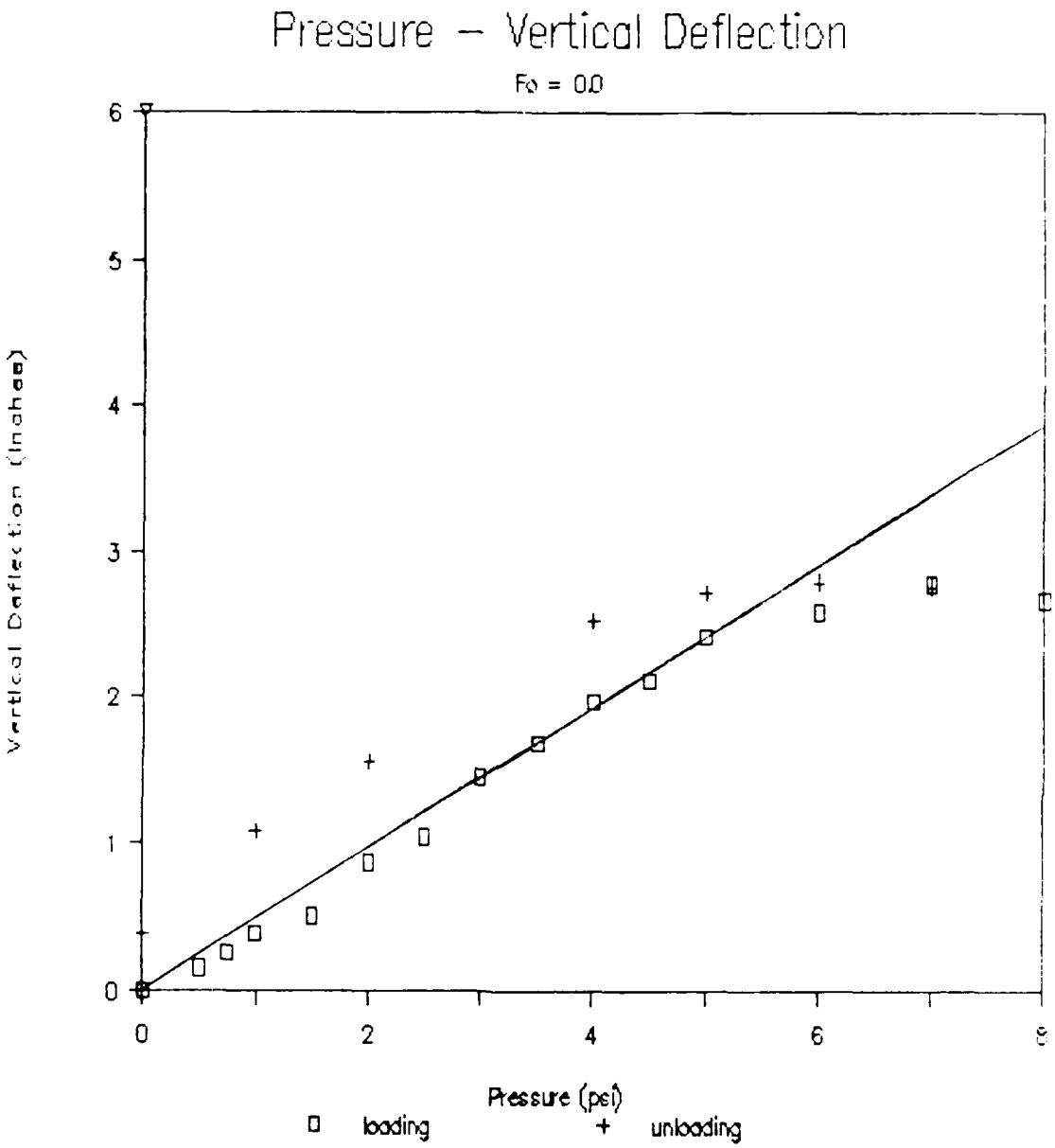

Figure 18: Experimental vertical tip deflection of small, optimum-gap bending element as a function of pressure, with no load at tip. Pressurization and depressurization of element shown.

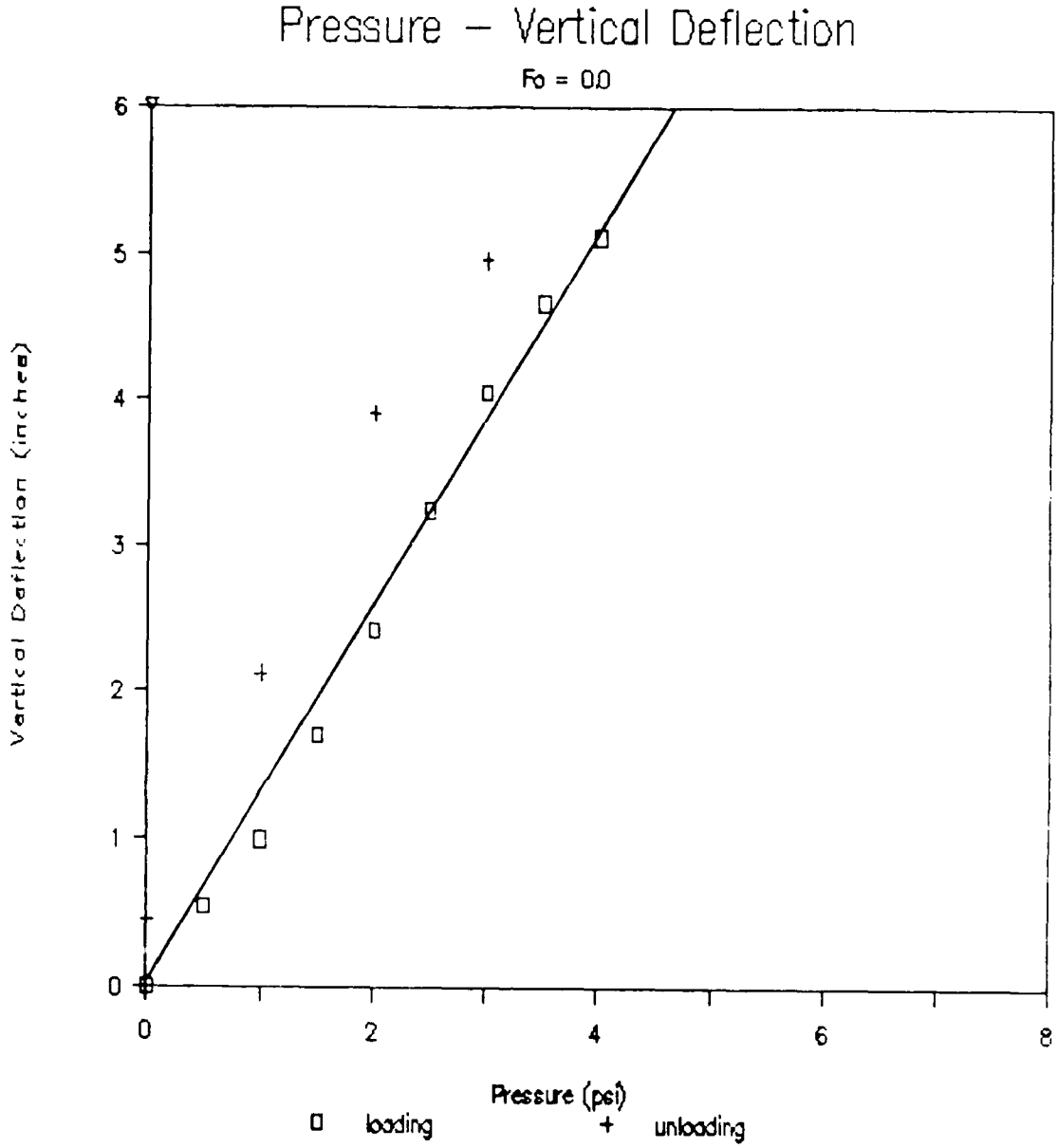

Figure 19 : Experimental vertical tip deflection of large, optimum-gap bending element as a function of pressure, with no load at tip. Pressurization and depressurization of element shown.

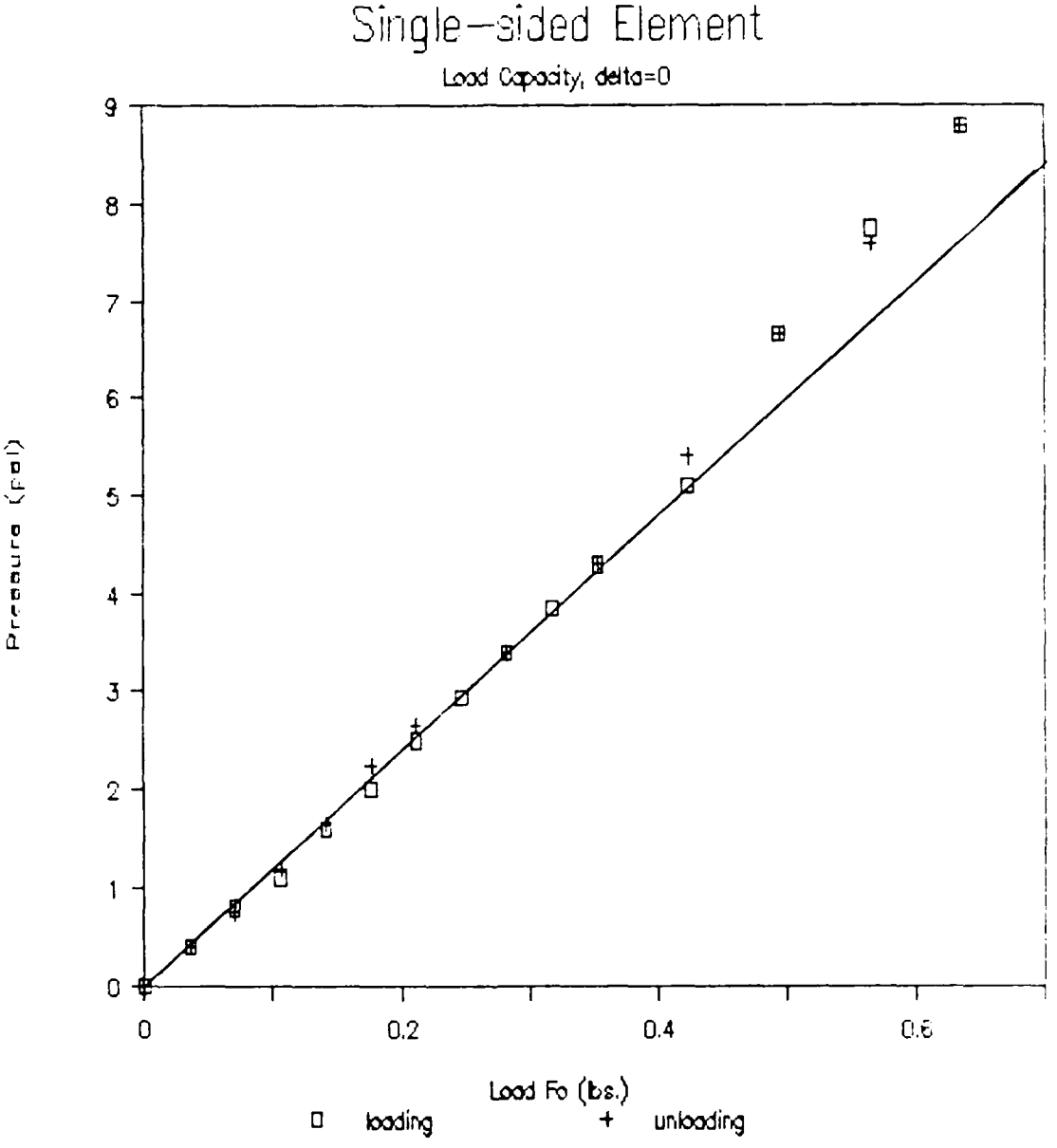

Figure 20 : Load capacity for single-sided, uniform-gap bending element; experimental pressure required to sustain load with zero tip deflection. Loading and unloading of element shown.

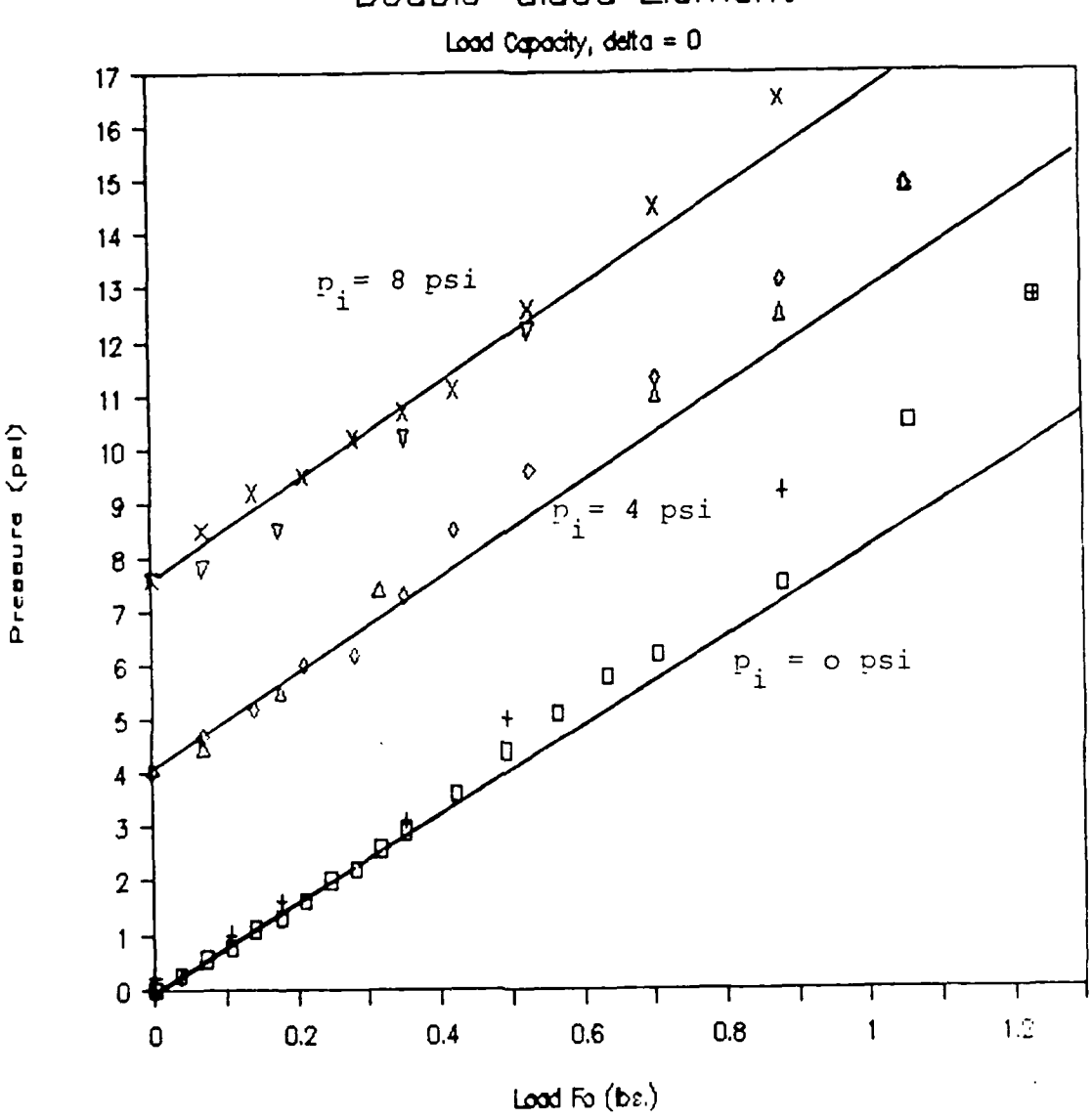

Figure 21 : Load capacity for double-sided, uniform-gap bending element; experimental pressure required to sustain load with zero tip deflection. Pressure in opposing bellows at 0, 4, and 8 psi. Loading and unloading of element shown.

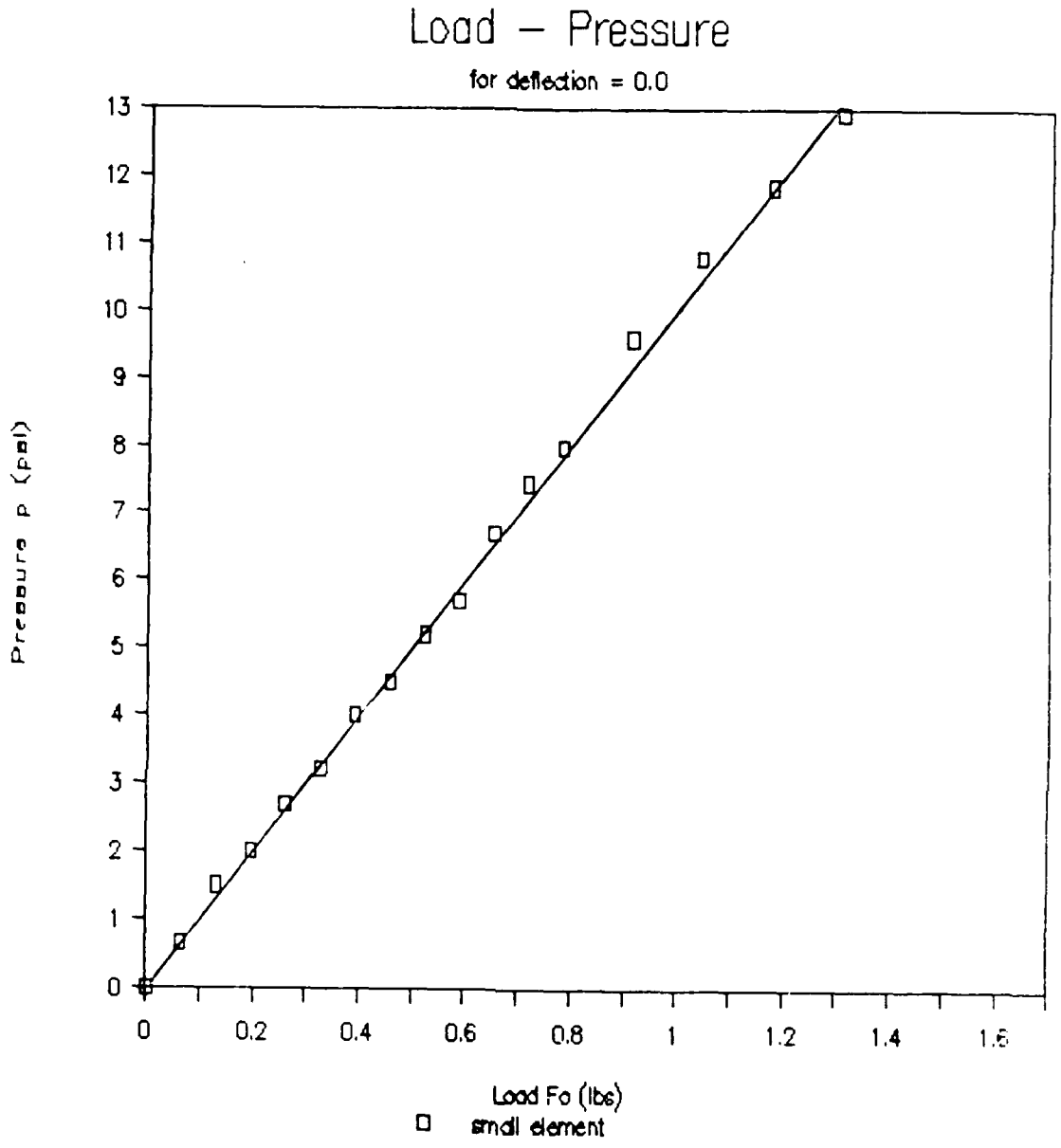

Figure 22: Load capacity for small, optimum-gap bending element; experimental pressure required to sustain load with zero tip deflection.

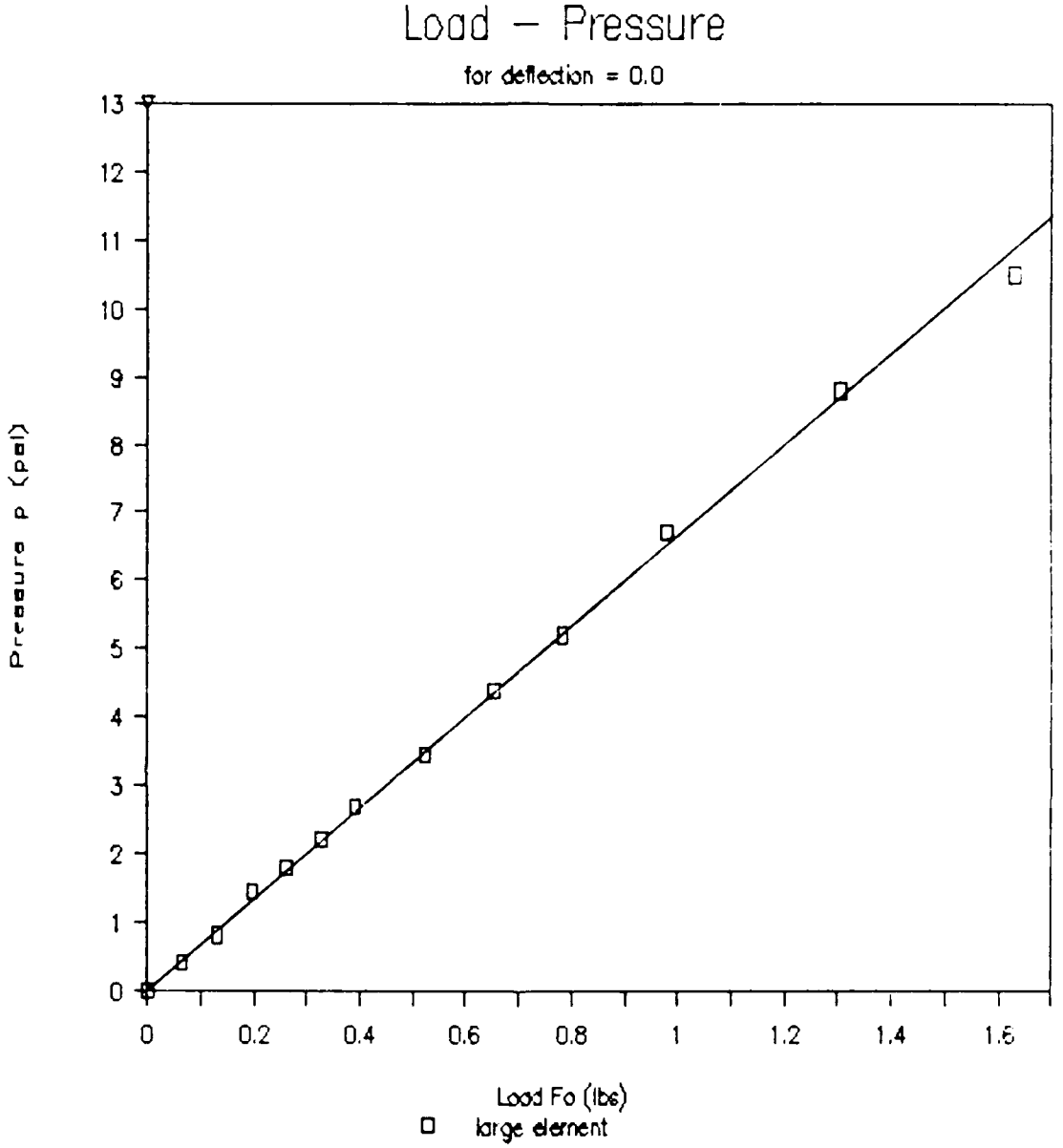

Figure 23: Load capacity for large, optimum-gap bending element; experimental pressure required to sustain load with zero tip deflection.

elements, represented by the pressure required to sustain the load with zero tip deflection. These figures also show the limits of linearity for these elements.

The slopes of the linear response ranges are listed in Table 1 and are compared to computed values. When deflection δ and end moment M_0 are zero, equation (1) becomes

$$\frac{F_0 L^3}{3EI_b} = \frac{M_p L^2}{2EI_b} \tag{14}$$

The computed values of p/F_0 based on equations (2)-(7) and (14) are listed in Table 1. The ratio p/F_0 is computed for a single value rather than a range of values since this ratio is independent of material modulus E.

Torque Element

Figures 24-26 show the results of the torque element experiments. The slopes for the linear range of behavior are listed in Table 2, along with calculated values.

To predict the behavior of the torque element, the ratio of the material modulus to bellows effective modulus E/E' for the bellows was calculated using the Haringx bellows model. The program used was HARINGX.FOR, which is listed in Appendix B. For the torque element tested:

$$E/E' = 6.08 \tag{15}$$

This value was then used with the results of Wilson and Orgill (1986) to predict values of shear strain $\gamma_{\theta z}$ as a function of bellows material and geometric parameters and pressure p and applied end torque T. $\gamma_{\theta z}$ was then used in equation (8) to obtain the desired values. Since our experiments showed that $\epsilon_{zz} << 1$, this quantity was neglected in subsequent calculations for the theoretical behavior of the torque element.

Rotation/Pressure:

The measured end rotation-internal pressure data are shown in Fig. 24. Note the nonlinear response at the higher pressure levels. In the linear range, the slope ϕ/p is 2.88 deg/psi.

The theoretical ratio ϕ/p for this torque element, for $E/E' = 6.08$, is based on the following results given in Fig. 2 of Wilson and Orgill (1986):

$$\gamma_{\theta z} = (3.06)\frac{pR}{Et} \tag{16}$$

where E is the material modulus, t is the bellows wall thickness, and R is the mean bellows radius. With equations (8) and (16) with $\epsilon_{zz} = 0$, the result is

$$\frac{\phi}{p} = (3.06)\frac{L}{Et} \tag{17}$$

Table 2 lists ϕ/p for lower and upper bounds of E.

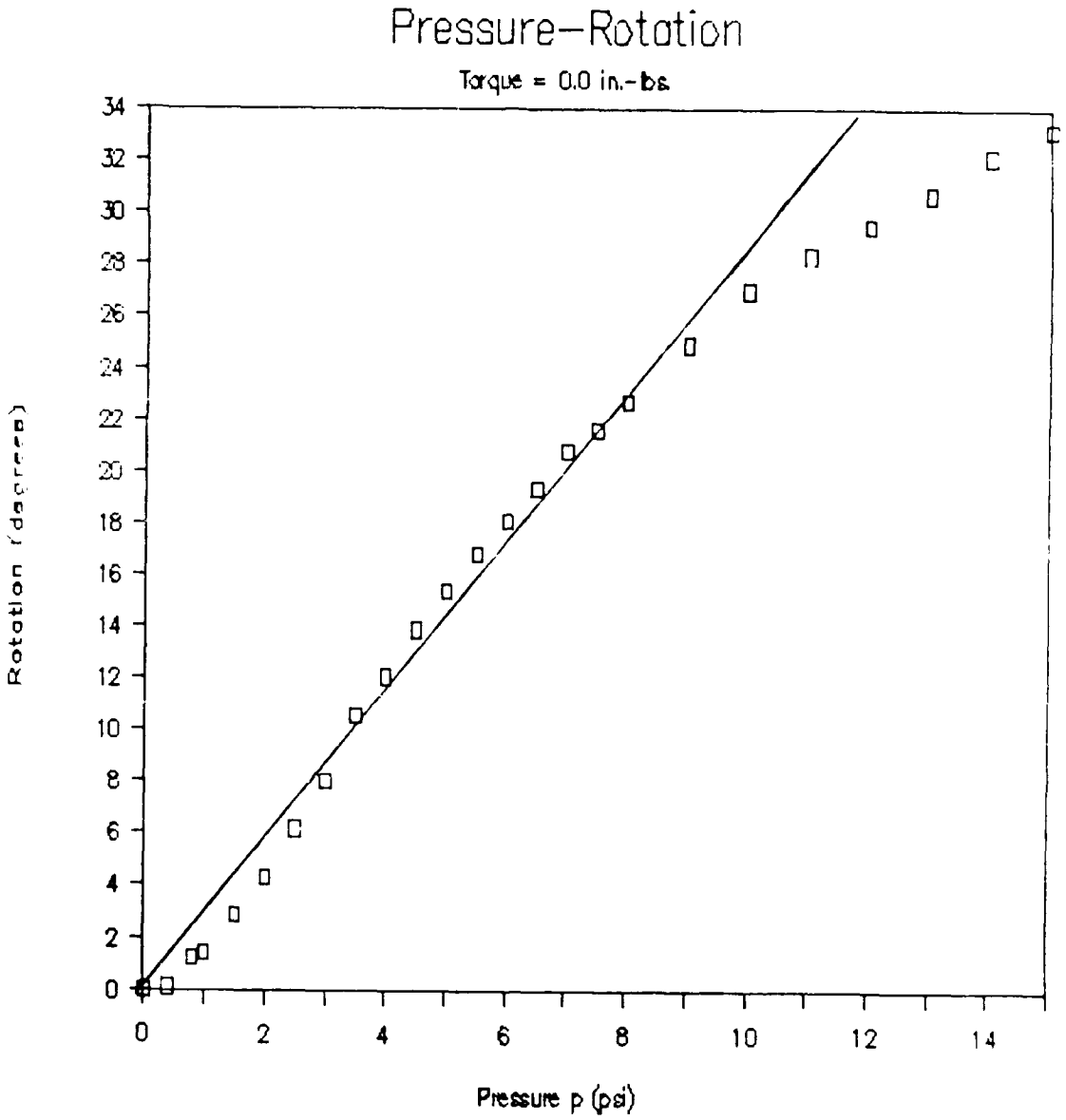

Figure 24: Experimental end rotation of torque element as a function of pressure, with no torque applied at end.

Pressure/Torque:

The measured pressure-torque data for zero rotation of the torque element are shown in Fig. 25. The slope p/T is 2.36 in-lb/psi and is approximately constant up to p = 10 psi.

The theoretical ratio p/T for E/E′ = 6.08, is based on Fig. 9 of Wilson and Orgill (1986), or

$$T = (3.68)pR^3 \tag{18}$$

Solving for T/p,

$$\frac{T}{p} = (3.68)R^3 \tag{19}$$

where T/p is independent of E. Here, R = 0.5 in. which gives p/T = 2.17.

Rotation/Torque:

The measured rotation-torque data are shown in Fig. 26. Here, the response is nearly linear for positive rotations up to 10 deg (rotations following the helix direction); and up to 20 deg for rotations in the opposite direction.

The shear strain-torque relationship, based on Fig. 4 of Wilson and Orgill (1986), is

$$\gamma_{\theta z} = (0.83)\frac{T}{EtR^2} \tag{20}$$

Substituting into (8) and solving for ϕ/T, where $\epsilon_{zz} = 0$, the result is

$$\frac{\phi}{T} = (0.83)\frac{L}{EtR^3} \tag{21}$$

Table 2 lists ϕ/T the lower and upper bounds of E.

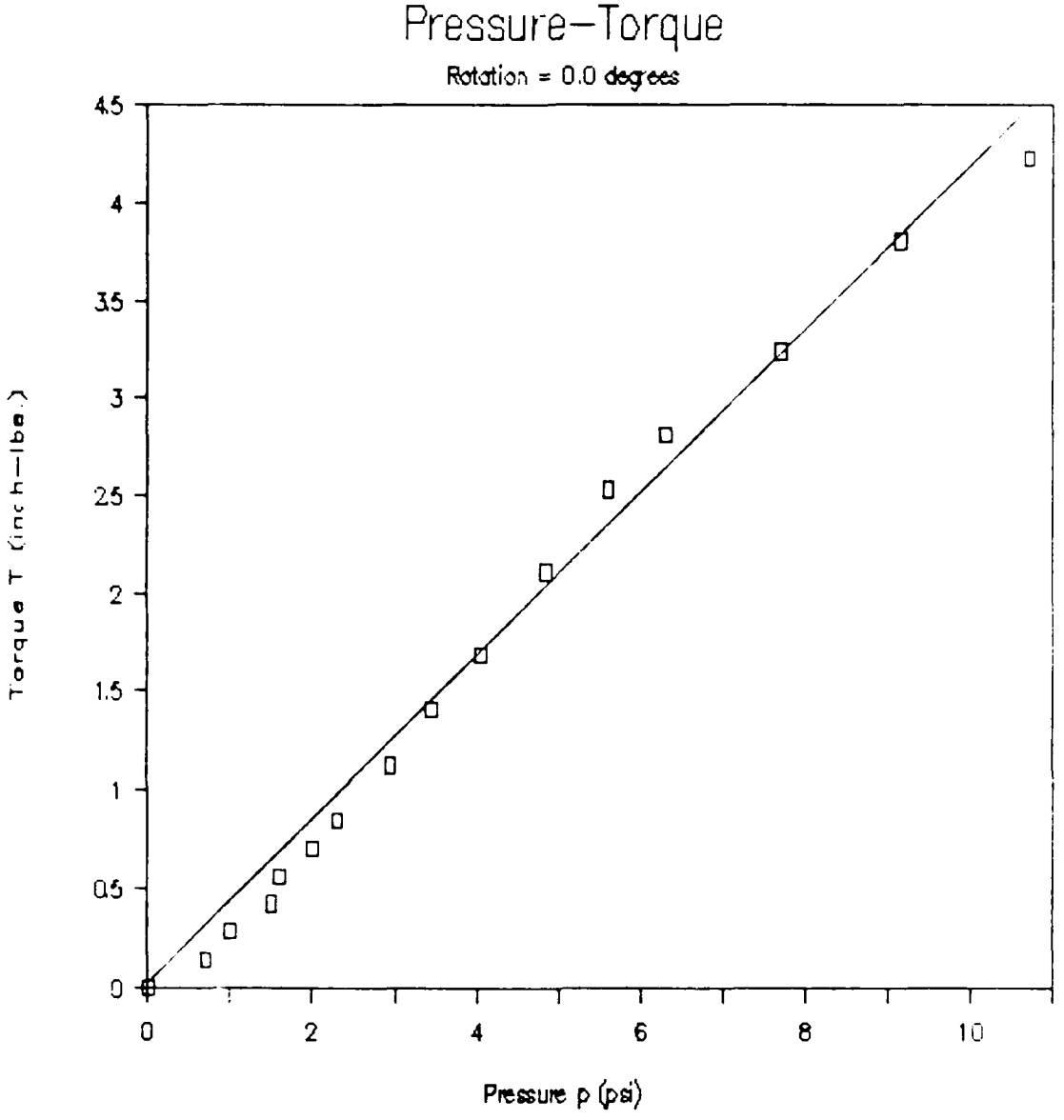

Figure 25: Torque capacity of torque element; experimental pressure required to sustain torque with zero end rotation.

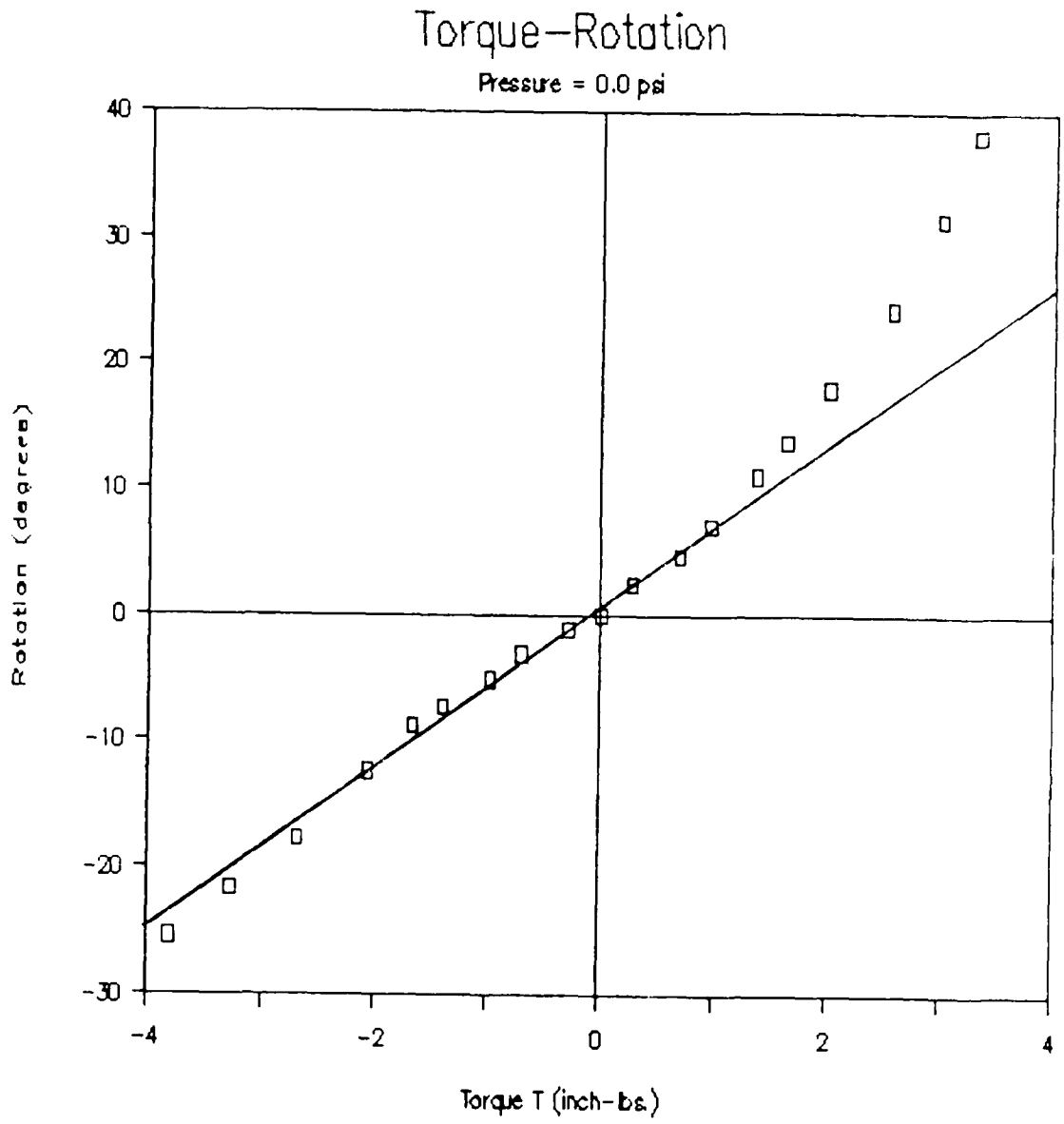

Figure 26: Experimental rotation of torque element as a function of torque applied at end, with zero internal pressure.

Table 1

BENDING ELEMENTS
Summary of Experimental and
Theoretical Behavior

Element	Test Performed	Experimental Behavior	Theoretical Behavior (E = 740 to 2330psi)	Units
single-sided	deflection/ pressure	$\delta/p = 0.884$	1.389 to .4411	in/psi
	pressure/ load	$p/F_0 = 12.0$	9.042	psi/lb
double-sided	deflection/ pressure	$\delta/p = 0.326$	.6280 to .1994	in/psi
	pressure/ load	$p/F_0 = 8.07$	9.042	psi/lb
small optimum	deflection/ pressure	$\delta/p = 0.481$	.9963 to .3164	in/psi
	pressure/ load	$p/F_0 = 10.1$	8.084	psi/lb
large optimum	deflection/ pressure	$\delta/p = 1.31$	2.671 to .8483	in/psi
	pressure/ load	$p/F_0 = 6.64$	3.526	psi/lb

Table 2

TORQUE ELEMENT
Summary of Experimental and
Theoretical Behavior

Element	Test Performed	Experimental Behavior	Theoretical Behavior (E = 740 to 2330psi)	Units
torque element	rotation/ pressure	$\phi/p = 2.88$	6.95 to 2.21	deg/psi
	pressure/ torque	$p/T = 2.36$	2.17	psi/in-lb
	rotation/ torque	$\phi/T = 6.50$	15.1 to 4.77	deg/in-lb

CONCLUSIONS

Our measured ratios deflection/pressure (for bending elements) and rotation/pressure (for torque elements) fell within predicted limits. As Tables 1 and 2 show, these experimental ratios always fell between the predicted upper bound based on E = 2330 psi for the cycled rubber, and the lower bound based on E = 740 psi for uncycled rubber. In general, the measured ratios were closer to the theoretical values based on the upper bound modulus.

Our studies of the ratios pressure/load and pressure/torque involved no element deformations and therefore were independent of the elastic moduli. For three of the four bending elements, the measured ratios pressure/load were higher than those predicted by theory. For the torque element, the measured pressure/torque ratio was within nine percent of that predicted by theory.

Our mathematical models that predict the mechanical behavior of bending and torque elements rely on linear theory and a knowledge of the following quantities: Young's modulus, the shear modulus, and Poisson's ratio for the material; the loading including the internal pressure; and element geometry. Our experiments herein serve to validate these mathematical models and show that they may be used with confidence in designing bending and torque elements.

REFERENCES

Ghattas, J.N., "Mechanics of Flexible Robotic Manipulator Elements," Masters Thesis, Civil Engineering Dept., Duke, University, (1988).

Haringx, J.A., "Instability of Bellows Subjected to Internal Pressure," Phillips Res. Rep. 7, 189, (1952).

Wilson, J.F., "Robotic Mechanics and Animal Morphology," NATO ASI Series, Vol. F11, Robotics and Artificial Intelligence, Springer-Verlag Berlin Heidelberg, (1984a).

Wilson, J.F., "Mechanics of Bellows: A Critical Survey," Int. J. Mech. Sci., Vol 26, No. 11/12, pp. 593-605, (1984b).

Wilson, J.F., "Material Properties and Mechanics of Pneumoelastic Bending Elements," Lord Corporation Report, (1986).

Wilson, J.F., and Orgill, G., "Linear Analysis of Uniformly Stressed, Orthotropic Cylindrical Shells," Journal of Applied Mechanics, Vol. 53, pp. 249-256, (1986).

Chapter III

CONTROL OF FLEXIBLE MANIPULATOR ARMS

James F. Wilson, Zhenhai Chen, and Rhett T. George, Jr.

INTRODUCTION

Flexible, corrugated tube elements made of black rubber or polyurethane are designed to bend when subjected to internal pressure. A typical configuration is shown in Figure 1. Analyses and experimental tal investigations of such elements were carried out by Wilson and Li (1987), who emphasized the control of two elements in parallel acting as a gripper. Multiple elements in series such as shown in Figure 2 can also be employed as manipulator arms. Previous analyses of such arms were made by Mahajan (1985) and Palaniappan (1986) who showed their feasibility. The purpose of the present investigation is to evaluate these arms experimentally.

The success of such an arm as a fast acting, smoothly operating manipulator depends on its pressure control system. This chapter describes the overall experimental system, two methods of pressure control, and typical experimental results. The experimental system consists of a pneumatic control module, an I/O board, a microcomputer, appropriate software, and the corrugated tube arm elements. The first of the two methods of element pressure control is based on timed sequencing: the valve-on condition in which air is admitted continuously until the desired element pressure level is reached; and the valve-off condition. The second method of element pressure control is based on pulsing the pressure of the admitted air. Both control methods are open-loop. The experiments involve using these methods, together with computer programs that specify different pressure-time histories for the arm elements, and then observing the speed and smoothness of arm and gripper motion. In a typical experiment, the gripper at the end of the arm grasps the payload from a lower platform, the arm lifts the load, places it on a higher platform, and returns to its original position without mishap. Experiments show that the fastest time for a 50 cm long arm to complete such a cycle is approximately five seconds.

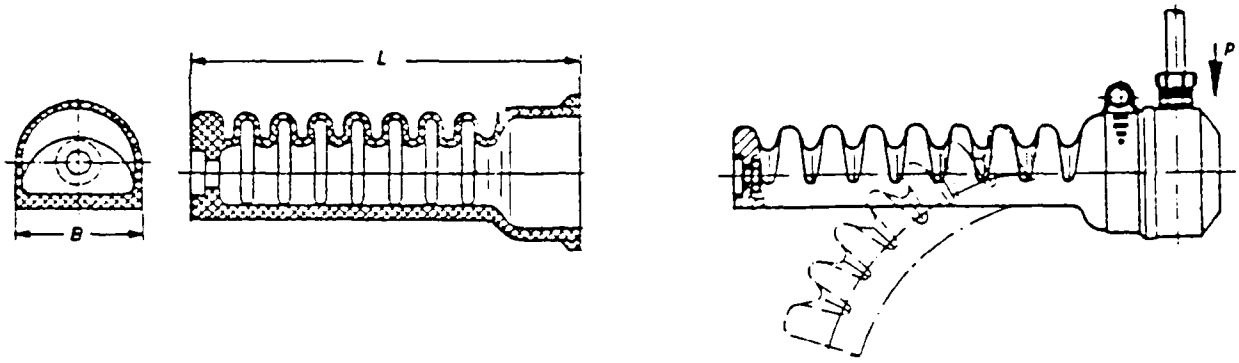

ELEMENT TYPE	DIMENSIONS (mm)	
	B	L
A-1, A-2	40	130
B-1, B-2	28	92
C-1, C-2	20	65

Figure 1 - The polyurethane SIMRIT finger, U.S. Patent No. 3,981,528, September, 1976.

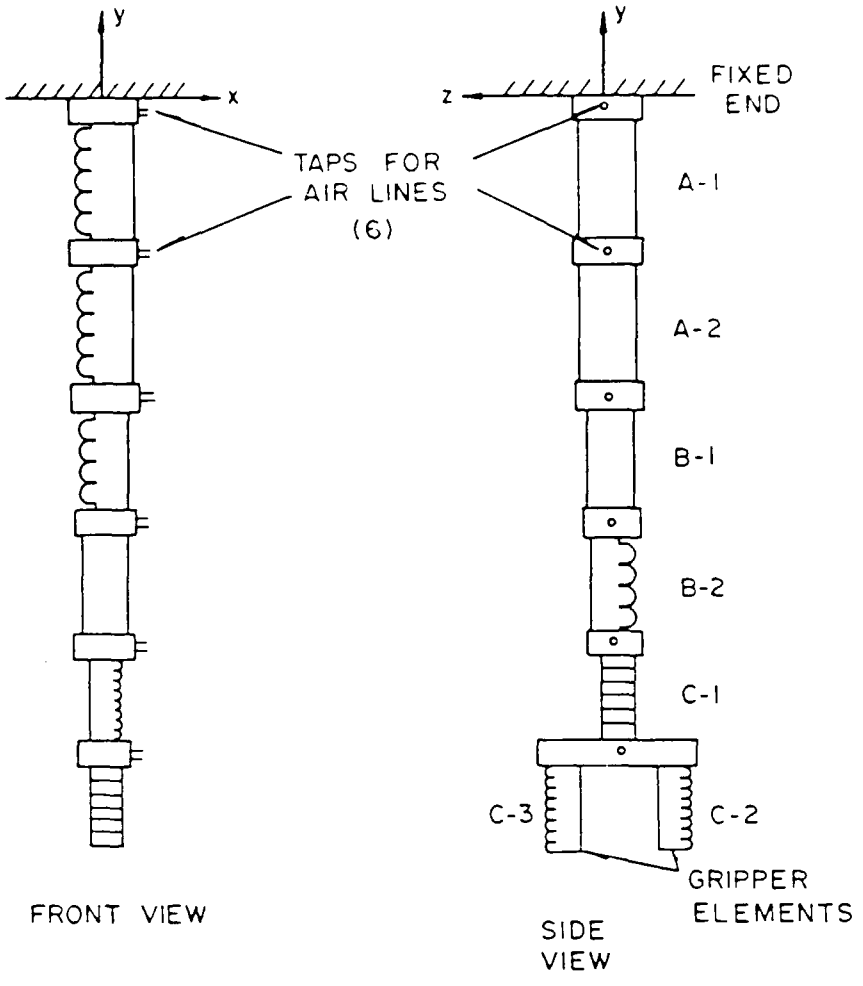

Figure 2 - First generation manipulator arm and gripper configuration.

MANIPULATOR ARM AND GRIPPER DESIGN

The first generation arm and gripper system was built with seven commercially available polyurethane bending elements. The outside dimensions of these component elements (three sizes) are shown in Figure 1; and the manipulator design is shown in Figure 2. The arm, which resembles somewhat the trunk of an elephant in both its outward form and manipulative function, is clamped at the top and hangs vertically when unpressurized and at rest. The largest elements, A-1 and A-2, are at the clamped end and these elements sustain the highest arm moments when the pressurized arm with the payload at the gripper is displaced from the vertical equlibrium position. In terms of the Cartesian coordinate system defined in Figure 2, arm elements A-1, A-2, B-1, and C-1 are aligned to bend in the x,y-plane; but element B-2 is aligned to bend in the y,z-plane. The latter element is effective in avoiding collisions of the arm with obstacles in the x,y-plane. Each arm element is a distinct pressure cell and has its own air supply line connected to the pneumatic control module. The two opposing elements of the gripper, however, have a common air supply.

Consider the mechanics of this manipulator system. When air pressure is increased in a particular element, its bellows portion expands and the element bends about its neutral axis located within its flat side. See Figure 1. As demonstrated by Wilson and Li (1987), the amount that a given element bends is proportional to both its internal pressure and its external end loads. Thus, for the manipulator arm to function properly, it is apparent that the internal pressure supplied to each of its elements must be of sufficient magnitude to overcome the opposing forces of the payload, the self weight of the arm and gripper, and the elastic resistance of the element material. Mahajan (1985) and Palaniappan (1986) studied the interrelationships among these system parameters and their results were used in the present study to estimate the element pressure levels required for practical manipulations of the experimental arm.

A typical pick-and-place maneuver cycle was chosen to evaluate

arm performance, especially to determine the shortest possible cycle times consistent with smoothness of arm motion. A photograph of this typical maneuver, taken with stroboscopic light, is shown in Figure 3. Here, the gripper is pressurized and grasps an object from the lower platform; the arm elements are selectively pressurized to lift the object to an upper platform while avoiding a collision with it; the gripper is depressurized and the object is released; the arm elements are repressurized to raise the arm somewhat; and then all elements are depressurized as the manipulator returns to its initial vertical equlibrium position. Of course, other maneuver cycles are also possible, including the retrieving of the object from the upper platform. What follows are descriptions of the experimental system used to achieve these maneuvers and discussions of typical experimental results.

CONTROL MODULE AND I/O BOARD

The control module contains 12 solenoid valves, five needle valves, 1/4 in. diameter flexible tubing and connectors for the fluid circuit, and the necessary electronics for interfacing the control module with a microcomputer. Each of the five arm bending elements and also the gripper has an independent fluid circuit with two solenoid valves: one for air intake control and one for exhaust control. The needle valve in each of the arm element fluid circuits is used to adjust both the intake and exhaust flow rate of the air. Figures 4 and 5 show the fluid circuit and the electronic circuit, respectively, for a bending element. In a typical arm maneuver, the intake air pressure for each of the arm elements is preset to a regulated value of 40 psi. However, the intake pressure for the gripper is preset at a higher pressure such as 70 psi to insure a sufficient gripping force.

The I/O board, a commercially available Techmar Lab Tender, was installed in an IBM pc-XT microcomputer. This board has the capabilities of performing four main functions: analog to digital conversion, digital to analog conversion, digital input-output control, and timing/counting. The digital to analog conversion and counting

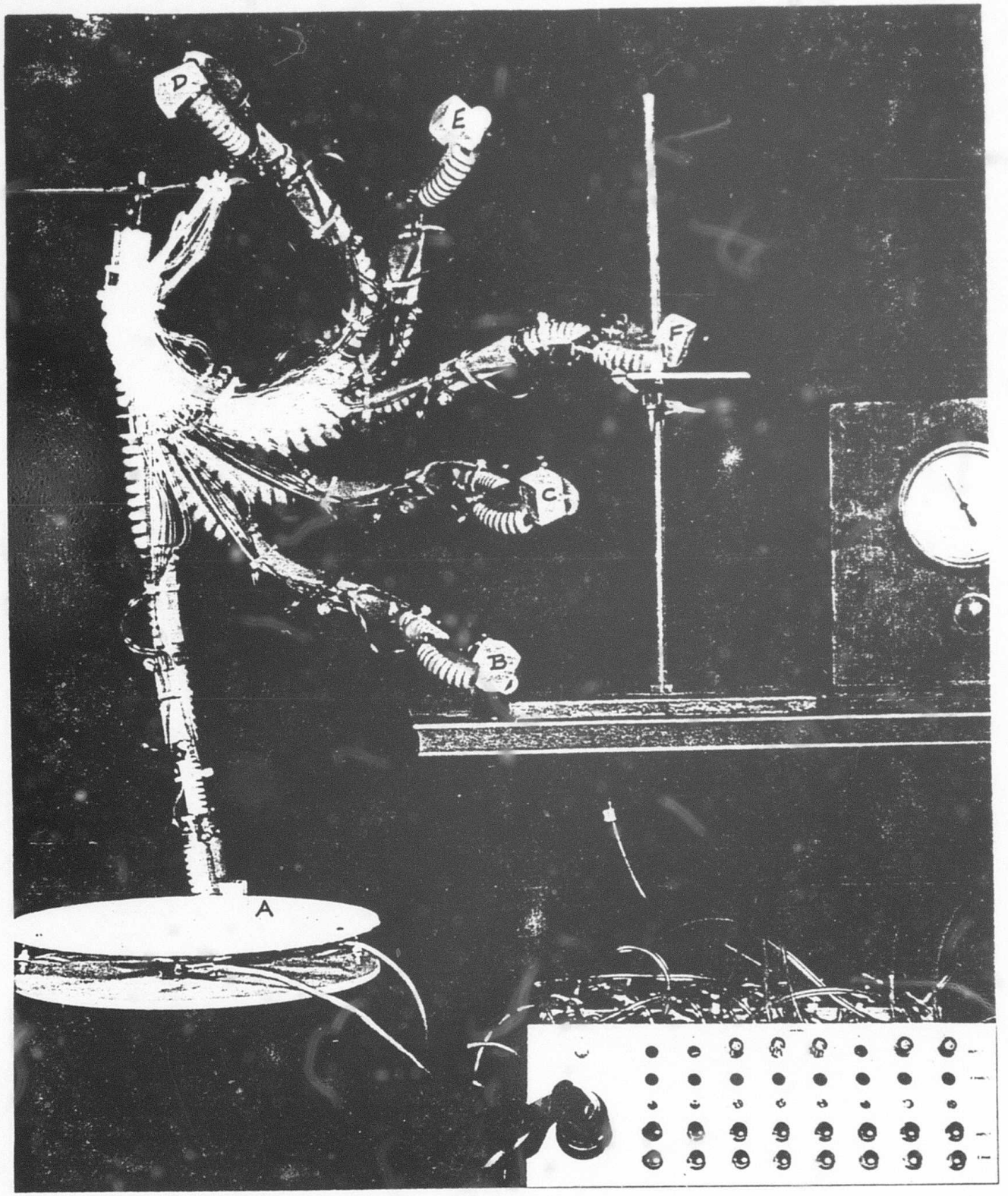

Figure 3 - Typical pick-and-place arm maneuver: A, pickup point; B,C,D,E, lifting cycle; F, placement on upper platform.

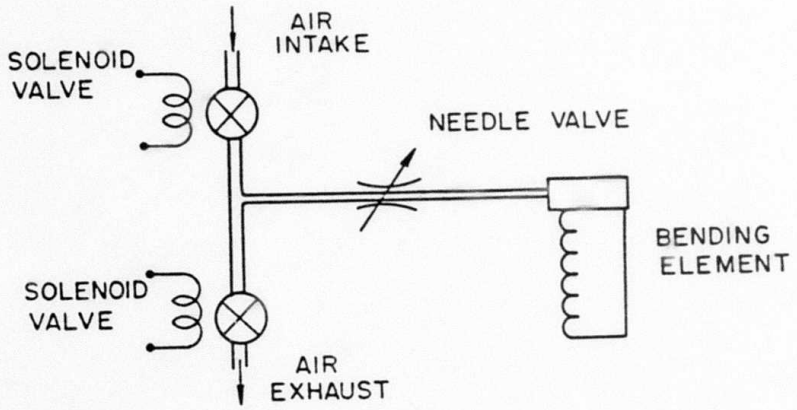

Figure 4 - Fluid circuit for control of a single element.

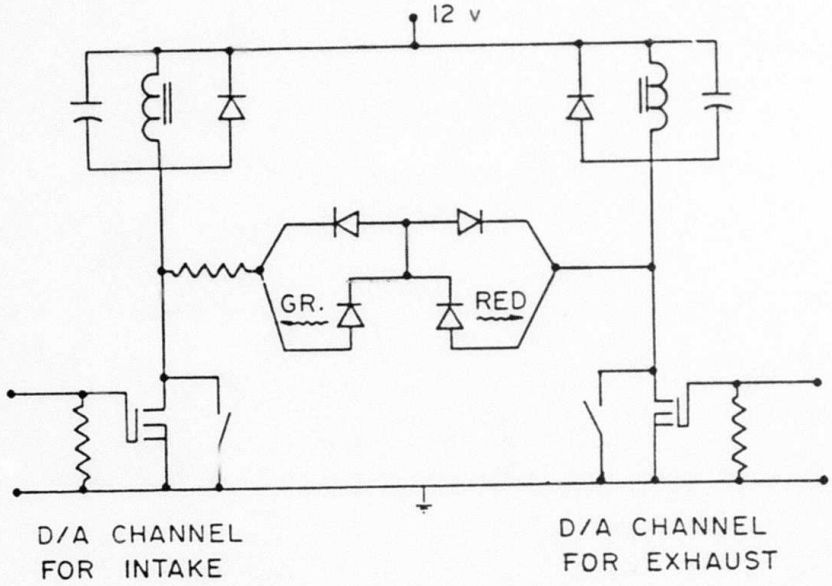

Figure 5 - Electronic circuit for D/A control of air intake and exhaust.

features of this Lab Tender board were utilized to develop system software for arm and gripper motion control. Two successful software control schemes were developed and these are discussed next.

SOFTWARE CONTROL SCHEMES

It became quite apparent in the early stages of this research project that a computer was needed to control the pressurized air to drive the arm. For instance, when an operator regulated the flow of air to the arm elements by manually pushing buttons to activate the solenoid valves, smooth arm motion could not be achieved. Even after some practice at hand control, an operator could not decrease to any significant extent the unwanted arm oscillations in attempting maneuvers such as depicted in Figure 3. Thus, computer controlled schemes were devised with a goal of achieving such a maneuver cycle in 10 seconds or less with motion as smooth as possible.

Early experiments on the system components, the solenoid valves and the individual bending elements, showed that their response times were sufficiently small: 12 milliseconds for the solenoids and no longer than one second for the largest bending element (type A) to fill with air and bend a full 90 degrees. A 0.3 sec response time was measured for elements B and C (Wilson, 1986).

With a knowledge of the solenoid valve and bending element response times, two open-loop software control schemes were developed to achieve the pick-and-place maneuver of Figure 3. The first control scheme is the timed sequencing method. For example, Figure 6 depicts the time sequences during which the intake and the exhaust solenoid valves are open to drive the pressure elements. The second control scheme is the pulsing method. Figure 7 shows the general form of this control signal for an intake or exhaust solenoid valve in which the valve is open during the pulse time interval and closed during the pulse gap interval. The desired arm motion is achieved by fixing the pulse time, the pulse gap, and the number of pulses for each solenoid valve in the system. To implement these two control schemes, the D/A converter and the timer of the Lab Tender were programmed as discussed in the following two sections.

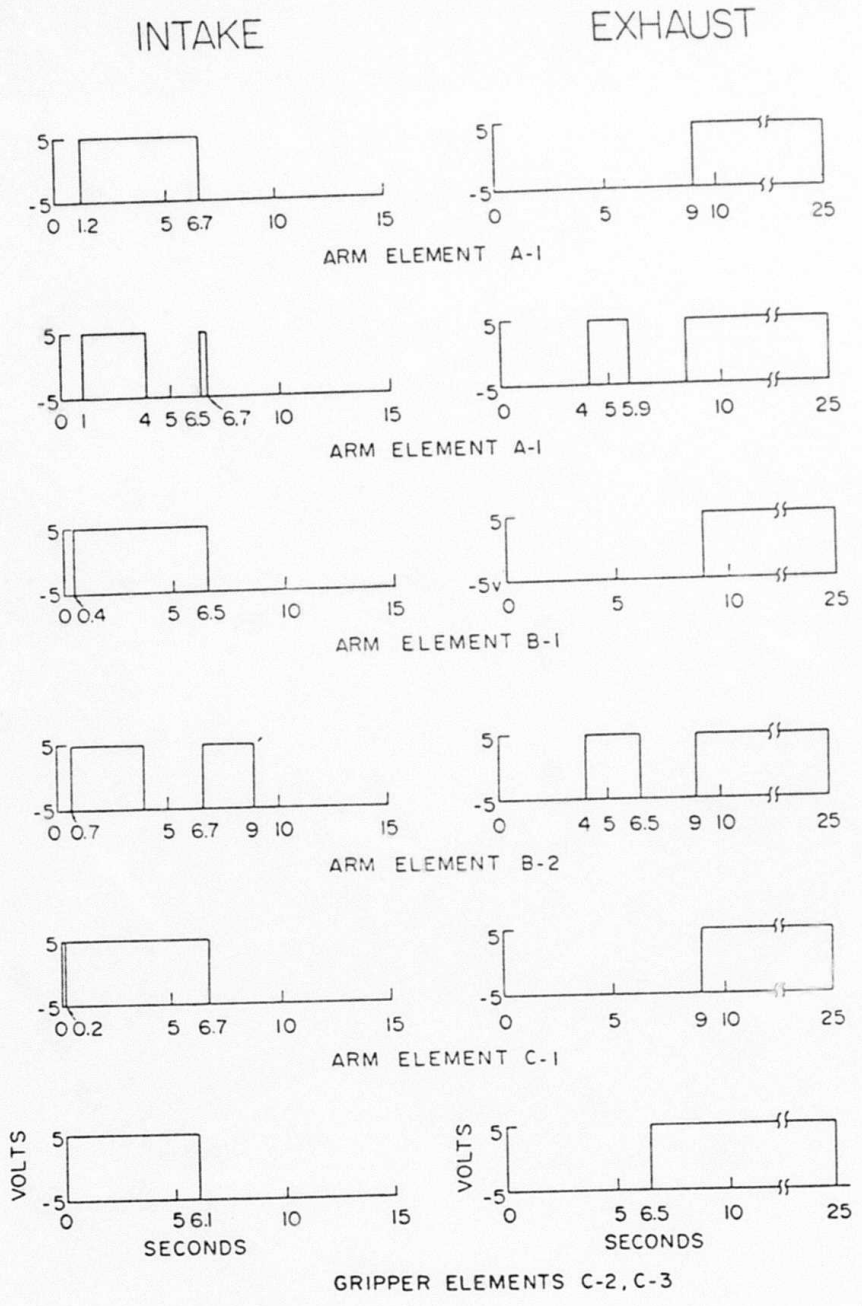

Figure 6 - Timed sequencing for a typical arm maneuver.

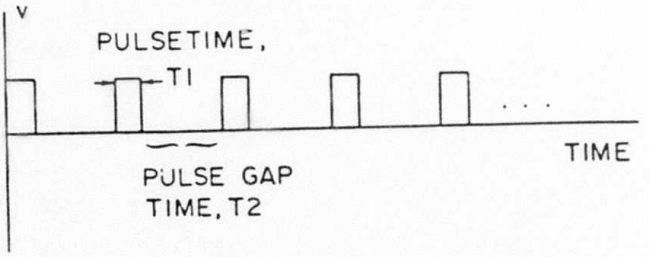

Figure 7 - Definition of the control signal for the pulsing method.

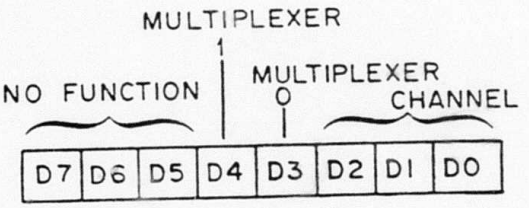

Figure 8 - Bit assignments for the D/A multiplexer control.

PROGRAMMING THE D/A CONVERTER

To operate the D/A section of the Lab Tender, the following sequence of commands are used.

1.Select a voltage to be output. The voltage is in offset binary which means that binary 0000 0000 equals -5.00 V, binary 1000 0000 equals 0.00 V, and binary 1111 1111 equals +4.96 V. Therefore, each increment of one bit increases the voltage by 0.04 V. The base address of the Lab Tender board is 816 and the address of the D/A data is BASE+5=816+5=821. Thus, a command to send +4.96 V out is (in BASIC):

```
10  OUT 821,255
```

2. Enable the channel for the previously selected voltage to be output on. The D/A converter has 16 channels divided equally among two multiplexers. Multiplexer 0 controls channels 0-7 while multiplexer 1 controls channels 8-15. The eight bit binary code is set up so that D0-D2 selects either channels 0-7 or 8-15, D3 either enables or disables multiplexer 0, D4 enables or disables multiplexer 1, and D5-D7 have no function. Figure 8 shows these bit assignments. Note that 0000 1001=9 enables multiplexer 0, channel 1, and that 0001 0011=19 enables multiplexer 1, channel 10. The multiplexer control address is located at 816+4=820. The previous two statements are programmed as:

```
20  OUT 820,9
30  OUT 820,19
```

3. Disable the multiplexers. This must be done between channel changes and D/A data changes or glitching may occur. To disable multiplexer 0, D3 must be 0, and to disable multiplexer 1, D4 must be 0. Therefore, outputting 0000 0000=0 disables both. This command is:

```
10  OUT 820,0
```

To illustrate the command sequence, consider the following program that outputs +4.96 volts on channels 0 and 9 and then outputs -5.00 volts on channels 1 and 10.

```
10   OUT 821,255          D/A +4.96 V
20   OUT 820,8            ENABLE CHANNEL 0
30   OUT 820,0            DISABLE MULTIPLEXER
40   OUT 820,17           ENABLE CHANNEL 9
50   OUT 820,0            DISABLE MULTIPLEXER
60   OUT 821,0            D/A -5.00 V
70   OUT 820,9            ENABLE CHANNEL 1
80   OUT 820,0            DISABLE MULTIPLEXER
90   OUT 820,18           ENABLE CHANNEL 10
100   OUT 820,0           DISABLE MULTIPLEXER
```

The output channels of the D/A multiplexers are sample/hold amplifiers that drift to their most negative voltages if they are not refreshed. Figure 9 shows the result of enabling a channel with +4.96 V, disabling it in the very next line of the program, and allowing it to drift to its most negative voltage. This channel was connected to a control module valve and the time and voltage at which the valve closed is shown as the circled coordinate in Figure 9.

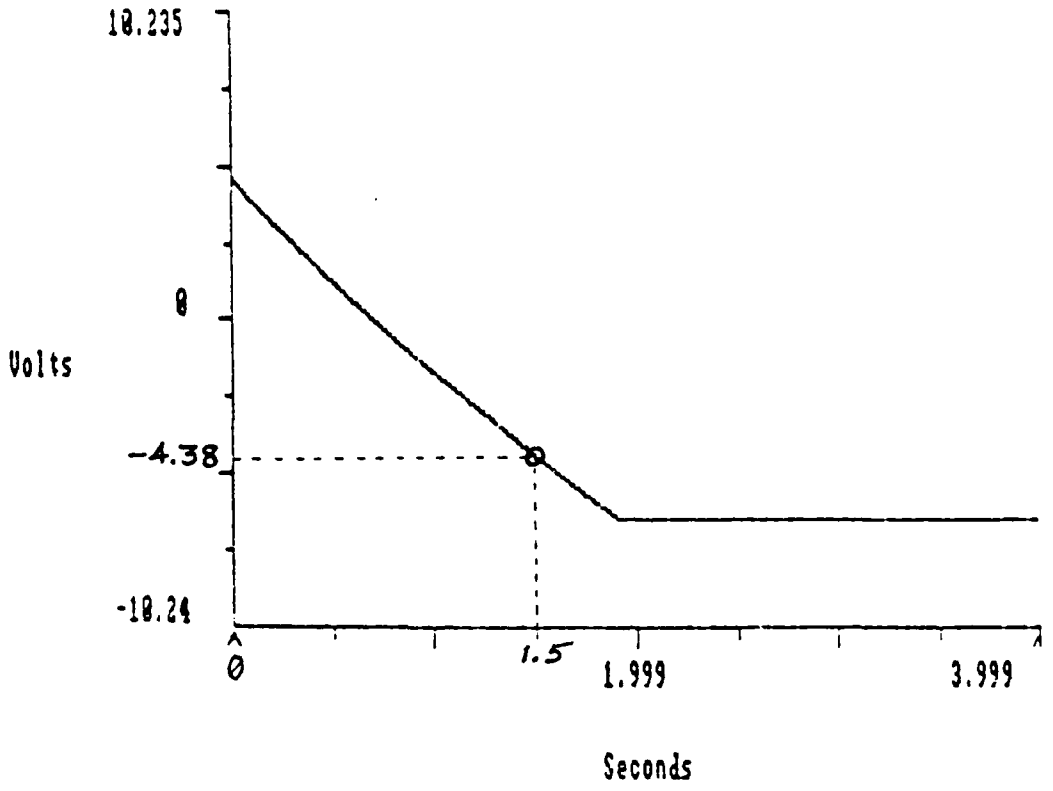

Figure 9 - Response of the D/A channel showing the valve cutoff point and drift to constant voltage.

PROGRAMMING THE TIMER

The timer in the Lab Tender uses an AM9513 System Timing Controller with five general-purpose, 16-bit counters, and internal oscillator and frequency scaling circuitry. Summarized below are the commands utilized in the timing controller in the present study.

1. Declare the maneuver cycle time.
2. Start the timing sequence.
3. Use programmed loops to check the current time and compare it to the time a given event should occur, such as turning a valve on or off.
4. Use programmed forward branching. If the timer value is greater than the desired event time, the program branches ahead to the desired subroutine for turning on or off the designated valves.
5. Use programmed backward branching. If the timer value is less than desired event time, the program branches back to the previous subroutines until the next event occurs. This procedure refreshes the sample/hold amplifiers in the D/A converter.

Just as the D/A data has an address of 821 and the D/A multiplexer has an address of 820, the timer has a Data Port at address 824 and a Command Port at address 825. Basically, the Command Port establishes where information from the Data Port should go. To set up the timer for a particular mode of

operation, the program must first set the Master Mode register, which consists of a 16 bit command code with bits assigned as shown in Figure 10. Since the IBM PC operates with an 8 bit bus, the command must be an input command for two consecutive statements. Of concern here is bit MM15, which is for scalar control; and bit MM14, which is for Data Pointer control. This program uses Binary Coded Decimal so MM15 is 1. The Data Pointer control is used to enable a sequencing mechanism when reading into or writing out of specific locations in the timer.

In the present application, the internal oscillators' frequency of 1 MHz was divided by 10,000 and counted by one of the five counters. Each counter has a Mode register, a Load register, and a Hold register. The Mode register establishes whether the counter counts up or down, repetitively or once. Its other functions are not used. The Load register contains the value that the counter will count to. In this application, the frequency coming in is 1 MHz/10,000=100 Hz. Thus, if the maneuver cycle time is set at 15 sec., the Load register contains 1500 counts. The Hold register is used to save the value in the counter without interupting the counting process. This value is read by the computer and compared to the preset time that a particular event is scheduled to occur.

The sequencing referred to above deals with the manner in which the Data Pointer accesses the Mode, Load, and Hold registers. If MM14 is a 1 in the Master Mode Register, the Data Pointer will increment through the registers as shown in Figure

11.

The bit assignment for the Counter Mode Register is shown in Figure 12. In the present application, the counter mode was set so that the Count Source Selection was F5, which divided the internal oscillator's frequency of 1 MHz by 10,000. The counter reloads from the load register each time, it counts once until armed again, and it counts down. The counting is done in the Binary Coded Decimal.

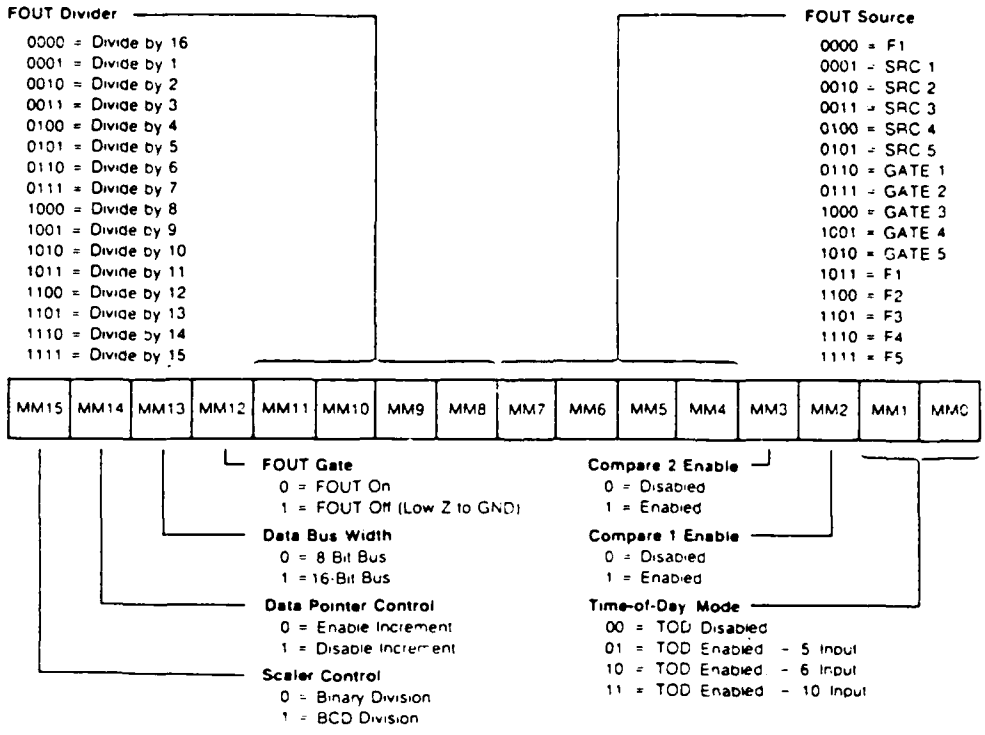

Figure 10 - Bit assignments for the master mode register.

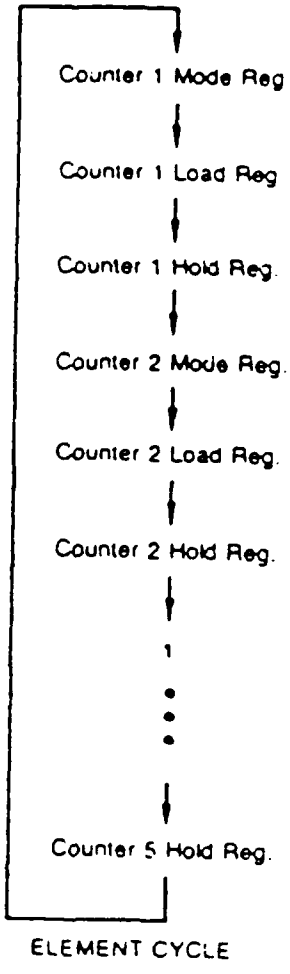

Figure 11 - Increments of the data pointer in an element cycle.

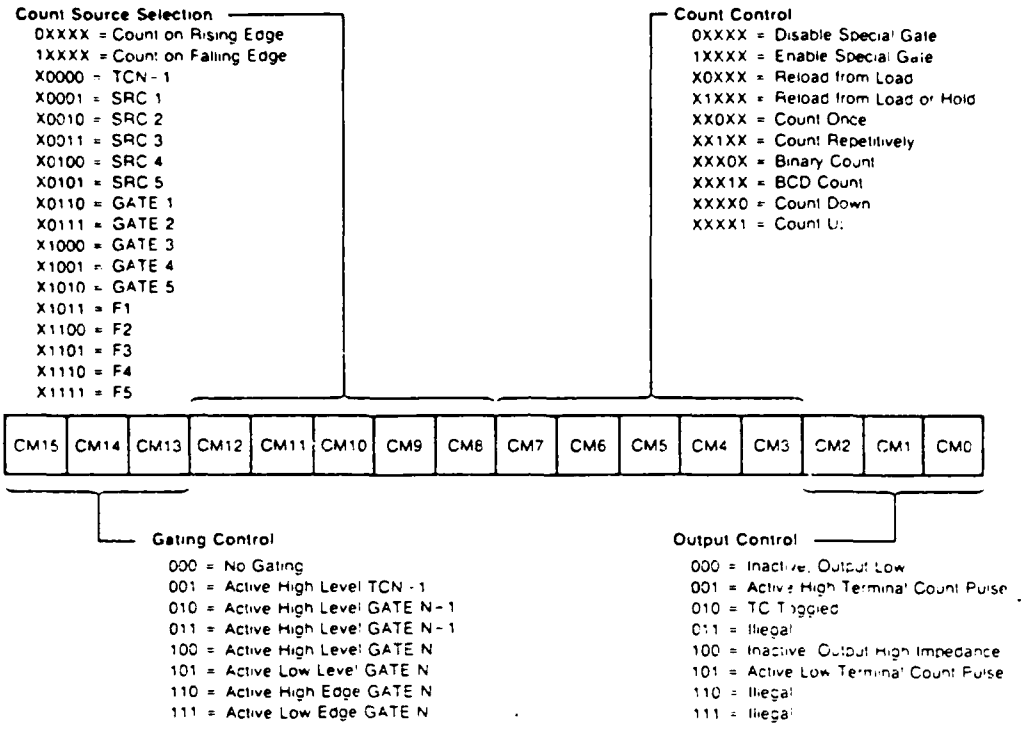

Figure 12 - Bit assignments for the counter mode register.

EXPERIMENTAL RESULTS AND DISCUSSION

For the manipulator arm and gripper defined in Figures 1 and 2, a series of experiments were performed to achieve the pick-and-place maneuver shown by the photograph of Figures 3. The coordinate system for this work space is defined in Figure 13. The manuevered object was a wood cube with an edge dimension of 2.54 cm., initially oriented with its sides parallel to the coordinate planes, with its cg located at position X = Y = Z = 0. After the gripper grasped the cube from this location on the lower platform, the arm deposited the cube at the target point on the upper platform, position X = 47 cm., Y = 49 cm, and Z = 5 cm., and the arm returned to its initial vertical position. The total time for this maneuver is defined as the cycle time T. The performance of the manipulator and the two control methods were evaluated on the following bases: qualitative observations of the smoothness of arm motion; quantatative data on the amplitude and frequency of arm motion at the end of the maneuver; measures of the deviations ΔX, ΔY, ΔZ from their respective target points; and the change in rotation $\Delta\theta$ of the cube about the Y-axis, from before to after placement.

The first series of experiments employed the timed sequencing control method with the basic pressure patterns of Figure 6. A general description and a printout of a typical computer program for this method is given in Appendix C. It was necessary to perform several experiments to determine the needle valve settings that minimized unwanted arm oscillations. Qualitative observations of these experiments are suummarized as follows. The smoothest arm motion occurred when the needle valves were set to greatly restrict the flow of air and the maneuver cycle times T in such cases were as high as 25 seconds. As the needle valves were opened to allow for higher air flow rates, the arm moved faster, and values of T as low as 5 seconds could be achieved. However, this fast action could be achieved only at the expense of an increase in unwanted arm oscillations during the maneuver cycle. Although the pick-and-place senario was achieved for many trials where T ranged from 5 to 25 seconds,

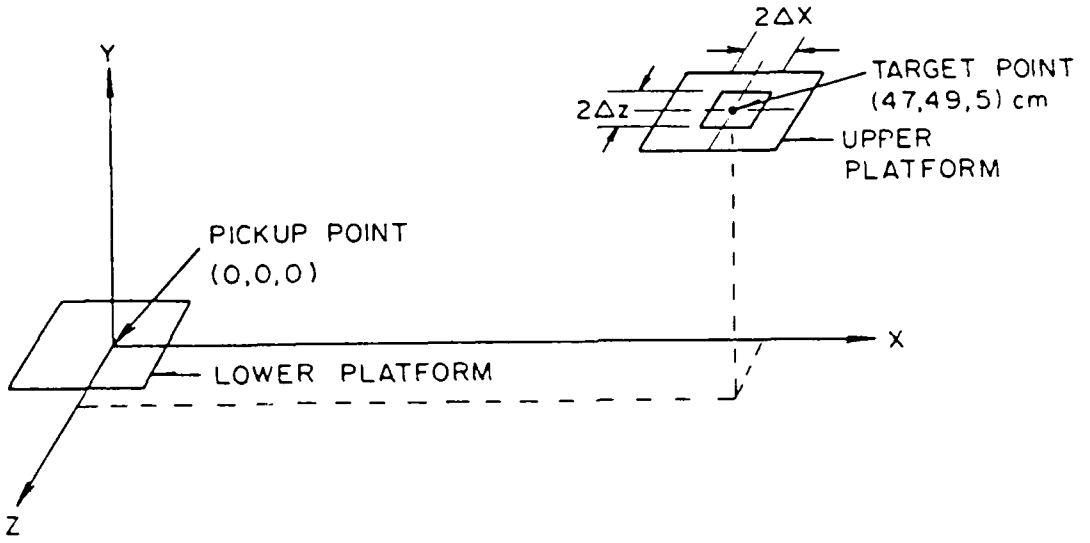

Figure 13 - Coordinate system for the pick-and-place maneuver.

there was still a need to achieve smoother arm motion, even at the higher cycle times.

A more versatile control method was sought, one without the need for needle valve adjustments to diminish unwanted arm oscillations. This lead to a second set of experiments based on the pulsing control method. A general description and a printout of a typical computer program for this method is given in Appendix D. In this method, each solenoid valve was activated at the proper preset time during an arm maneuver, analogous to the plan in Figure 6. The method employed three software timers, one for the pulse time T1, one for the pulse gap time T2, and the third for the delay time, or the time required to grip the object at the pickup point and to release the object from the grips at the target point. In programming a maneuver, these three time intervals may take on different values and this versatility allowed for the design of maneuvers with smoother arm motions over the 5 to 25 second cycle time than were possible for the timed sequenced control method.

Typical experimental results showing the accuracy of object placement for the pick-and-place maneuver are summarized in Table 1. In each of the two programs, the time intervals for the maneuver cycle, the pulse, and the gap were fixed. For each program, the change in the object rotation $\Delta\theta$ and the deviations ΔX and ΔZ from the object's target values were measured in repeated trials. Table 1 gives the maximum measured $\Delta\theta$ and the maximum percent deviation from the target coordinates, based on ten trials for each program. Also listed is the maximum amplitude of free oscillation A which occurs at the end of the maneuver, when the arm is depressurized and swings about its vertical equlibrium position.

The experimental results for the two methods of arm motion control are compared and summarized as follows.

1. If the gap time interval T2 is chosen as zero for the pulsing method, as for Program 2 of Table 1, then the two control methods are the same.
2. Both control methods may be used successfully for pick-and-place manipulation cycle times T as small as 4.2 seconds.
3. The pulsing method is superior to the timed sequence method

TABLE 1 - Typical Experimental Results

	T (s)	T1 (ms)	T2 (ms)	Δx (mm)	Δz (mm)	$\frac{\Delta x}{x}$ x100%	$\frac{\Delta z}{z}$ x100%	(deg)	A (cm)
PROGRAM I	16.42	70	210	$\pm$2	$\pm$2.5	$\pm$0.43%	$\pm$5%	22	4
PROGRAM II	4.22	105	0	$\pm$4	$\pm$4.5	$\pm$0.85%	$\pm$9%	15	7

because the pulsing method affords more versatile programming and gives smoother arm motion at a fixed T.

4. The object positioning errors for coordinates X and Z were at most 9% for T2 = 0 and T = 4.2 sec. However, these errors decreased when both T2 and T were increased.
5. Object rotations $\Delta\theta$ up to 22 deg were measured.
6. The amplitude A of the end-cycle, free swinging arm oscillations were at most 7 cm, but decreased when both T2 and T were increased.

These results show the need to improve the accuracy of object placement and to decrease the end-cycle oscillations. These improvements may be implemented by introducing positioning feedback and damping into the control system. However, the present new-concept manipulator arm with its pulsing, open-loop control method may be practical in applications where high accuracy of object placement is not a requirement; but where a fast-acting, light weight, robust, and relatively simple arm structure is a requirement.

REFERENCES

1. Mahajan, U. (1985), "Mechanics of a Continuous Manipulator Made of a Nonlinear, Composite Material," Master's Thesis, Dept. of Civil Engineering, Duke University.
2. Palaniappan, M. (1986), "Large Deflections of Continuous Elastic Structures," Master's Thesis, Dept. of Civil Engineering, Duke University.
3. Wilson, J. F. and Li, D. (1987), "Mechanics and Active Control of Polymeric Grippers," submitted to the Journal of Dynamic Systems, Measurement, and Control.
4. Wilson, J. F. (1986), "Compliant Robotic Structures-Part II," U.S. Dept. of Defense, DTIC, MDA903-84-C-0243.

APPENDIX A

Computer Code for the Elastica

```
      PROGRAM STATIC
      REAL*8 ALPHA,XA,YA
      REAL*8 WBAR,PBAR,DBAR,BETA,PI,EPS,THETA
      REAL*8 A,B,E,KSQ,DCADRE,AERR,RERR,ERROR,F,FX,FY
      REAL*8 TEMP,TEMP1,TEMP2,ALPHA1,ALPHA2
      REAL*8 C,X,Y,XT,YT
      INTEGER II,III,IJ,IK,IL,IER,IFLAG,NC1,NC2
      INTEGER IFILE,NL
      EXTERNAL F,FX,FY
      COMMON /SET1/ WBAR,PBAR,DBAR,BETA
      COMMON /SET2/ E,KSQ,THETA
      COMMON /SET3/ A,B,PI,IFLAG
C
      IFILE=1
      IF(IFILE .EQ. 1)REWIND(10)
C
      PI=3.14159265358979D+00
      EPS=.1D-06
      BETA=.00D+00
      WBAR=7.5D+00
      NL=20
      DBAR=0.20D+00
      AERR=0.00D+00
      RERR=.1D-09
      DO 1000 II=120,130,1
      PBAR=DFLOAT(II)/1.D+01
C      IF(II .EQ. 15)PBAR=14.4D+00
C      IF(II .EQ. 20)PBAR=14.5D+00
      PRINT*
      PRINT*
C
      PRINT 501,WBAR,DBAR,PBAR
      PRINT*,'       INTERMEDIATE COMPUTED DATA'
C
C
      TEMP1=-1.00D+00
C
      DO 1001 IJ=1,60,1
      ALPHA=DFLOAT(IJ)*PI/20.D+00
      CALL COMP(ALPHA)
C
      IF(IFLAG .EQ. 1)GOTO 1003
      TEMP2=DCADRE(F,A,B,AERR,RERR,ERROR,IER)-1.D+00
C
C
      IF(TEMP2 .GE. 0.0D+00)GOTO 1002
 1001 CONTINUE
      PRINT*,'POSITIVE LIMIT COULD NOT BE FOUND,STEP1'
      STOP
C
 1003 ALPHA1=ALPHA-PI/20.D+00
      ALPHA2=ALPHA
      DO 1005 IJ=1,25,1
      ALPHA=.5D+00*(ALPHA1+ALPHA2)
      CALL COMP(ALPHA)
      IF(IFLAG .EQ. 1)THEN
       ALPHA2=ALPHA
       GOTO 1005
      ENDIF
      TEMP2=DCADRE(F,A,B,AERR,RERR,ERROR,IER)-1.D+00
      IF(TEMP2 .GE. 0.0D+00)THEN
       GOTO 1002
```

```
      ENDIF
      ALPHA1=ALPHA
 1005 CONTINUE
      PRINT*,'POSITIVE LIMIT COULD NOT BE FOUND,STEP2'
      STOP
C
 1002 IF(DABS(TEMP2) .LT. EPS)GOTO 2000
      ALPHA1=0.0D+00
      ALPHA2=ALPHA
      DO 1004 IK=1,180,1
      ALPHA=ALPHA1-(ALPHA2-ALPHA1)*(TEMP1/(TEMP2-TEMP1))
      CALL COMP(ALPHA)
C
      TEMP=DCADRE(F,A,B,AERR,RERR,ERROR,IER)-1.D+00
C
      IF(DABS(TEMP) .LT. EPS)GOTO 2000
      IF(TEMP .GT. 0.0D+00)THEN
       TEMP2=TEMP
       ALPHA2=ALPHA
      ENDIF
      IF(TEMP .LT. 0.0D+00)THEN
       TEMP1=TEMP
       ALPHA1=ALPHA
      ENDIF
 1004 CONTINUE
      PRINT*,'ALPHA COULD NOT BE FOUND IN 180 ITERATIONS'
      STOP
C
 2000 XA=DCADRE(FX,A,B,AERR,RERR,ERROR,IER)
      YA=DCADRE(FY,A,B,AERR,RERR,ERROR,IER)
      TEMP=DCADRE(F,A,B,AERR,RERR,ERROR,IER)
C
      PRINT 503,XA,YA,ALPHA,TEMP
C
       PRINT*,'KSQ=',KSQ,'THETA=',THETA
       PRINT*,'A=',A,'B=',B
       PRINT*,'E=',E
      PRINT*
      DO 1010 IJ=0,NL,1
      C=DFLOAT(IJ)*ALPHA/DFLOAT(NL)
      C=A+C/2.D+00
      X=DCADRE(FX,C,B,AERR,RERR,ERROR,IER)
      Y=DCADRE(FY,C,B,AERR,RERR,ERROR,IER)
      XT=XA-X
      YT=YA-Y
      PRINT 500,IJ,C,X,Y,XT,YT
      IF(IFILE .EQ. 1)WRITE(10,FMT=502)XT,YT
 1010 CONTINUE
 1000 CONTINUE
C
  500 FORMAT(6X,I2,4X,'C=',D13.6,2X,'X=',D13.6,2X,'Y=',D13.6,10X,
     S'XT=',D13.6,2X,'YT=',D13.6)
  501 FORMAT(4X,'WBAR=',D13.6,2X,'DBAR=',D13.6,8X,'PBAR=',D13.6)
  502 FORMAT(2D16.8)
  503 FORMAT(6X,'XA=',D23.16,2X,'YA=',D23.16,2X,'ALPHA=',D23.16,
     S10X,'L=',D23.16)
      STOP
      END
C
C
      SUBROUTINE COMP(ALPHA)
      REAL*8 ALPHA,WBAR,PBAR,DBAR,BETA,TESTA,TESTB
```

```
      REAL*8 CA,SA,CB,SB,A,B,C,D,E,THETA,KSQ,PI,EPS,TEST
      INTEGER IFLAG
      COMMON /SET1/ WBAR,PBAR,DBAR,BETA
      COMMON /SET2/ E,KSQ,THETA
      COMMON /SET3/ A,B,PI,IFLAG
      EPS=1.D-09
      CA=DCOS(ALPHA)
      SA=DSIN(ALPHA)
      CB=DCOS(BETA)
      SB=DSIN(BETA)
      A=-(PBAR*CA+WBAR*CB)*2.D+00
      B=-(PBAR*SA+WBAR*SB)*2.D+00
C
      C=-A*CA-B*SA+(PBAR*DBAR)**2
      D=DSQRT(A*A+B*B)
      E=2.D+00/DSQRT(D+C)
      KSQ=D/(D+C)+D/(D+C)
      THETA=DATAN2(B,A)
      TEST=D*DCOS(THETA)-A
      IF(ABS(TEST) .GT. EPS)GOTO 300
      TEST=D*DSIN(THETA)-B
      IF(ABS(TEST) .GT. EPS)GOTO 300
      A=-.5D+00*THETA
      B=.5D+00*ALPHA+A
      IF(KSQ .LT. 1.0D+00)GOTO 100
      IF(DABS(A) .GE. (PI*.5D+00))GOTO 200
      IF(DABS(B) .GE. (PI*.5D+00))GOTO 200
      TESTA=KSQ*DSIN(A)**2
      TESTB=KSQ*DSIN(B)**2
      IF(TESTA .GE. 1.00D+00)GOTO 200
      IF(TESTB .GE. 1.00D+00)GOTO 200
  100 IFLAG=0
      RETURN
  200 IFLAG=1
      RETURN
  300 PRINT*,'TEST FAILED IN SUBROUTINE COMP'
      STOP
      END
C
C
      FUNCTION F(X)
      REAL*8 F,X,E,KSQ,THETA
      COMMON /SET2/ E,KSQ,THETA
      F=1.D+00-KSQ*DSIN(X)**2
      F=E/DSQRT(F)
      RETURN
      END
C
      FUNCTION FX(X)
      REAL*8 FX,X,E,KSQ,THETA
      COMMON /SET2/E,KSQ,THETA
      FX=1.D+00-KSQ*DSIN(X)**2
      FX=E/DSQRT(FX)
      FX=FX*DCOS(X+X+THETA)
      RETURN
      END
C
      FUNCTION FY(X)
      REAL*8 FY,X,E,KSQ,THETA
      COMMON /SET2/E,KSQ,THETA
      FY=1.-KSQ*DSIN(X)**2
      FY=E/DSQRT(FY)
```

```
      FY=FY*DSIN(X+X+THETA)
      RETURN
      END
```

APPENDIX B

Computer Codes for Bending Elements:

LINDEFL.FOR
HARINGX.FOR

```
CCCCCCCCCCCCCCCCCCCCCCCCCCCCCCCCCCCCCCCCCCCCCCCCCCCCCCCCCCCCCCCCCCCCCCC
C                Program LINDEFL.FOR                                    C
C                                                                       C
C    This program computes the relationships between deflection,C
C    end load, and moment for single and double-sided bending   C
C    elements using simple beam theory and Haringx model for    C
C    bellows stiffness.                                         C
CCCCCCCCCCCCCCCCCCCCCCCCCCCCCCCCCCCCCCCCCCCCCCCCCCCCCCCCCCCCCCCCCCCCCCC

      REAL Mo,L,VAL(200)
111   FORMAT (I1)
100   WRITE (*,'(''Enter:'')')
001   WRITE (*,'(A)')
      WRITE (*,'(A)')'       1) INPUT DIFFERENT VALUES'
      WRITE (*,'(A)')'       2) KEEP SAME VALUES'
      WRITE (*,'(A)')'       3) QUIT PROGRAM'
      READ (*,111) I
      write(*,'(''Input E : '')')
      read (*,*) E
      IF (I.EQ.1) THEN
         WRITE (*,'(A)')' INPUT S1: '
         READ (*,'(F6.4)')S1
         WRITE (*,'(A)')' INPUT S2: '
         READ (*,'(F6.4)')S2
         WRITE (*,'(A)')' INPUT L : '
         READ (*,'(F6.4)')L
         WRITE (*,'(A)')' INPUT D1: '
         READ (*,'(F6.4)')D1
         WRITE (*,'(A)')' INPUT D2: '
         READ (*,'(F6.4)')D2
         WRITE (*,'(A)')' INPUT D3: '
         READ (*,'(F6.4)')D3
         WRITE (*,'(A)')' INPUT D4: '
         READ (*,'(F6.4)')D4
         WRITE (*,'(A)')' INPUT ALPHA 0: '
         READ (*,'(F6.4)')ALPHA0
         WRITE (*,'(A)')' INPUT t :'
         READ (*,'(F6.4)')t
         WRITE (*,'(A)')' INPUT R : '
         READ (*,'(F6.4)')R
         WRITE (*,'(A)')' INPUT Ro: '
         READ (*,'(F6.4)')Ro
         WRITE (*,'(A)')' INPUT H : '
         READ (*,'(F6.4)')H
         WRITE (*,'(A)')' INPUT b : '
         READ (*,'(F6.4)')b
      ELSEIF (I.EQ.2) THEN
          GOTO 007
      ELSEIF (I.EQ.3) THEN
          GOTO 1000
      ELSE
         WRITE (*,'(A)')' TRY AGAIN'
         GOTO 100
      ENDIF
      Em=0.00
```

```
      V=0.5
      RHO=(1.0-H/R)/(1.0+H/R)
      RLAM=R*T/b/b
      Qu=(3.0*(1.0-V*V))**0.25/(RLAM*(1.0+H/R))**0.5
      Qi=(3.0*(1.0-V*V))**0.25/(RLAM*(1.0-H/R))**0.5
      RLAMu=(SINH(2.*Qu)+SIN(2.*Qu))/(2.*Qu)/(COSH(2.*Qu)+COS(2.*Qu))
      RLAMi=(SINH(2.*Qi)+SIN(2.*Qi))/(2.*Qi)/(COSH(2.*Qi)+COS(2.*Qi))
      A=(1.-RHO*RHO+2.*RHO*RHO*ALOG(RHO))**2*RLAMu
      BB=RHO*(1.-RHO*RHO+2.*ALOG(RHO))**2*RLAMi
      C=(1.-RHO*RHO)*((1.-RHO*RHO)**2-(2.*RHO*ALOG(RHO))**2)
007   WRITE (*,'(A)')
      WRITE (*,'(A)')
      WRITE (*,'(A)')
      WRITE (*,'(A)')
      WRITE (*,'(A)')
002   WRITE (*,'(A)')' DO YOU WANT TO:'
      WRITE (*,'(A)')
      WRITE (*,'(A)')'     1) KEEP CHI=1'
      WRITE (*,'(A)')'     2) CALCULATE CHI'
      READ (*,111)I4
      IF (I4.EQ.1) THEN
          CHI=1.0
      ELSEIF (I4.EQ.2) THEN
          CHI=1.+(2.*(b/R))/(1.+(H/R))*(A/C+BB/C)
      ENDIF
     FLAG1=3.*R/4./t*CHI*(1.+H/R)**2*(1.-V*V)/RLAM/(B/R)**3/(1.-RHO**2)
      FLAG2=FLAG1*((1.-RHO**2)**2-(2.*RHO*ALOG(RHO))**2)
      WRITE (*,'(A)')
      WRITE (*,'(A)')
      WRITE (*,'(A)')
      WRITE (*,'(A)')
      WRITE (*,'(A)')
      WRITE (*,'(A)')' CHOOSE ONE:'
      WRITE (*,'(A)')
      WRITE (*,'(A)')' 1) OUTPUT DELTA/Fo FOR Mo=0 AND P=0'
      WRITE (*,'(A)')' 2) OUTPUT DELTA/P FOR Fo=0 AND Mo=0'
      WRITE (*,'(A)')' 3) OUTPUT Fo/P FOR DELTA=0 AND Mo=0'
      WRITE (*,'(A)')' 4) OUTPUT DELTA AT MIDPOINT FOR DELTA(END)=0 AND
     i Mo=0'
      WRITE (*,'(A)')' 5) OUTPUT DELTA/P FOR A GIVEN Fo AND Mo'
      write (*,'(a)')' 6) same as (1), double sided element'
      write (*,'(a)')' 7)    "   "  (2),    "       "      "     '
      write (*,'(a)')' 8)    "   "  (3),    "       "      "     '
      write (*,'(a)')' 9)    "   "  (4),    "       "      "     '
      write (*,'(a)')'10)    "   "  (5),    "       "      "     '
      READ (*,111) II
112   FORMAT (F9.4)
      IF (II.EQ.1.or.ii.eq.6) THEN
          PP=0.0
          Mo=0.0
          Fo=1.0
      ELSEIF (II.EQ.2.or.ii.eq.7) THEN
          Fo=0.0
          Mo=0.0
          PP=1.0
```

```
      ELSEIF (II.EQ.3.OR.II.EQ.4.or.ii.eq.8.or.ii.eq.9) THEN
          Mo=0.0
          PP=1.0
      ELSEIF (II.EQ.5.or.ii.eq.10) THEN
          WRITE (*,'(A)')' INPUT Fo: '
          READ (*,'(F7.3)') Fo
          WRITE (*,'(A)')' INPUT Mo: '
          READ (*,'(F7.4)') Mo
      WRITE (*,'(A)')' INPUT STARTING PRESSURE: '
      READ (*,'(I3)')IPS
      WRITE (*,'(A)')' INPUT ENDING PRESSURE: '
      READ (*,'(I3)')IPE
      WRITE (*,'(A)')' INPUT DELTA PRESSURE: '
      READ (*,'(I3)')IDP
      ENDIF
      IF (II.EQ.5) THEN
       DO 114 IPP=IPS,IPE,IDP
        PP=REAL(IPP)
        VAL(IPP)=VALUE(II,T,PP,D1,D2,D3,D4,ALPHA0,Ro,R,L,FLAG2,Em,
     1    E,Fo,Mo,YBAR,Yc,RMULT,Ap)
  114   CONTINUE
      ELSE
       VALM=VALUE(II,t,PP,D1,D2,D3,D4,ALPHA0,Ro,R,L,FLAG2,Em,E,Fo,Mo,
     1YBAR,Yc,RMULT,Ap,xIbase)
      ENDIF
      WRITE (*,'(A)')
      WRITE (*,'(A)')
      WRITE (*,'(A)')
      write (*,'(a)')
      write (*,'(a)')
      write (*,'(a)')
      if (ii.eq.1.or.ii.eq.2.or.ii.eq.3.or.ii.eq.4.or.ii.eq.5)then
         WRITE (*,'(A)')' Single-Sided Element'
      else
         WRITE (*,'(A)')' Double-Sided Element'
      endif
      WRITE (*,'(A)')
      WRITE (*,151)D1,D2,D3
  151 FORMAT(' D1=',F9.4,'      D2=',F9.4,'      D3=',F9.4)
      WRITE (*,152)D4,t,R
  152 FORMAT(' D4=',F9.4,'      t =',F9.4,'      R =',F9.4)
      WRITE (*,153)Ro,ALPHA0,L
  153 FORMAT(' Ro=',F9.4,'    ALPHA0=',F9.4,'    L =',F9.4)
      WRITE (*,154)S1,S2,B,H
  154 FORMAT(' S1=',F9.4,'      S2=',F9.4,'      B=',F9.4,'      H=',F9.4)
      EPRIME=E/FLAG2
      WRITE (*,155)E,Em,EPRIME
  155 FORMAT(' E =',F9.2,'      Em=',F9.4,'     Eprime=',F9.4)
      WRITE (*,157)YBAR,Yc,RMULT,Ap
  157 FORMAT (' Ybar=',F9.4,'    Yp=',F9.4,'    E*Ibar=',F9.4,'    Ap='
     1,F9.4)
      EIbase = E*xIbase
      write(*,'('' E*Ibase = '',F9.4)')EIbase
      WRITE (*,156)CHI
  156 FORMAT (' CHI = ',F9.4)
```

```
      WRITE (*,'(A)')
      WRITE (*,'(A)')
      WRITE (*,'(A)')
      WRITE (*,'(A)')
      IF (II.EQ.1.or.ii.eq.6) THEN
         WRITE (*,500) Fo,Mo,PP,VALM
500      FORMAT (' FOR THE GIVEN:',/,'  Fo=',F4.2,/,'  Mo=',F4.2,/,
     1'  P=',F4.2,/,'  DEFLECTION IS:  ',F9.4)
      ELSEIF (II.EQ.2.or.ii.eq.7) THEN
         WRITE (*,501) Fo,Mo,PP,VALM
501      FORMAT (' FOR THE GIVEN:',/,'  Fo=',F4.2,/,'  Mo=',F4.2,/,
     1'  P=',F4.2,/,'  DEFLECTION IS:  ',F9.4)
      ELSEIF (II.EQ.3.or.ii.eq.8) THEN
         WRITE (*,503) DLETA,Mo,PP,VALM
503      FORMAT (' FOR THE GIVEN:',/,'  DELTA=',F4.2,/,'  Mo=',F4.2,/,
     1'  P=',F4.2,/,'  FORCE IS:  ',F9.4)
      ELSEIF (II.EQ.4.or.ii.eq.9) THEN
         WRITE (*,504) DELTA,Mo,PP,VALM
504    FORMAT (' FOR THE GIVEN:',/,'  DELTA(END)=',F4.2,/,'  Mo=',F4.2,
     1/,'  P=',F4.2,/,'  THE MIDPOINT DEFLECTION IS:  ',F9.6)
      ELSEIF (II.EQ.5.or.ii.eq.10) THEN
         WRITE (*,505)Fo,Mo
505      FORMAT (' FOR THE GIVEN: ',/,'  Fo= ',F7.4,'  Mo= ',F8.4)
         DO 506 IPP=IPS,IPE,IDP
          WRITE (*,507) IPP,VAL(IPP)
507       FORMAT (I3,'      ',F6.4)
506      CONTINUE
      ENDIF
      WRITE (*,'(A)')
      WRITE (*,'(A)')
      WRITE (*,177)
177   FORMAT (' DO YOU WANT TO CONTINUE?    (1 FOR YES, 2 FOR NO)')
      READ (*,'(I1)') ICON
      IF (ICON.EQ.1) THEN
          GOTO 001
      ELSE
          GOTO 1000
      ENDIF
1000  END

c.....................................................................
.......
      FUNCTION VALUE(II,t,PP,D1,D2,D3,D4,ALPHA0,Ro,R,L,FLAG2,Em,E,Fo,
     1Mo,YBAR,Yc,RMULT,Ap,xIbase)
      REAL IBAR,Ir,Iw,Is,Ib,Mp,L,Mo
      IF (ALPHA0.LT.3.14159) THEN
         ALPHA=2.*(ACOS(COS(ALPHA0/2.)/R*Ro))
      ELSE
         ALPHA=ALPHA0
      ENDIF
      Se=(Em/E)*S1
      Te=(1/FLAG2)*t
      Ab=ALPHA*R*Te
      Yb=2.*R/ALPHA*SIN(ALPHA/2.)-Ro*COS(ALPHA/2.)+D2
      Ib=2.*R**3*Te*(ALPHA+SIN(ALPHA)-4./ALPHA*(1.-COS(ALPHA)))
```

```
      Ar=D1*D3
      Yr=.5*D3
      Ir=(1./12.)*D1*D3**3
      Aw=2.*D4*(D2-D3)
      Yw=.5*(D2+D3)
      Iw=(1./6.)*D4*(D2-D3)**3
      As=Se*S2
      Ys=-(.5)*S2
      Is=(1./12.)*Se*S2*S2*s2
      A=Ab+Ar+Aw+As
      YBAR=(1./A)*(Yb*Ab+Yr*Ar+Yw*Aw+Ys*As)
      XXXX=Ib+Ir+Iw+Is+Ab*(YBAR-Yb)**2+Ar*(YBAR-Yr)**2
      IBAR=XXXX+Aw*(YBAR-Yw)**2+As*(YBAR-Ys)**2
      xIbase=Ib+Ir+Iw+Is +Ab*Yb**2+ Ar*Yr**2+ Aw*Yw**2+ As*Ys**2
      IF (ALPHA.LT.3.14159) THEN
        A1=.5*ALPHA*R*R-R*R*SIN(ALPHA/2.)*COS(ALPHA/2.)
        A2=(D2-D3)*(D1-2.*D4)
        Yc2=.5*(D2+D3)
        XXX=2.*R*R*R/3./A1*(1.-COS(ALPHA/2.)**2)*SIN(ALPHA/2.)
        YC1=XXX-R*COS(ALPHA/2.)+D2
        Ap=A1+A2
    write(*,*)'Ap=',Ap
        Yc=(1./Ap)*(Yc1*A1+YC2*A2)
      ELSE
        A2=(D2-D3)*(D1-2.*D4)
        A3=0.5*ALPHA*R*R
        YC3=4.0*R/3.0/ALPHA*SIN(ALPHA/2.0)-Ro*COS(ALPHA/2.0)+D2
        A4=-0.5*Ro*(D1-2.0*D4)*COS(ALPHA/2.0)
        YC4=-(1./3.)*Ro*COS(ALPHA/2.)+D2
        YC2=.5*(D2+D3)
        Ap=A2+A3+A4
        Yc=(1./Ap)*(YC2*A2+YC3*A3+YC4*A4)
      ENDIF
      RMULT=E*IBAR
      Mp=(Yc-YBAR)*PP*Ap
      if (ii.eq.6.or.ii.eq.7.or.ii.eq.8.or.
     1     ii.eq.9.or.ii.eq.10 ) then
         xIeff = xIbase * 2.
      else
         xIeff = Ibar
      endif
      IF (II.EQ.1.OR.II.EQ.2.OR.II.EQ.5.or.
     1     ii.eq.6.or.ii.eq.7.or.ii.eq.10) THEN
         VALUE=Fo*L**3/3./E/xIeff+(Mo+Mp)*L*L/2./E/xIeff
      ELSEIF (II.EQ.3.or.ii.eq.8) THEN
         VALUE = -(Mo+Mp)*3.0/2.0/L
      ELSEIF (II.EQ.4.or.ii.eq.9) THEN
         VALUE=Mp*L*L/32.0/E/xIeff
      ENDIF
    END
```

```
CCCCCCCCCCCCCCCCCCCCCCCCCCCCCCCCCCCCCCCCCCCCCCCCCCCCCCCCCCCCCCCCCCCCCCCCCC
C                    Program HARINGX.FOR                                    C
C   Computes bellows stiffness according to Haringx model.                  C
CCCCCCCCCCCCCCCCCCCCCCCCCCCCCCCCCCCCCCCCCCCCCCCCCCCCCCCCCCCCCCCCCCCCCCCCCC
c       V=0.5
c       b =.1162
c       R = ( .5/cos(70.) + .5 )/2.
c       t = .1
c       h = .08
        RHO=(1.0-H/R)/(1.0+H/R)
        RLAM=R*T/b/b
        Qu=(3.0*(1.0-V*V))**0.25/(RLAM*(1.0+H/R))**0.5
        Qi=(3.0*(1.0-V*V))**0.25/(RLAM*(1.0-H/R))**0.5
        RLAMu=(SINH(2.*Qu)+SIN(2.*Qu))/(2.*Qu)/(COSH(2.*Qu)+COS(2.*Qu))
        RLAMi=(SINH(2.*Qi)+SIN(2.*Qi))/(2.*Qi)/(COSH(2.*Qi)+COS(2.*Qi))
        A=(1.-RHO*RHO+2.*RHO*RHO*ALOG(RHO))**2*RLAMu
        BB=RHO*(1.-RHO*RHO+2.*ALOG(RHO))**2*RLAMi
        C=(1.-RHO*RHO)*((1.-RHO*RHO)**2-(2.*RHO*ALOG(RHO))**2)
002     WRITE (*,'(A)')' DO YOU WANT TO:'
        WRITE (*,'(A)')'     1) KEEP CHI=1'
        WRITE (*,'(A)')'     2) CALCULATE CHI'
        READ  (*,*) I4
        IF (I4.EQ.1) THEN
            CHI=1.0
        ELSEIF (I4.EQ.2) THEN
            CHI=1.+(2.*(b/R))/(1.+(H/R))*(A/C+BB/C)
        ENDIF
        FLAG1=3.*R/4./t*CHI*(1.+H/R)**2*(1.-V*V)/RLAM/(B/R)**3/(1.-RHO**2)
        FLAG2=FLAG1*((1.-RHO**2)**2-(2.*RHO*ALOG(RHO))**2)
        WRITE (*,'(''E/Eprime = '',\)')
        WRITE (*,*) flag2
        END
```

Pressure-Deflection

```
Single-Sided Element

D1=    0.5000      D2=    0.0500      D3=    0.0500
D4=    0.0000      t =    0.0500      R =    0.4000
Ro=    0.5000   ALPHA0=    5.3600    L =    3.0000
S1=    0.0000      S2=    0.0000      B=    0.0500      H=    0.1000
E =    740.00      Em=    0.0000    Eprime=   12.6557
Ybar=    0.0618    Yp=    0.4710   E*Ibar=    0.7168    Ap=    0.5407
E*Ibase =     0.7928
CHI =     2.4573



FOR THE GIVEN:
 Fo=0.00
 Mo=0.00
 P=1.00
 DEFLECTION IS:      1.3890

DO YOU WANT TO CONTINUE?    (1 FOR YES. 2 FOR NO)



Single-Sided Element

D1=    0.5000      D2=    0.0500      D3=    0.0500
D4=    0.0000      t =    0.0500      R =    0.4000
Ro=    0.5000   ALPHA0=    5.3600    L =    3.0000
S1=    0.0000      S2=    0.0000      B=    0.0500      H=    0.1000
E =  2330.00      Em=    0.0000    Eprime=   39.8483
Ybar=    0.0618    Yp=    0.4710   E*Ibar=    2.2571    Ap=    0.5407
E*Ibase =     2.4961
CHI =     2.4573



FOR THE GIVEN:
 Fo=0.00
 Mo=0.00
 P=1.00
 DEFLECTION IS:      0.4411

DO YOU WANT TO CONTINUE?    (1 FOR YES, 2 FOR NO)
```

```
Double-Sided Element

D1=    0.5000      D2=    0.0500      D3=    0.0500
D4=    0.0000      t =    0.0500      R =    0.4000
Ro=    0.5000   ALPHA0=    5.3600    L =    3.0000
S1=    0.0000      S2=    0.0000      B=    0.0500      H=    0.1000
E =    740.00      Em=    0.0000    Eprime=   12.6557
Ybar=    0.0618    Yp=    0.4710   E*Ibar=    0.7168    Ap=    0.5407
E*Ibase =     0.7928
CHI =     2.4573



FOR THE GIVEN:
 Fo=0.00
 Mo=0.00
 P=1.00
 DEFLECTION IS:      0.6280

DO YOU WANT TO CONTINUE?    (1 FOR YES, 2 FOR NO)



Double-Sided Element

D1=    0.5000      D2=    0.0500      D3=    0.0500
D4=    0.0000      t =    0.0500      R =    0.4000
Ro=    0.5000   ALPHA0=    5.3600    L =    3.0000
S1=    0.0000      S2=    0.0000      B=    0.0500      H=    0.1000
E =   2330.00      Em=    0.0000    Eprime=   39.8483
Ybar=    0.0618    Yp=    0.4710   E*Ibar=    2.2571    Ap=    0.5407
E*Ibase =     2.4961
CHI =     2.4573



FOR THE GIVEN:
 Fo=0.00
 Mo=0.00
 P=1.00
 DEFLECTION IS:      0.1994

DO YOU WANT TO CONTINUE?    (1 FOR YES, 2 FOR NO)
```

Single-Sided Element

```
D1=    0.5000      D2=    0.0500      D3=    0.0500
D4=    0.0000      t =    0.0500      R =    0.4000
Ro=    0.5000   ALPHA0=    5.3600    L =    3.0000
S1=    0.0000      S2=    0.0000      B=    0.0500      H=    0.1000
E =  1000.00       Em=    0.0000    Eprime=   17.1023
Ybar=    0.0618    Yp=    0.4710   E*Ibar=    0.9687    Ap=    0.5407
E*Ibase =     1.0713
CHI =     2.4573
```

FOR THE GIVEN:
DELTA=????
Mo=0.00
P=1.00
FORCE IS: -0.1106

DO YOU WANT TO CONTINUE? (1 FOR YES, 2 FOR NO)

Double-Sided Element

```
D1=    0.5000      D2=    0.0500      D3=    0.0500
D4=    0.0000      t =    0.0500      R =    0.4000
Ro=    0.5000   ALPHA0=    5.3600    L =    3.0000
S1=    0.0000      S2=    0.0000      B=    0.0500      H=    0.1000
E =  1000.00       Em=    0.0000    Eprime=   17.1023
Ybar=    0.0618    Yp=    0.4710   E*Ibar=    0.9687    Ap=    0.5407
E*Ibase =     1.0713
CHI =     2.4573
```

FOR THE GIVEN:
DELTA=????
Mo=0.00
P=1.00
FORCE IS: -0.1106

DO YOU WANT TO CONTINUE? (1 FOR YES, 2 FOR NO)

Pressure-Deflection
(small, optimum bend.)

```
Single-Sided Element

D1=    0.5000      D2=    0.3750      D3=    0.3750
D4=    0.0000      t =    0.0460      R =    0.3980
Ro=    0.5230   ALPHA0=    5.1070    L =    3.7500
S1=    0.0000      S2=    0.0000      B=    0.0777      H=    0.1250
E =    740.00      Em=    0.0000    Eprime=    8.1662
Ybar=    0.1914    Yp=    0.7941   E*Ibar=    2.1831    Ap=    0.5133
E*Ibase =     7.2930
CHI =     2.5795



FOR THE GIVEN:
 Fo=0.00
 Mo=0.00
 P=1.00
 DEFLECTION IS:      0.9963


DO YOU WANT TO CONTINUE?    (1 FOR YES, 2 FOR NO)



Single-Sided Element

D1=    0.5000      D2=    0.3750      D3=    0.3750
D4=    0.0000      t =    0.0460      R =    0.3980
Ro=    0.5230   ALPHA0=    5.1070    L =    3.7500
S1=    0.0000      S2=    0.0000      B=    0.0777      H=    0.1250
E =  2330.00      Em=    0.0000    Eprime=   25.7123
Ybar=    0.1914    Yp=    0.7941   E*Ibar=    6.8739    Ap=    0.5133
E*Ibase =    22.9632
CHI =     2.5795



FOR THE GIVEN:
 Fo=0.00
 Mo=0.00
 P=1.00
 DEFLECTION IS:      0.3164


DO YOU WANT TO CONTINUE?    (1 FOR YES, 2 FOR NO)
```

Load-Pressure
(small optimum bend. el.)

Single-Sided Element

```
D1=    0.5000      D2=    0.3750      D3=    0.3750
D4=    0.0000      t =    0.0460      R =    0.3980
Ro=    0.5230   ALPHAO=    5.1070    L =    3.7500
S1=    0.0000      S2=    0.0000      B=    0.0777      H=    0.1250
E =  1000.00       Em=    0.0000    Eprime=   11.0353
Ybar=    0.1914    Yp=    0.7941   E*Ibar=    2.9502    Ap=    0.5133
E*Ibase =     9.8555
CHI =     2.5795



FOR THE GIVEN:
 DELTA=????
 Mo=0.00
 P=1.00
 FORCE IS:     -0.1237
```

DO YOU WANT TO CONTINUE? (1 FOR YES, 2 FOR NO)

Pressure-Deflection
(large, optimum bend. el.)

```
Single-Sided Element

D1=    0.7500      D2=    0.5620      D3=    0.5620
D4=    0.0000      t =    0.0460      R =    0.6010
Ro=    0.7730   ALPHA0=    5.6400    L =    6.4540
S1=    0.0000      S2=    0.0000      B=    0.1128      H=    0.1720
E =    740.00      Em=    0.0000    Eprime=    4.6649
Ybar=    0.2835   Yp=    1.2268   E*Ibar=    9.5151    Ap=    1.2936
E*Ibase =    34.6454
CHI =     2.5075



FOR THE GIVEN:
 Fo=0.00
 Mo=0.00
 P=1.00
 DEFLECTION IS:      2.6709


DO YOU WANT TO CONTINUE?    (1 FOR YES, 2 FOR NO)



Single-Sided Element

D1=    0.7500      D2=    0.5620      D3=    0.5620
D4=    0.0000      t =    0.0460      R =    0.6010
Ro=    0.7730   ALPHA0=    5.6400    L =    6.4540
S1=    0.0000      S2=    0.0000      B=    0.1128      H=    0.1720
E =   2330.00      Em=    0.0000    Eprime=   14.6880
Ybar=    0.2835   Yp=    1.2268   E*Ibar=   29.9597    Ap=    1.2936
E*Ibase =   109.0862
CHI =     2.5075



FOR THE GIVEN:
 Fo=0.00
 Mo=0.00
 P=1.00
 DEFLECTION IS:      0.8483


DO YOU WANT TO CONTINUE?    (1 FOR YES, 2 FOR NO)
```

Load-Pressure
(large, optimum bend. el.)

```
Single-Sided Element

D1=    0.7500      D2=    0.5620      D3=    0.5620
D4=    0.0000      t =    0.0460      R =    0.6010
Ro=    0.7730   ALPHA0=    5.6400    L =    6.4540
S1=    0.0000      S2=    0.0000      B=    0.1128      H=    0.1720
E =  1000.00       Em=    0.0000    Eprime=    6.3039
Ybar=    0.2835   Yp=    1.2268   E*Ibar=   12.8582   Ap=    1.2936
E*Ibase =    46.8181
CHI =     2.5075



FOR THE GIVEN:
 DELTA=????
 Mo=0.00
 P=1.00
 FORCE IS:     -0.2836    =>

DO YOU WANT TO CONTINUE?    (1 FOR YES, 2 FOR NO)
```

APPENDIX C

Computer Code for the Timed Sequencing Control Method

PROGRAM I: TIMED SEQUENCE

LINE	DESCRIPTION
1	Turns off any channels that may have been left on.
10-20	Defines a function to convert Binary Coded Decimal into decimal.
30-60	Sets the Master Mode Register (see figure 8). Line 50 contains the low byte and line 60 contains the high byte.
70-100	Sets the Counter Mode Register for Counter #1 (see figure 9). The low byte isin line 90 and the high byte is in line 100.
110-130	Loads 2500 into the Load Register. Notice that since the Data Pointer Increment is enabled, there is no need to address this register. Once the counter was addressed in line 80, it automatically incremented to the load register. This feature makes it very easy to load data into all the counters if necessary.
140-150	Disables Data Pointer Increment
160-180	This command loads the 2500 from the Load Register into the counter and arms it. Arming a counter starts the counting process. Line 180 immediately branches the program to the subroutine which grasps the object.
190	Branches the program to the subroutine at line 900 which sends a command to save the the value of the counter in the Hold Register of the counter without interupting the counting process. The low byte contains 1/100's of a second while the high byte contains the seconds.
200-570	Checks to see if the value of the counter is greater than the time the next event should occur (remember, the timer counts down). If it is, it goes back and

	refreshes the sample/hold amplifiers. If the counter is less than the time of the next event, it goes ahead and performs it
900-990	Subroutine for checking time. Time is saved from hold register, data poniter is put back to the hold register, and the time is converted from BCD.
1000-15270	Subroutines for controlling D/A channels.

```
1 GOSUB 15000       'TURN ALL VALVES OFF
10 REM               DEFINE BCD-DECIMAL CONVERSION
20 DEF FNDCONV(X)=X-6*(X\16)
30 REM               SET MASTER MODE
40 OUT 825,23
50 OUT 824,0
60 OUT 824,128
70 REM               SET COUNTER MODE
80 OUT 825,1
90 OUT 824,16
100 OUT 824,15
110 REM              SET LOAD FOR 25 SECONDS
120 OUT 824,0
130 OUT 824,37
140 REM              DISABLE SEQUENCING
150 OUT 825,232
160 REM              LOAD AND ARM
170 OUT 825,97
180 GOSUB 1000                          'BEGINNING OF SEQUENCE
190 GOSUB 900
200 IF C>24.8 THEN GOTO 180
210 GOSUB 2000
220 GOSUB 900
230 IF C>24.6 THEN GOTO 210
240 GOSUB 3000
250 GOSUB 900
260 IF C>24.3 THEN GOTO 240
270 GOSUB 4000
280 GOSUB 900
290 IF C>24! THEN GOTO 270
300 GOSUB 5000
310 GOSUB 900
320 IF C>23.8 THEN GOTO 300
330 GOSUB 6000
340 GOSUB 900
350 IF C>21! THEN GOTO 330
360 GOSUB 7000
370 GOSUB 900
380 IF C>19.1 THEN GOTO 360
390 GOSUB 9000
400 GOSUB 900
410 IF C>18.9 THEN GOTO 390
420 GOSUB 8000
430 GOSUB 900
440 IF C>18.5 THEN GOTO 420
450 GOSUB 10000
460 GOSUB 900
461 IF C>18.3 THEN GOTO 450
462 GOSUB 10500
463 GOSUB 900
470 IF C>17! THEN GOTO 462
480 GOSUB 11000
490 GOSUB 900
500 IF C>16.5 THEN GOTO 480
510 GOSUB 12000
```

```
520 GOSUB 900
530 IF C>16! THEN GOTO 510
540 GOSUB 13000
550 GOSUB 900
560 IF C>9! THEN GOTO 540
570 GOSUB 15000
580 END
900 REM              SUB FOR CHECKING TIME
901 REM              SAVE COUNTER 1
910 OUT 825,161
920 REM              DATA POINTER HOLD
930 OUT 825,17
940 REM              READ COUNTER 1
950 A=INP(824)
960 B=INP(824)
965 B=FNDCONV(B)
970 A=.01*FNDCONV(A)
980 C=A+B
990 RETURN
1000 REM               SUB FOR TURNING ON CHANNEL 8
1010 OUT 820,0        'TURN MULTIPLEXERS OFF
1020 OUT 821,255      '4.96 VOLTS
1030 OUT 820,8        'ENABLE CHANNEL 8
1040 OUT 820,0        'DISABLE CHANNEL 8
1050 RETURN
2000 REM               SUB TO TURN ON CHANNELS 8 AND 22
2010 OUT 821,255      '5.00 VOLTS
2015 OUT 820,8        'ENABLE
2020 OUT 820,0        'DISABLE
2030 OUT 820,22
2040 OUT 820,0
2041 REM      LINES TO KEEP 16 OFF
2042 OUT 821,0
2043 OUT 820,16
2044 OUT 820,0
2050 RETURN
3000 REM               SUB FOR TURNING ON CHANNELS 8,22,18
3010 OUT 821,255
3020 OUT 820,8        'ENABLE 8
3030 OUT 820,0        'DISABLE
3040 OUT 820,22
3050 OUT 820,0
3060 OUT 820,18
3070 OUT 820,0
3071 REM       LINES TO KEEP 16 OFF
3072 OUT 821,0
3073 OUT 820,16
3074 OUT 820,0
3080 RETURN
4000 REM              SUB TO TURN ON 8,22,20,18
4010 OUT 821,255
4020 OUT 820,8
4030 OUT 820,0
4040 OUT 820,22
4050 OUT 820,0
```

```
4060 OUT 820,20
4070 OUT 820,0
4080 OUT 820,18
4090 OUT 820,0
4091 REM   LINES TO KEEP 16 OFF
4092 OUT 821,0
4093 OUT 820,16
4094 OUT 820,0
4100 RETURN
5000 REM                SUB TO TURN ON 8,22,20,18,16
5010 OUT 821,255
5020 OUT 820,8
5030 OUT 820,0
5040 OUT 820,22
5050 OUT 820,0
5060 OUT 820,20
5070 OUT 820,0
5080 OUT 820,18
5090 OUT 820,0
5100 OUT 820,16
5110 OUT 820,0
5120 RETURN
6000 REM                SUB TO TURN ON 8,22,20,18,16,10
6010 OUT 821,255
6020 OUT 820,8
6030 OUT 820,0
6040 OUT 820,22
6050 OUT 820,0
6060 OUT 820,20
6070 OUT 820,0
6080 OUT 820,18
6090 OUT 820,0
6091 OUT 820,16
6092 OUT 820,0
6093 OUT 820,10
6100 OUT 820,0
6110 RETURN
7000 REM                SUB TO TURN OFF 20,16 AND TURN ON 8,22,18,10,17,21
7010 OUT 821,0
7020 OUT 820,20
7030 OUT 820,0
7040 OUT 820,16
7050 OUT 820,0
7060 OUT 821,255
7070 OUT 820,8
7080 OUT 820,0
7090 OUT 820,22
7100 OUT 820,0
7110 OUT 820,18
7120 OUT 820,0
7130 OUT 820,10
7140 OUT 820,0
7150 OUT 820,17
7160 OUT 820,0
7170 OUT 820,21
```

```
7180 OUT 820,0
7181 REM    LINES TO KEEP 16 OFF
7182 OUT 821,0
7183 OUT 820,16
7184 OUT 820,0
7190 RETURN
8000 REM                SUB TO TURN OFF 8 AND TURN ON 22,18,10,21,9
8010 OUT 821,0
8020 OUT 820,8
8030 OUT 820,0
8031 REM    LINES TO KEEP 16 OFF
8032 OUT 820,16
8033 OUT 820,0
8040 OUT 821,255
8050 OUT 820,22
8060 OUT 820,0
8070 OUT 820,18
8080 OUT 820,0
8090 OUT 820,10
8100 OUT 820,0
8130 OUT 820,21
8140 OUT 820,0
8150 OUT 820,9
8160 OUT 820,0
8161 REM    LINES TO KEEP 16 OFF
8162 OUT 821,0
8163 OUT 820,16
8164 OUT 820,0
8170 RETURN
9000 REM                SUB TO TURN OFF 17 AND TURN ON 22,18,21,8,10
9010 OUT 821,0
9020 OUT 820,17
9030 OUT 820,0
9031 REM     LINES FOR 16
9032 OUT 821,0
9033 OUT 820,16
9034 OUT 820,0
9040 OUT 821,255
9050 OUT 820,10
9060 OUT 820,0
9070 OUT 820,22
9080 OUT 820,0
9090 OUT 820,18
9100 OUT 820,0
9110 OUT 820,21
9120 OUT 820,0
9130 OUT 820,8
9140 OUT 820,0
9150 RETURN
10000 REM               SUB TO TURN ON 9,10,16,18,22
10040 OUT 821,255
10070 OUT 820,9
10080 OUT 820,0
10090 OUT 820,10
10100 OUT 820,0
```

```
10110 OUT 820,16
10120 OUT 820,0
10130 OUT 820,18
10140 OUT 820,0
10150 OUT 820,22
10160 OUT 820,0
10161 REM    LINE TO KEEP 8 OFF
10162 OUT 821,0
10163 OUT 820,8
10164 OUT 820,0
10170 RETURN
10500 REM          SUB TO TURN OFF 21,10,16,18,22 AND TURN ON 20
10510 OUT 821,0
10511 REM   LINE TO KEEP 8 OFF
10512 OUT 820,8
10513 OUT 820,0
10520 OUT 820,21
10530 OUT 820,0
10550 OUT 820,10
10560 OUT 820,0
10570 OUT 820,16
10580 OUT 820,0
10590 OUT 820,18
10600 OUT 820,0
10610 OUT 820,22
10620 OUT 820,0
10630 OUT 821,255
10640 OUT 820,20
10645 OUT 820,0
10650 RETURN
11000 REM          SUB TO TURN OFF 18,10,16,22, AND TURN ON 20,11
11010 OUT 821,0
11020 OUT 820,18
11030 OUT 820,0
11040 OUT 820,10
11050 OUT 820,0
11060 OUT 820,16
11070 OUT 820,0
11080 OUT 820,22
11090 OUT 820,0
11100 OUT 821,255
11110 OUT 820,20
11120 OUT 820,0
11130 OUT 820,11
11140 OUT 820,0
11150 RETURN
12000 REM          SUB TO TURN OFF 20 AND TURN ON 21,17
12010 OUT 821,0
12020 OUT 820,20
12030 OUT 820,0
12040 OUT 821,255
12050 OUT 820,17
12060 OUT 820,0
12070 OUT 820,21
12080 OUT 820,0
```

```
12090 RETURN
13000 REM          SUB TO TURN ON 19,23
13010 OUT 821,255
13020 OUT 820,19
13030 OUT 820,0
13040 OUT 820,23
13050 OUT 820,0
13060 REM     LINES TO KEEP INTAKE VALVES OFF
13070 OUT 821,0
13080 OUT 820,8
13090 OUT 820,0
13100 OUT 820,10
13110 OUT 820,0
13120 OUT 820,16
13130 OUT 820,0
13140 OUT 820,0
13150 OUT 820,20
13160 OUT 820,0
13170 OUT 820,22
13180 OUT 820,0
13190 RETURN
14000 REM        SUB TO TURN OFF 10 AND TURN ON 11,23,17,19,21,9
14010 OUT 821,0
14020 OUT 820,10
14030 OUT 820,0
14040 OUT 821,255
14050 OUT 820,11
14060 OUT 820,0
14070 OUT 820,23
14080 OUT 820,0
14090 OUT 820,17
14100 OUT 820,0
14110 OUT 820,19
14120 OUT 820,0
14130 OUT 820,21
14140 OUT 820,0
14150 OUT 820,9
14160 OUT 820,0
14170 RETURN
15000 REM        SUB TO TURN OFF EVERYTHING
15010 OUT 821,0
15020 OUT 820,8
15030 OUT 820,0
15040 OUT 820,9
15050 OUT 820,0
15060 OUT 820,10
15070 OUT 820,0
15080 OUT 820,11
15090 OUT 820,0
15100 OUT 820,16
15120 OUT 820,0
15130 OUT 820,17
15140 OUT 820,0
15150 OUT 820,18
15160 OUT 820,0
```

```
15170 OUT 820,19
15180 OUT 820,0
15190 OUT 820,20
15200 OUT 820,0
15210 OUT 820,21
15220 OUT 820,0
15230 OUT 820,22
15240 OUT 820,0
15250 OUT 820,23
15260 OUT 820,0
15270 RETURN
```

APPENDIX D

Computer Code for the Pulsing Control Method

PROGRAM II: PULSE METHOD

LINE	DESCRIPTION
40	Get pulse time
50	Get pulse gap
60	Disable the Multiplexer
70-80	Close gripper
90-220	Lift the object and put it on the upper platform
230-240	Open gripper
250-380	Return to the initial position
390-1430	Subroutines for operating gripper and fingers
1440-1580	Timer

```
10 REM File Name: REPORT.BAS
20 REM PULSE METHOD: TYPICAL MANEUVER
30 REM N--Delay; N1--Pulse Time; N2--Pulse Gap
40 N1=20
50 N2=60
60 OUT 820,0
70 M1=8 : GOSUB 390
80 N=400 : GOSUB 1440
90 K=1  : M1=18  : GOSUB 440
100 K=8
110 M1=10 : M2=20 : M3=18 : M4=16
120 GOSUB 920
130 K=5
140 M1=10  : M2=16  : M3=18  : M4=21
150 GOSUB 920
160 K=1
170 M1=11 : M2=16 : M3=22
180 GOSUB 720
190 K=3
200 M1=10 : M2=17 : M3=22 : M4=18
210 GOSUB 920
220 N=200  : GOSUB 1440
230 M1=9 : GOSUB 390
240 N=400  : GOSUB 1440
250 K=3
260 M1=16 : M2=18 : M3=10
270 GOSUB 720
280 K=2  : M1=20
290 GOSUB 440
300 K=4  : M1=20  : M2=11
310 GOSUB 560
320 K=6
330 M1=11 : M2=17 : M3=21 : M4=23
340 GOSUB 920
350 K=6
360 M1=17 : M2=19 : M3=21 : M4=11
370 GOSUB 920
380 END
390 REM SUB 1: GRIPPER OPERATE
400 OUT 821,255
410 OUT 820,M1
420 OUT 820,0
430 RETURN
440 REM SUB 2: ONE FINGER OPERATE
450 FOR L=1 TO K
460 OUT 821,255
470 OUT 820,M1
480 OUT 820,0
490 GOSUB 1490
500 OUT 821,0
510 OUT 820,M1
520 OUT 820,0
530 GOSUB 1540
540 NEXT
550 RETURN
```

```
560 REM SUB 3: TWO FINGERS OPERATE
570 FOR L=1 TO K
580 OUT 821,255
590 OUT 820,M1
600 OUT 820,0
610 OUT 820,M2
620 OUT 820,0
630 GOSUB 1490
640 OUT 821,0
650 OUT 820,M1
660 OUT 820,0
670 OUT 820,M2
680 OUT 820,0
690 GOSUB 1540
700 NEXT
710 RETURN
720 REM SUB 4: THREE FINGERS OPERATE
730 FOR L=1 TO K
740 OUT 821,255
750 OUT 820,M1
760 OUT 820,0
770 OUT 820,M2
780 OUT 820,0
790 OUT 820,M3
800 OUT 820,0
810 GOSUB 1490
820 OUT 821,0
830 OUT 820,M1
840 OUT 820,0
850 OUT 820,M2
860 OUT 820,0
870 OUT 820,M3
880 OUT 820,0
890 GOSUB 1540
900 NEXT
910 RETURN
920 REM SUB 5: FOUR FINGERS OPERATE
930 FOR L=1 TO K
940 OUT 821,255
950 OUT 820,M1
960 OUT 820,0
970 OUT 820,M2
980 OUT 820,0
990 OUT 820,M3
1000 OUT 820,0
1010 OUT 820,M4
1020 OUT 820,0
1030 GOSUB 1490
1040 OUT 821,0
1050 OUT 820,M1
1060 OUT 820,0
1070 OUT 820,M2
1080 OUT 820,0
1090 OUT 820,M3
1100 OUT 820,0
```

```
1110 OUT 820,M4
1120 OUT 820,0
1130 GOSUB 1540
1140 NEXT
1150 RETURN
1160 REM SUB 6: FIVE FINGERS OPERATE
1170 FOR L=1 TO K
1180 OUT 821,255
1190 OUT 820,M1
1200 OUT 820,0
1210 OUT 820,M2
1220 OUT 820,0
1230 OUT 820,M3
1240 OUT 820,0
1250 OUT 820,M4
1260 OUT 820,0
1270 OUT 820,M5
1280 OUT 820,0
1290 GOSUB 1490
1300 OUT 821,0
1310 OUT 820,M1
1320 OUT 820,0
1330 OUT 820,M2
1340 OUT 820,0
1350 OUT 820,M3
1360 OUT 820,0
1370 OUT 820,M4
1380 OUT 820,0
1390 OUT 820,M5
1400 OUT 820,0
1410 GOSUB 1540
1420 NEXT
1430 RETURN
1440 REM SUB 7: TIMER 1
1450 FOR I=1 TO N
1460 J=I+1
1470 NEXT
1480 RETURN
1490 REM SUB 8: TIMER 2
1500 FOR I=1 TO N1
1510 J=I+1
1520 NEXT
1530 RETURN
1540 REM SUB 9: TIMER 3
1550 FOR I=1 TO N2
1560 J=I+1
1570 NEXT
1580 RETURN
```